EXPERIMENTAL INVESTIGATIONS ON DIAMOND BURNISHING OF 17-4 PH STAINLESS STEEL UNDER SUSTAINABLE COOLING ENVIRONMENTS

Thesis

Submitted in partial fulfillment of the requirements for the degree of

DOCTOR OF PHILOSOPHY

by

SACHIN B

DEPARTMENT OF MECHANICAL ENGINEERING
NATIONAL INSTITUTE OF TECHNOLOGY KARNATAKA
SURATHKAL, MANGALORE-575025

OCTOBER, 2019

Dedicated to….

My beloved Parents,

Family members…

&

All my Teachers and Colleagues who taught and encouraged me with positive thoughts…

DECLARATION

By the Ph.D. Research Scholar

I hereby declare that the Research Thesis entitled **"EXPERIMENTAL INVESTIGATIONS ON DIAMOND BURNISHING OF 17-4 PH STAINLESS STEEL UNDER SUSTAINABLE COOLING ENVIRONMENTS"** which is being submitted to the **National Institute of Technology Karnataka, Surathkal** in partial fulfillment of the requirements for the award of the degree of **Doctor of Philosophy** in **Mechanical Engineering** is a bonafide report of the research work carried out by me. The material contained in this Research Thesis has not been submitted to any other Universities or Institutes for the award of any degree.

Register Number: **165091ME16F14**

Name of the Research Scholar: **Sachin B**

Signature of the Research Scholar:

Department of Mechanical Engineering

Place: NITK-Surathkal

Date:

CERTIFICATE

This is to certify that the Research Thesis entitled **"EXPERIMENTAL INVESTIGATIONS ON DIAMOND BURNISHING OF 17-4 PH STAINLESS STEEL UNDER SUSTAINABLE COOLING ENVIRONMENTS"** submitted by **Mr. Sachin B** (Register Number: ME16F14) as the record of the research work carried out by him, is accepted as the Research Thesis submission in partial fulfillment of the requirements for the award of the degree of **Doctor of Philosophy**.

Research Guides

Prof. Narendranath. S
Professor
Department of Mechanical Engineering
NITK, Surathkal
Date:

Dr. D. Chakradhar
Assistant Professor
Department of Mechanical Engineering
IIT Palakkad
Date:

Chairman-DRPC
Date:

DEPARTMENT OF MECHANICAL ENGINEERING
NATIONAL INSTITUTE OF TECHNOLOGY KARNATAKA, SURATHKAL
MANGALORE - 575025

ACKNOWLEDGMENT

I am indebted to my supervisors **Prof. Narendranath. S**, Professor, Department of Mechanical Engineering, National Institute of Technology Karnataka, Surathkal and **Dr. D. Chakradhar**, Assistant Professor, Department of Mechanical Engineering, Indian Institute of Technology Palakkad, for their excellent guidance and support throughout the research work. Their constant encouragement, help, and review of the entire work during the investigation are invaluable.

I wish to thank Research Progress Assessment Committee members **Prof. Lakshman Nandagiri**, Professor, Department of Applied Mechanics and Hydraulics Engineering and **Prof. Prasad Krishna**, Professor, Department of Mechanical Engineering for their unbiased appreciation and criticism all through this research.

I am immensely grateful to **Prof. Shrikantha. S. Rao**, Professor, and Head, Department of Mechanical Engineering for extending the Departmental facilities, which ensured the satisfactory progress of my research work. I wish to express my sincere gratitude to **Prof. Vijay Desai,** Professor, Department of Mechanical Engineering, for his valuable suggestions to perform this research work.

I want to thank all the teaching and non-teaching staff members of the Department of Mechanical Engineering of NITK Surathkal for their continuous help and support throughout the research work.

I thank **Ms. Rashmi Banjan** of Department of Metallurgical and Materials Engineering, for her support in connection with the use of a Scanning Electron Microscope. I want to thank CMTI Bengaluru for research support during all years of my research. I also like to thank **Mr. Puneeth** and **Mrs. Sushma** for their support in connection with the use of a confocal microscope and X-Ray diffraction measurement system.

I owe my deepest gratitude to supporting staff of the Department of Mechanical Engineering, **Mr. Jaya Devadiga**, **Mr. C. A. Varghese**, **Mr. Gangadhar, Mr. Krishna Kumar, Mr. Mahesh**, **Mr. Pradeep**, **Mr. Sudhakar** and **Mr. Mahaveer** for their help during the conduction of experiments.

I thank the Director and the administration of NITK Surathkal for permitting me to pursue my research work at the Institute.

I would like to thank my co-researchers and friends **Ms. Charitha. M. Rao**, **Mr. Gajanan. M. Naik, Mr. Vinay Varghese, Dr. Sivaiah**, **Mr. Puneeth**, **Dr. Venkatesh**, **Dr. Hargovind Soni, Mr. Abhinaba Roy, Mr. Manoj, Mr. Prithivirajan, Mr. Ravindra Badiger, Mr. Mahesh Davangeri, Mr. Gopal, Mr. Kishan, Mr. Renjith Joy, Mr. Vasu, Mr. Nuthan,** for their kind help, encouragement for successful completion of this research work.

I would like to thank my colleagues **Mr. Manjunath HN, Mr. Ramesh Babu, Dr. Kiran Aithal**, **Dr. V. R. Kabadi,** Department of Mechanical Engineering, NITTE Meenakshi Institute of Technology, Bangalore, and **Prof. N. R. Shetty**, Director, NITTE Meenakshi Institute of Technology, Bangalore for their kind help and suggestions throughout the research work. I am immensely indebted to the continual help and support I received from **Dr. Shailesh Rao**, Department of Industrial and Production Engineering, National Institute of Engineering, Mysuru and **Mr. Pawar**, Mech-India Pvt. Ltd. Mumbai, during my research work.

I am indebted to all my friends from the Department of Mechanical Engineering and other Departments of NITK Surathkal for their constant help and encouragement during the research work.

I would also like to share the happiest moment of my life with my respected parents. Their blessings, guidance, and endeavor kept my moral high throughout the research. I feel happy to express my sincere appreciation to all my family members, for their understanding, care, support, and encouragement.

The list goes on, and there are many others I should mention. There are people who had helped me all the way and supported me when I didn't even realize I needed it, or needed it now, or needed it constantly. Listing all of them would fill a book itself, so I merely will have to limit myself to a few words: I THANK YOU ALL……!

Sachin B

ABSTRACT

The materials which initiate more tool wear, heat, cutting force, and poor surface finish during machining are termed to be difficult-to-cut materials. The precipitation hardenable (PH) stainless steel is one of the interesting family of steels which can attain hardness up to 49 HRC. In these family of stainless steels, 17-4 PH stainless steel has attracted engineers across the world because of its superior corrosion resistance and high strength, which is not possible to find in any of the steel grades. Owing to low thermal conductivity, high strength and admirable wear resistance properties, it has been classified under difficult to cut materials. It is a special type of PH martensitic stainless steel which consists of martensite along with a small quantity of austenite. Compressor blades of steam turbines are subjected to high temperature, vibration, and stress inducement. These issues can cause damage to the engine. Hence, the first set of compressor blades can be manufactured with PH stainless steel to avoid the problems arising due to foreign object damage. Machining of such kind of steels results in poor surface quality and also the production cost is more. Burnishing is one of the preferred secondary finishing operations which is usually performed after machining to achieve the mirror finish of the surface. To achieve the superior surface characteristics of the difficult to cut material, it is preferred to cool the burnishing zone with an appropriate lubricant.

Millions of workers throughout the world get affected by working under different kinds of cutting fluids or coolants. Aerosol particles or mist are some of the hazardous elements which will be generated during the application of different types of cutting fluids during machining and which affects the operator's health. Cryogenic machining has emerged as an alternative cutting fluid in the last two decades. Liquid nitrogen (LN_2) will be sprayed at the interface of the tool and workpiece. It is environmental friendly coolant when compared to other conventional coolants. During the burnishing process, because of the pressure created in the burnishing zone, the temperature at that region increases. By the application of LN_2, the temperature can be reduced, which results in improved surface integrity of the material.

A high-quality finishing of the mechanical parts is necessary to attain the improved fatigue resistance and a low friction ratio. Hence the finishing processes are turned out to be a major drive for industrial innovation all over the globe. Some of the secondary finishing processes such as grinding, lapping, honing, and polishing have been widely used to achieve the super finish of the surface. However, to improve the surface quality and geometrical accuracy of the component, burnishing has been introduced. Burnishing is also one of the well-known secondary finishing process used to improve the functional performance of the component. Diamond burnishing is one of the chipless finishing processes where the spherical tip of the tool made up of natural diamond, slides on the surface of the workpiece which causes plastic deformation. Directly after machining, the workpiece can be diamond burnished to acquire improved surface integrity. It is an economical and compatible process which can be applied on ferrous and nonferrous materials to achieve the mirror-like surface finish. It has a higher level of efficiency when compared to grinding, lapping, and polishing processes.

The main objective of this research work is to investigate the influence of process parameters on the surface integrity characteristics while diamond burnishing of 17-4 PH stainless steel under varying working environments. To achieve the best feasible surface integrity properties of the material, the present research work has been classified into four phases. In the first phase, one factor at the time approach (OFATA) was used to find out the influence of control factors such as burnishing speed, burnishing feed and burnishing force on performance characteristics such as surface roughness, surface hardness, surface morphology, surface topography, subsurface microhardness and residual stress using a commercially available diamond burnishing tool. The cryogenic cooling, minimum quantity lubrication (MQL), and dry environments were considered for the study. In the second phase, a novel diamond burnishing tool was designed and fabricated to improve the performance characteristics of the material. To analyze its performance under all the three environments, OFATA was used. Further, the study was extended to investigate the influence of two more process parameters such as the number of tool passes and diamond sphere diameter on the performance characteristics in the cryogenic cooling condition. In

the third phase, the optimization of process parameters was performed by Taguchi's Grey Relational Analysis (TGRA). In the fourth phase, a mathematical model was developed for surface roughness and surface hardness by Response Surface Methodology (RSM). The developed regression equation was used to perform multi-objective optimization using genetic algorithm (GA). The optimal process parameters were achieved, which will be beneficial in improving the performance of the component.

Keywords: 17-4 PH stainless steel; Sustainable burnishing; Cryogenic burnishing; MQL; A novel diamond burnishing tool; Surface integrity characteristics; Grey Relational Analysis, Response Surface Methodology, Genetic Algorithm.

CONTENTS

LIST OF FIGURES

LIST OF TABLES

LIST OF ABBREVIATIONS AND SYMBOLS

RSM	Response surface methodology
LN_2	Liquid nitrogen
TGRA	Taguchi's grey relational analysis
OFATA	One factor at the time approach
ANOVA	Analysis of variance
MOGA	Multi-objective genetic algorithm
GA	Genetic algorithm
GRA	Grey relational analysis
GRG	Grey relational grade
MQL	Minimum quantity lubrication
PH	Precipitation hardenable
CCD	Central composite design
Std. Dev	Standard deviation
CV	Coefficient of variation
PRESS	Predicted residual error sum of squares
R^2	coefficients of determination
df	Degrees of freedom
Adj	Adjusted
Adeq	Adequate
Pred	Predicted
Prob	Probability

CHAPTER-1

INTRODUCTION

The surface properties and dimensional precision of the components are the two most crucial factors which are considered seriously in modern machining industries. High-quality finishing of the mechanical parts is necessary to obtain the improved fatigue resistance and a low friction ratio. Hence the finishing processes turn out to be a major drive for industrial innovation across the globe. Technological quality of the component can be estimated by an important factor known as surface quality. Wear resistance and fatigue strength are the two major factors which are influenced by the surface roughness of the component. The surface generated by machining will have irregularities, and hence it is difficult to produce a flat surface. To obtain a super finished surface, some of the secondary finishing operations have to be performed. The surface layer of the components is subjected to heavy loads. The surface layer aspects such as residual stresses, microhardness are to be given more importance to improve the lifetime of the components. The required set of improved surface properties could be achieved by improving the microhardness, residual stress, grain refinement, and surface finish.

1.1 NEED FOR THE ENHANCEMENT OF SURFACE QUALITY

During the machining operation of some of the materials, namely hardened steels, titanium alloys, and refractory metals, tool wear is a common issue which has to be considered seriously. Increasing tool wear results in poor surface properties of the material and it also leads to the inducement of tensile residual stresses. The functional performance will get affected by the poor fatigue strength of the material. The machining process causes the dramatic failure of the components because of the damage caused by the process to the components, especially which are made up of difficult to cut materials. To overcome these issues, a secondary finishing process has to be performed which is capable of producing a

modified surface characteristic of the material. Modern industries demand advanced materials which can yield improved corrosion and wear resistance. However, procuring of these material results in an increase in the cost of the production. The failure of the components is initiated from the surface due to the chemical and mechanical interaction with the surrounding environment. On the other hand, the environmental attack and intensity of external stress will be highest at the surface. To eliminate these issues during machining, the surface modification techniques have been performed on the surface of the material (Liu et al. 2016). Surface modification is treated as one of the crucial technique in improving the surface integrity characteristics of the material. The service life of the components is being enhanced by advanced technology such as laser treatment and coating. It has a drawback of the high cost involved in the production of the components, and it demands a high level of surface finish. Hence from the economical point of view, it is not feasible for all the components. Few researchers have shown interest in post machining and finishing operations in improving the surface characteristics of the materials (Shapiro, 1970; Timoshchenko and Dubenko, 1976; Ruseva and Fuks, 1978; Rajesham and Tak, 1989).

To enhance the life of the critical components, a variety of surface treatment methods have been employed, as shown in Figure 1.1. The basic types of surface enhancement techniques are thermal and mechanical surface treatment techniques. In the case of a thermal method, the material is subjected to heating to modify its microstructure, which yields improved hardness and fatigue strength of the material. Thermal treatment methods are classified as case hardening, nitriding, and induction hardening. In the nitriding process, nitrogen will be introduced into the surface of the material. Case hardening is a process where the metal surface will harden, and a thin layer of the hardened alloy will be formed on the surface. Induction hardening will be carried out by heating a metal and quenching it to obtain an improved brittleness and hardness by the martensitic transformation. Thermal treatment techniques have enormous advantages, but after processing the surface becomes brittle, and also grain boundaries will become weak. Mechanical techniques are used for

improving the fatigue life, corrosion resistance, and wear resistance of the components (Tolga, 2005).

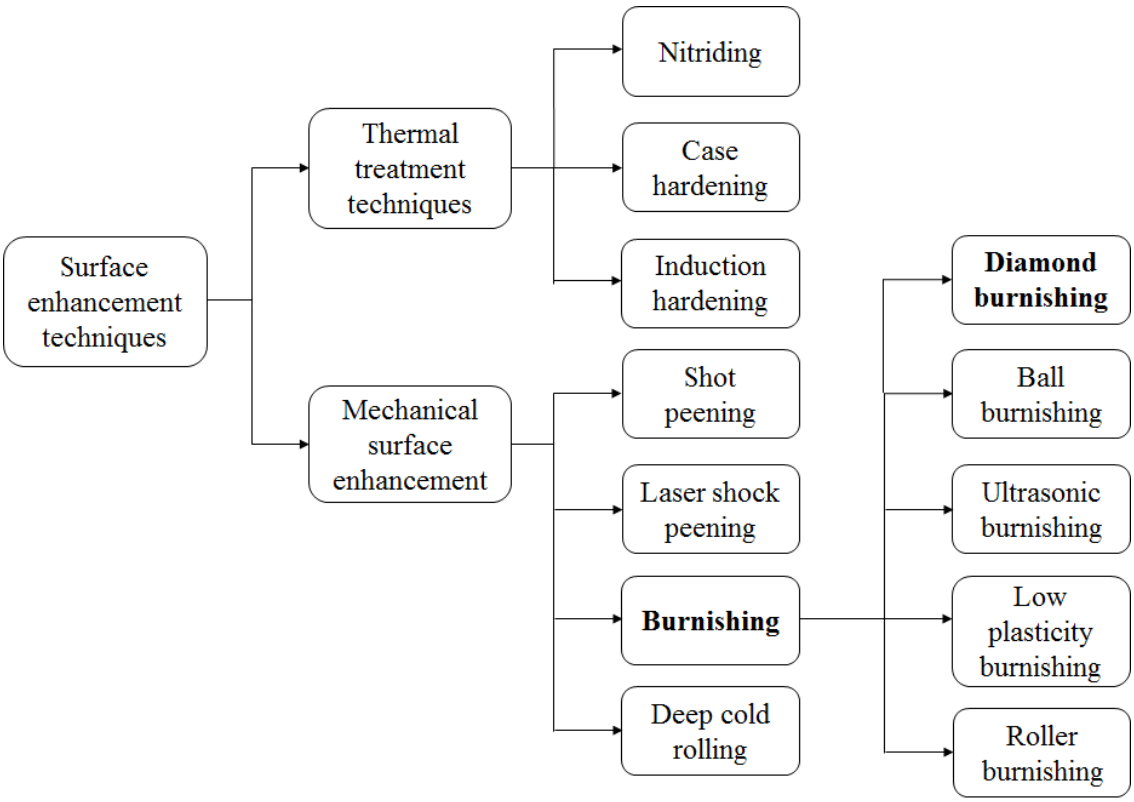

Figure 1.1 Surface enhancement methods (Revankar et al. 2014).

In shot peening, particles are imparted to the surface of the metal in a predefined way. It can be used on large or small area depending upon the requirement and also the cost involved is low. However, excessive surface damage and poor surface finish are the notable disadvantages of the shot peening process. Ultrasonic and laser shot peening is considered to be expensive because it requires a protected environment and skilled manpower for treatment. To eliminate such drawbacks experienced by other techniques, burnishing has been introduced. Burnishing is a surface finishing technique which enhances the surface properties of the material, and it has to be performed after machining. Generation of compact and wear resistance surface is possible through burnishing, which enhances the life of the product. Formation of compressive residual stresses and super finished surface layer separates it from other surface treatment methods (Wang, 2009). Maawad et al.

(2011) investigated the performance of burnishing and proved it to be a superior process to shot peening, laser shock peening, and ultrasonic shot peening.

1.2 BURNISHING

Burnishing is a popular mechanical treatment method which induces compressive residual stresses by severe plastic deformation. It is also popularly known as a surface smoothening process (Sayahi et al. 2013). The superior surface finish and hardness are the two important requirements of the manufacturing industries which can be easily attained by implementing burnishing. Fatigue life is one of the important property of the material and failure of the engineering components are initiated because of the lack of fatigue strength. Some of the factors which have an impact on fatigue life are size, surface finish, and shape of the components.

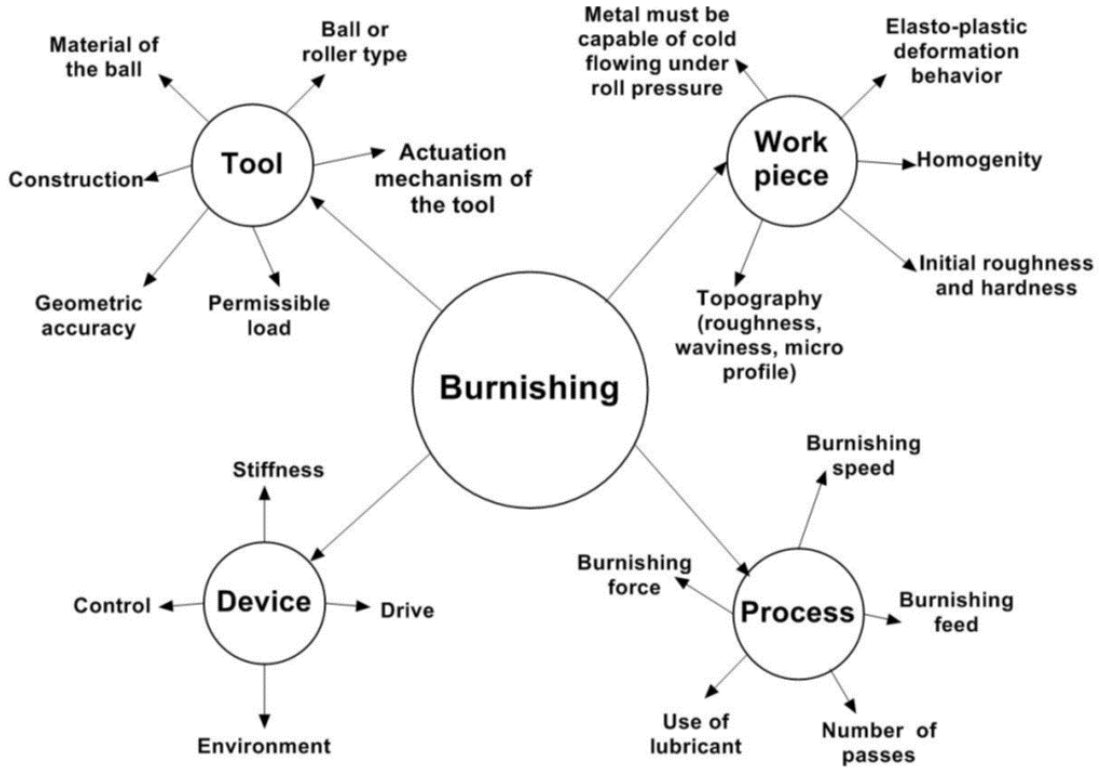

Figure 1.2 Influence of parameters on burnishing (Revankar et al. 2014).

Figure 1.2 describes the influence of parameters on the burnishing process. Among these, surface roughness causes microscopic stress concentrations, which is one of the strong reason for the reduction in the fatigue strength of the material. Fatigue will be initiated on the surface because of the formation of cracks. Hence, fatigue strength is directly dependent on the surface roughness of the component (Herbert, 1927). Some of the irregularities present over the surface after initial machining operation can be removed by secondary finishing operations, namely burnishing, grinding, lapping, honing, and polishing. Some of the commonly employed material for burnishing are brass, bronze, stainless steel, cast iron, copper, aluminum, titanium alloy, etc. Another basic requirement of burnishing is the hardness of the material should not be more than 40 HRC, and also the cold flow of the material should take place under the applied pressure. It is a chipless process in contrast with other finishing processes. The inducement of compressive residual stresses after burnishing is key to improve the fatigue strength of the material. Burnishing process induces a combination of improved surface characteristics of the material, and it is a widely accepted super finishing process (Loh and Tam, 1988).

To understand the burnishing mechanism more clearly, it can be divided into three segments as follows:

1. Geometrical mechanism
2. Mechanical mechanism
3. Metallurgical mechanism

Geometrical mechanism refers to the changes happening in the surface roughness of the material. Mechanical mechanism is defined as the characteristics which induce cold-work hardening and compressive residual stresses. Closure of surface cracks, refinement of the grains (Wang et al. 2009), and texture orientation (Zaborski et al. 2000) are some of the characteristics of the metallurgical mechanism. Further, burnishing can be performed in conventional machines with less skilled operators, and it is a cost-effective process. The working principle of the burnishing process is based on an indenting tool which moves along the cylindrical length of the workpiece. Due to the force acting on the workpiece by the tool-tip, the plastic flow of the asperities occurs from the peak to the valley, and the

surface will be flattened. A schematic diagram of the burnishing process is as depicted in Figure 1.3.

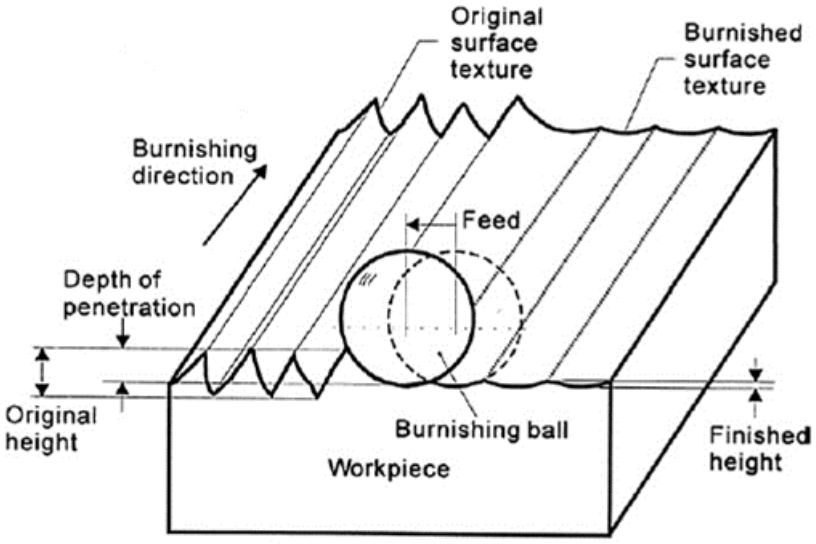

Figure 1.3 Burnishing process (Fang and Chuing, 2010).

Burnishing has been classified into three types, i.e., Ball burnishing, roller burnishing, and slide/diamond burnishing. All the three methods differ from each other in terms of the tool, but the mechanism of working remains the same for all the kinds. In ball burnishing a ball made up of different materials will be placed in the tool tip. The applied burnishing force causes the rotation of the ball when it comes in direct contact with the workpiece. Here ball acts as a rotating device to super finish the workpiece into the required surface quality. Usually, carbide rollers will be used to improve the surface quality of the material. The ball burnishing process is depicted in Figure 1.4. In roller burnishing, a small roller will be placed at the tip of the tool which rotates on the circumference of the workpiece. The application of force tries to apply more pressure by the roller to the workpiece, which substantially improves the surface quality of the workpiece. The roller burnishing process uses a tool, as shown in Figure 1.5. In the case of diamond/slide burnishing, a diamond tip will be used to super finish the workpiece. Superior surface finish can be obtained as the tip of the tool moves over the workpiece. Compared to ball and roller burnishing, diamond burnishing method is the most preferred one to improve the surface quality of the

workpiece. In the present study, diamond burnishing process has been performed. It is one of the preferred technology used by the production industries to enhance the surface characteristics of the material. Diamond burnishing process is a chipless process which typically consists of a spherical diamond tip which applies pressure on the workpiece, which leads to plastic deformation of the asperities. Directly after machining, the workpiece can be diamond burnished to obtain improved surface integrity properties.

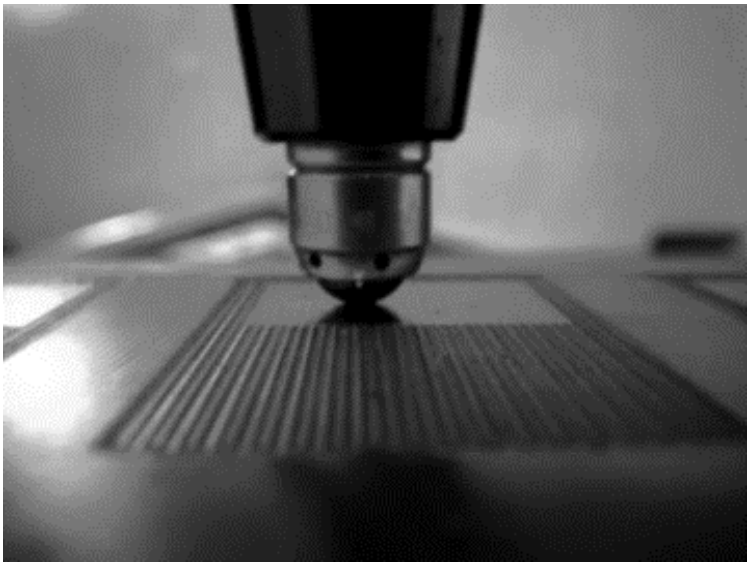

Figure 1.4 Ball burnishing process (López et al. 2011).

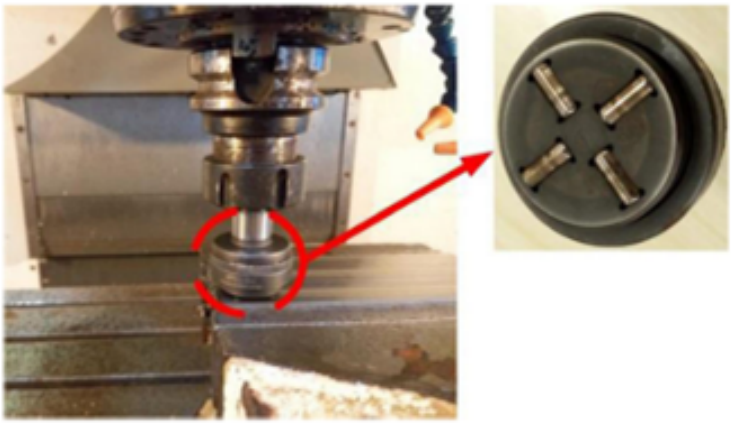

Figure 1.5 Roller burnishing process (Yuan et al. 2016).

The careful selection of the control variables can yield superior surface characteristics of the material during the diamond burnishing process. It is one of the cost-effective technique which has been implemented in the manufacturing sectors to improve the productivity and quality of the components. To obtain the close tolerance of the components which are used in aircraft, machine tools, defense, and automobile parts, diamond burnishing operation is being performed (John et al. 2016). It is an economical and compatible process which can be applied on ferrous and nonferrous materials to obtain a superior surface finish. It has a higher level of efficiency when compared to grinding, lapping, and polishing processes. Figure 1.6 illustrates the diamond burnishing process.

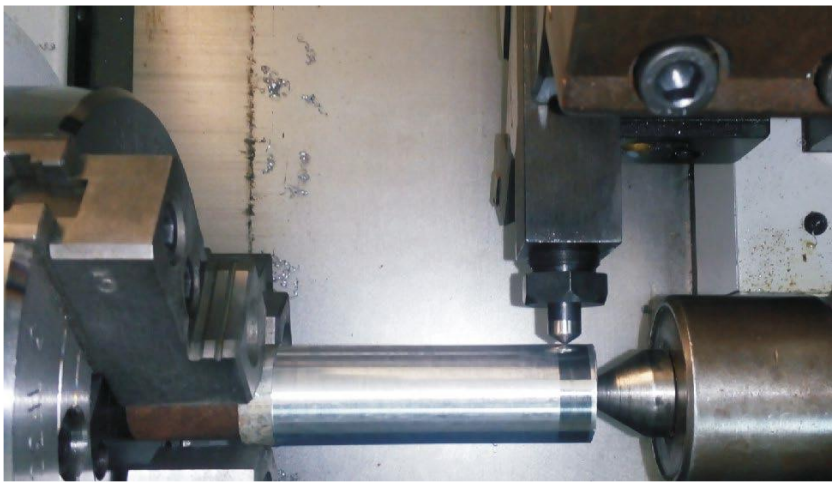

Figure 1.6 Diamond burnishing process (Maximov et al. 2017).

1.2.1 Control variables

For the successful development of a product, the appropriate selection of process parameters and their levels are crucial. The improper selection of the process parameters and their levels may lead to poor surface integrity characteristics of the material. Improper selection of the control variables affects the productivity of the components. Hence it is very much necessary to focus on the most required process parameters for obtaining improved surface characteristics of the material. In the present study, some of the process parameters such as burnishing speed, burnishing feed, burnishing force, diamond sphere diameter, and number of tool passes have been considered.

1.2.1.1 Burnishing speed

It is defined as the speed at which the burnishing process is performed. The range of burnishing speed varies from 21 m/min to 113 m/min. From the preliminary experimentation, it was found that a medium range of burnishing speed is preferred to obtain a good surface finish and low burnishing speed is preferred to obtain high surface hardness of the material. The higher range of burnishing speed may lead to possible chatter, which affects the surface quality of the components. Fundamentally, any range of burnishing speed may be chosen for the burnishing process based on the requirement.

1.2.1.2 Burnishing feed

In the burnishing process, there are certain parameters which have to be controlled properly to obtain a quality surface of the component. Burnishing feed is one among those parameters which have to be controlled properly to avoid poor surface finish of the component. Burnishing feed is defined as the distance covered by the tool during one revolution of the workpiece. Based on the manufacturer's recommendation, for diamond burnishing, the feed range should not exceed 0.1 mm/rev. Hence in the present study, the burnishing feed was varied from 0.048 mm/rev to a maximum of 0.096 mm/rev.

1.2.1.3 Burnishing force

To attain the maximum surface hardness of the material after burnishing, the burnishing force parameter has to be controlled properly. It is treated to be one of the important process parameters to perform diamond burnishing. Basically for diamond burnishing the application of a higher range of burnishing force is usually not preferred because the diamond tip is capable of producing exceptional surface finish even at a low range of burnishing force. Based on the requirement of the present study, the burnishing force has been selected from 50 N to 200 N. Application of burnishing force to the workpiece leads to permanent plastic deformation which is the basic principle of burnishing. The burnishing force can be applied to the workpiece by applying suitable pressure on the tool, which

results in compression of the spring. The spring movement is necessary for applying a suitable burnishing force on the material.

1.2.1.4 Diamond sphere

For diamond burnishing process, a spherical diamond sphere will be used to provide a sliding movement on the workpiece. The variation of the surface characteristics of the material may be expected with the varying diamond sphere diameter of the tool-tip. Small diamond sphere diameter is preferred to attain maximum surface hardness, and moderated sphere diameter is preferred for obtaining a superior surface finish of the components. In the current study, the diamond sphere diameters of 6 mm, 8 mm, and 10 mm have been used.

1.2.1.5 Number of passes

The number of passes is defined as the repetitive movement of the tool over the same area of the workpiece. The present investigation introduces two working schemes for diamond burnishing. The repetitive movement of the tool in the same area of the workpiece leads to repeated plastic deformation of the material and work hardening takes place at this condition. Fundamentally number of passes need not be necessarily considered for carrying out diamond burnishing. However, for increasing the surface hardness, the number of passes can be considered as one of the parameters. In the present research work, two number of passes have been considered to perform diamond burnishing.

1.2.2 Applications of burnishing process

By the effective use of burnishing, the secondary finishing methods can be avoided with an appreciable improvement in surface characteristics. The burnishing process has been extensively used in industries such as defense, mining, railways, automobile, spacecraft, agriculture, textile, aircraft, machine tools for the production of piston, connecting rod bores, brake system components, torque converter hubs, motors, pump, transmission parts, etc. (Boyer, 1996; Cui, 2011).

1.2.3 Recent trends in aerospace industries

In aerospace industries, burnishing process has emerged as an innovative technique in improving the characteristics of the material. Enormous research work has been performed in this area. The modern aircraft engine works in a hectic environment which involves critical parts. The material used should be expected to have high strength, good corrosion resistance, and ductility.

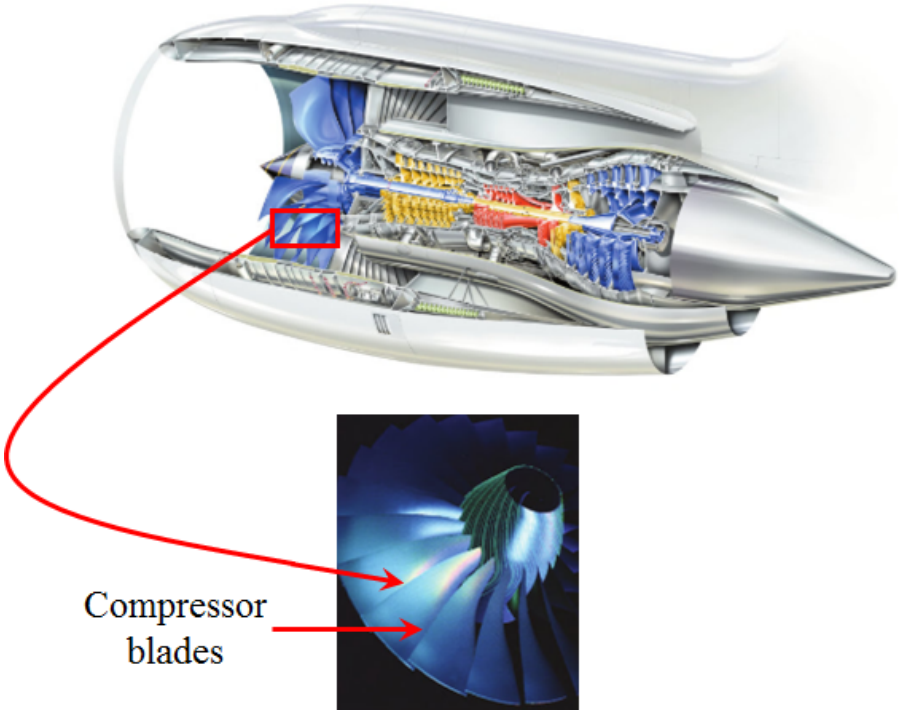

Figure 1.7 Aero-engine compressor blades (Rolls Royce, 2015).

Figure 1.7 depicts the compressor blades used in aero-engine. Failure occurring in the compressor blades is the only reason for compromising safety. The first stage compressor blades are treated to be important in aero-engine because most of the accidents take place due to the failure occurring at these blades. The major causes for this failure are rectified to be sand and bird hits. The root causes for the failure of these blades are focussed mainly on foreign object damage (FOD), which significantly affects the fatigue life of the components (Silveira et al. 2008). Research work performed on the first stage of compressor blades shows that the application of burnishing has improved its fatigue life.

Titanium and aluminum based alloys are commonly used for aerospace compressor blades because of its admirable properties (Zhang et al. 2015). However, the first stage of compressor blades demands high strength material to withstand ingested debris. Out of all the sets of compressor blades, the first five to eight stages are made up of martensitic stainless steel like 15-5 PH (Boyce and Meherwan, 2006). 17-4 PH stainless steel has high strength and corrosion resistance, which makes it preferred selection for the first stage of compressor blades used in aerospace compressor blades (Bressana et al. 2008). 17-4 PH stainless steel is used for the first stage of compressor blades employed in T56 turboprop engine. It was also observed that 17-4 PH stainless steel has better results in stress corrosion cracking and high cycle fatigue test by the application of low plasticity burnishing in contrast with alloy 450 (Zhang et al. 2015).

1.3 INFLUENCE OF HIGH TEMPERATURE ON BURNISHING

In manufacturing industries, burnishing is treated to be the essential technique to improve the surface characteristics of the material. Difficult to cut materials are drawing interest among the researchers on account of its excellent mechanical properties. Therefore it is essential to increase the performance of the components manufactured from these materials without compromising on its quality and cost. Some of the nonconventional machining processes can be used to machine difficult to cut materials (Li et al. 2015; Liu et al. 2015). However, they have a lot of limitations in its productivity on account of high machining cost and low material removal rate. Generally, during machining, heat will be generated due to the impact of a higher range of machining parameters, which results in poor surface finish and tool wear (Sharma et al. 2009). The productivity of the components will also get affected by these issues. In burnishing, when the tool and the workpiece come in contact with each other, friction will be generated due to the sliding movement of the tool and application of a higher range of input parameters. At the burnishing zone, the formation of high temperature takes place, which gradually affects the performance of the components. The sliding action of the burnishing tool results in tool wear. The performance characteristics will be severely affected by the generation of high temperature in the burnishing zone. Friction is another major issue which will be observed during burnishing.

High-temperature generation at the burnishing zone induces thermal stresses on the burnishing tool which also results in thermal softening of the burnishing tool leading to failure of the tool. Some of the general drawbacks as a result of higher burnishing zone temperature are poor dimensional accuracy, poor surface quality, non-beneficial surface characteristics, and reduced tool life. At a higher range of process parameters, the possible chattering may be experienced, which reduces the surface quality of the material because of the formation of surface defects (Dhar et al. 2001). The surface integrity characteristics of the material will be greatly affected by the tool wear (Kaynak et al. 2014). Few other factors have an immense influence on the formation of higher burnishing zone temperatures such as tool material, selection of the process parameters, workpiece material, tool geometry, and burnishing lubricants used for reducing the temperature at the burnishing zone.

1.4 LUBRICATION APPROACHES

The tool life and performance of the product can be improved by various effective lubrication methods. If the heat generation at the burnishing zone increases, then the performance of the surface characteristics decreases. It is essential to handle this issue more carefully with the intention of improving the performance characteristics during burnishing. To decrease the heat generation at the tool-workpiece interface, several kinds of lubrication methods have been successfully used. The notable cooling techniques are cryogenic cooling, allied cooling, MQL, high-pressure coolant, flood cooling, and solid lubricant. Most of the manufacturing industries are using conventional fluids to overcome the temperature rise in the burnishing zone (Baradie, 1996a). It was also found that the flood cooling methods used to reduce the heat generated at the machining zone cannot be able to reduce the temperature (Shaw et al. 1951; Cassin and Boothroyd, 1965). It was investigated that the conventional fluids cause health issues and environmental problems, which is a matter of concern for most of the manufacturers (Baradie, 1996b). The predicted cost of lubricants in the machining of difficult to cut materials will be 20-30% of the total manufacturing cost (Pusavec et al. 2010). Moreover, the disposal of the cutting fluids is also expensive because it could cost up to 2 to 4 times its purchase cost (Chetan et al. 2016).

Most of the organizations have restricted the use of cutting fluids in industries because of the above-mentioned issues. Various sustainable manufacturing methods used in industries are illustrated in Figure 1.8. The sustainable machining choices available are depicted in Figure 1.9.

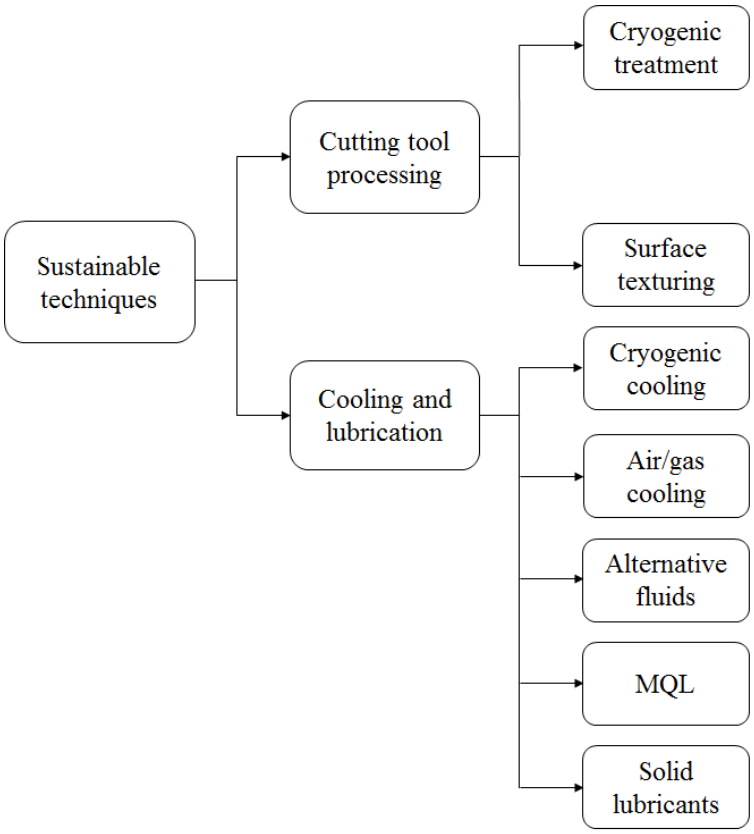

Figure 1.8 Cooling techniques in metal cutting (Chetan et al. 2016).

In MQL system, a mist of fluid will be used in the burnishing zone at a flow rate of 50-500 ml/hr. It is believed that the consumption of fluid in MQL is 10,000 times lesser than the conventional coolants (Dhar et al. 2006b). MQL machining is reported to be non-feasible in industries due to the fact that it causes health problems due to the continuous supply of oil mist at the working zone (Aoyama et al. 2008). Air/gas cooling method is not effective in reducing the temperature developed at the burnishing zone, and also it requires a special equipment for cooling the interface. Solid lubricant requires more production cost and

similar to the air cooling, it also requires a special equipment to supply the lubricant. Usually, in flood cooling techniques, some of the lubricants, namely ionic liquids and vegetable oil is widely used, which are cost effective and also biodegradable. The major drawback of these kinds of oils is they have poor thermal stability and is not capable of removing the heat generated efficiently.

Figure 1.9 Sustainable machining choices (Jawahir et al. 2016).

1.5 MINIMUM QUANTITY LUBRICATION

The remarkable negative effects of flood cooling on environment and health have resulted in switching over to the next level of lubrication methods. To meet the requirements of the manufacturers and also to make it more environmentally friendly, the researchers are concentrating on minimum use of lubrication during manufacturing. MQL is one among those techniques which could reduce the use of extensive fluids for lubrication. The flow rate of the lubricant will be usually set in the range of 10 to 100 ml/hour. The quantity of lubricant used in the MQL system will be reduced to ten-thousandth times in contrast with flood lubrication (Autret et al. 2003). This technique is also termed as near dry machining because of the minimum quantity of the fluid used. This method works on the principle of atomization in which the air flow splits the drop of fluid, and the dispersed fluid follows the direction of air flow. Most of the researchers have attempted to improve the machining characteristics during turning, drilling, and milling by the extensive use of MQL

(Wakabayashi et al. 1998; Dhar et al. 2006a; Davim et al. 2007; Kamata and Obikawa, 2007).

The metal cutting operations demand the use of lubrication because it increases the tool life, enhances the quality of the component, and it also prevents damages caused during machining on the surface layer of the component. The problems associated with the conventional lubricants are more such as environmental issues, health problems due to the smoke, airborne mist, etc. Some of the health issues faced by the workers are asthma, tuberculosis, respiratory problems, bronchitis, allergic reactions and skin eruptions, etc. (Sivaiah and Chakradhar, 2017). Due to the above problems encountered during machining, the manufacturing industries are constantly trying to explore a new technique for the lubrication to limit the use of conventional lubricants. By reducing the abundant use of lubricants, the wastage can be reduced along with the price of production. Some of the instances have proved that the cost of cutting fluids exceeds the cost of the tool (Klocke et al. 1997). The development of MQL was initiated because of economical and environmental concerns. In the modern manufacturing industries, the focus of the researchers is laid on the careful selection of the cutting fluids which eliminates all the issues faced by the workers (Sreejith and Ngoi, 2000; Sokovic and Mijanovic, 2001). The use of MQL is an attractive alternative in contrast with dry and flood lubrication methods to reduce the amount of fluid. By the effective use of MQL, surface quality, and tool life of the components can be improved. The benefits of MQL has led us to improve the surface quality of the product. Some of the benefits of MQL are yet to be explored. Hence an attempt has been made in this research work to explore the benefits of MQL during diamond burnishing of 17-4 PH stainless steel.

1.6 SIGNIFICANCE OF CRYOGENIC BURNISHING

The practice of sustainability principles in product development has become an emerging trend in manufacturing. The abundant usage of lubrication, cost, and energy consumption have become major sustainability concern. The cryogenic machining/burnishing is one of the commonly used technique which can improve the material properties. LN_2 has been

widely used in machining/burnishing as a reason for its availability. Usually, cryogenics has been referred to as the temperature of the liquid below 0 ˚C (Abelle and Schramm, 2008; De Chiffre et al. 2007; Dix et al. 2014). LN_2 can be produced by fractional distillation of liquid air (Yildiz and Nalbant, 2008). It is a non-toxic, environmentally friendly, and contributes to the sustainability aspects of manufacturing (Jayal et al. 2010). Nitrogen constitutes 79% of air and disperses into the air during burnishing. The maintenance issues, disposal, cleaning problems can be reduced by the successful use of LN_2. The liquid gases, namely carbon dioxide, helium, and nitrogen can be used for burnishing as a substitute for oil or water-based lubricants (Jawahir et al. 2016).

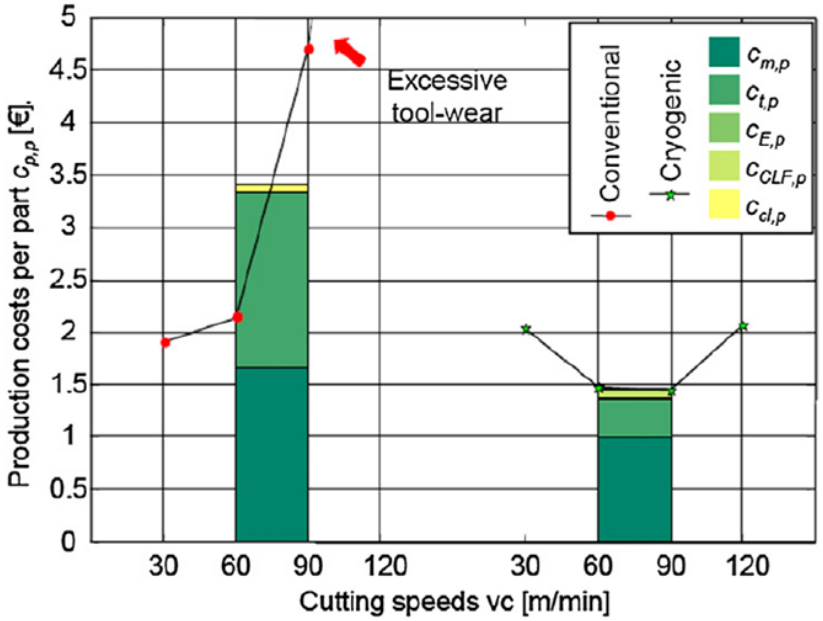

Figure 1.10 Comparative study of cryogenic and conventional machining (Jawahir et al. 2016).

Cryogenic burnishing can alter the performance characteristics of the material and the tool. Lower temperature yields improved hardness, the toughness of tool material, higher productivity, and lower energy consumption. Recent studies on cryogenic machining reveal a significant enhancement in the corrosion resistance, wear and fatigue strength (Jayal et al. 2010; Kaynak et al. 2014; Pu et al. 2012a; Pu et al. 2012b). Furthermore, it can

dissipate the heat generated at the burnishing zone (Dillon et al. 1990; Hong and Ding, 2001a; Hong and Zhao, 1999). Cryogenic burnishing can yield an engineered surface by minimizing the damage to the external surface of the component. A comparison study has shown that conventional machining is more expensive than cryogenic machining as framed in Figure 1.10. A recent technology of hybrid cooling, which includes a small quantity of MQL and LN_2 has proved to be a better choice to improve the functional performance of the product. Table 1.1 shows the effect of various lubrication methods and their advantages.

Table 1.1 Effect of lubrication (Jawahir et al. 2016).

Effects of cooling and lubrication strategy	**Flood**	**Dry**	**MQL**	**Cryogenics**	**Hybrid**
Cooling	Good	Poor	Marginal	Excellent	Excellent
Lubrication	Excellent	Poor	Excellent	Marginal	Excellent
Chip removal	Good	Good	Marginal	Good	Good
Machine cooling	Good	Poor	Poor	Marginal	Good
Workpiece cooling	Good	Poor	Poor	Good	Good
Dust/particle control	Good	Poor	Marginal	Marginal	Good
Product quality	Good	Poor	Marginal	Excellent	Excellent

1.7 PRECIPITATION HARDENABLE STAINLESS STEEL

The materials which cause more tool wear, heat, cutting force, and poor surface finish during machining processes are termed to be difficult to machine materials. Some of the difficult to cut materials such as titanium alloy, precipitation hardenable stainless steel has high strength, high hardness, excellent corrosion resistance, and low thermal conductivity. Hence, these materials have various industrial applications which involve marine, automobile, aerospace, chemical and nuclear, etc. (Shokrani et al. 2012). In several critical applications such as chemical, food processing, petrochemical, and aerospace, the most indispensable materials are precipitation hardenable stainless steels, namely PH 13-8 Mo, 17-7 PH, and 17-4 PH (Kochmański and Nowacki, 2006; Mohanty et al. 2016). The PH

stainless steel is one of the interesting family of steels which can attain hardness up to 49 HRC. Out of these family of stainless steels, 17-4 PH stainless steel has attracted engineers across the world on account of its superior strength and corrosion resistance which is not possible to find in any of the steel grades (Mirzadeh et al. 2009). Owing to low thermal conductivity, high strength and admirable wear resistance properties, it has been classified under hard to machine materials. It develops more adhesion wear on the tool. It is a special type of PH martensitic stainless steel which consists of martensite and along with a small quantity of austenite. Strengthening of this steel can be performed by precipitation of copper-rich phases in the martensitic matrix through the aging process and a simple solution treatment (Mirzadeh and Najafizadeh, 2009). In recent years the critical components which are being used in the aircraft engines have been replaced with 17-4 PH stainless steel in place of titanium alloys and polymeric composite materials because these components will be subjected to high cyclical thermal and mechanical loads. In the meanwhile, improved fatigue strength and surface integrity are expected in such kind of heavy duty components (Wang et al. 2011; Liu et al. 2016). Compressor blades of steam turbines are subjected to high temperature, high vibration, and formation of high stresses. These issues can cause damage to the engine. Hence, it could be a better choice to be used for the first set of aerospace compressor blades to avoid the problems arising due to foreign object damage. Machining of such kind of steels results in poor surface quality and also the cost involved for production is more. Hence to obtain the superior surface characteristics of the difficult to cut material, it is essential to cool the tool-workpiece interface with lubricant/coolant to reduce the temperature generated during burnishing.

1.8 OPTIMIZATION AND MODELING TECHNIQUES

The conventional methods of optimization are tedious and challenging to use. To minimize the effort needed to design the experiments, Taguchi method has been used (Phadke, 1989; Ross, 1996). Besides, to reduce the complication in number of experiments, this method has been extensively used. The effects of the control variables will be understood by the simple orthogonal array design and a minimum set of experiments (Taguchi, 1986). It uses a parametric design which yields the optimum process variables along with the quality of

the performance with the minimum possible noise deviation. TGRA is considered to be one of the scientific methods to solve a multi-objective problem. In this method, the multi-objective optimization of the output responses can be performed. The grades of the grey relation define the optimal control setting for the process to obtain improved functional performance of the product. Analysis of variance (ANOVA) yields the significance of each term used in the process.

The quality of the surface plays a significant role in defining the life of the manufactured component. To achieve superior quality surface, the parameter setting and the prediction of the dimensional properties are important by theoretical modeling (Sahin and Motorcu, 2004). RSM is an effective modeling technique which helps in predicting the responses by generating a regression equation (Ozel and Karpat, 2005). This technique reduce the time and cost, along with the interaction effect of the control variables (Montgomery, 2005). In general, a second-order model is used in RSM to determine the appropriate approximation for the functional relationship between the independent variables (Kwak, 2005; Montgomery, 2005). Various experimental designs can be selected based on the requirement of the process. The lower and upper limit will be defined as (−1, 1) in terms of coded factors.

To solve a multi-objective problem, a genetic algorithm (GA) is preferred to be the best-suited method. It is an adaptive heuristic search algorithm which works on the idea of survival of the fittest population amid the interbreeding population to generate a search strategy (Kumar and Sait, 2017). The conventional methods are found to be deterministic. Whereas, GA applies mutation and crossover functions amongst the created set of the population of solutions which yield the best solution to the problem. At each cycle, the weak generation fades away retaining strong off-springs. Depending upon the fitness values used, the different set of the selection procedure will be used in GA. The present investigation optimizes the control variables using the generated regression equation from RSM. The best optimal solution will be achieved to improve the functional performance of the component.

1.9 NEED FOR THE CURRENT INVESTIGATION

Surface integrity characteristics of a machined component are one of the most important factors which have to be considered seriously to improve the performance of the product. The poor performance of the product may lead to decreased productivity and quality of the engineered surface. Machining of 17-4 PH stainless steel is a challenging task because it causes more tool wear, which in turn affects the surface quality of the component (Mohanty et al. 2016). Manufacturing industries are facing difficulty in using conventional lubrication strategies because of the regulations, health issues, disposal, and environmental problems, etc. One of the most challenging tasks is to couple all these issues together to produce an improved performance of the product. Henceforth, the industries are constantly trying to improve productivity by introducing new sustainable manufacturing concepts. In continuation with the need of investigation as described in P-18-19, it is very much essential to perform a broad study on the diverse machinability perspectives. From the previous studies, it has been observed that inadequate literature is available on surface integrity investigation of diamond burnishing process under cryogenic, MQL, and dry environments. There are not many evidence present in the literature regarding the potential of diamond burnishing in improving the quality of the surface of 17-4 PH stainless steel. Hence there is a necessity to understand the effect of control factors on diamond burnishing of 17-4 PH stainless steel under cryogenic, MQL, and dry environments. To fulfill the requirements of the diamond burnishing process and to overcome the drawbacks faced by the manufacturers while using a conventional tool, a novel diamond burnishing tool has been used in the present investigation. To the author's knowledge, not many kinds of literature are available on diamond burnishing process with the proposed novel diamond burnishing tool. Hence, the main objective of the current investigation is to study the influence of control variables on surface integrity properties of 17-4 PH stainless steel under cryogenic, MQL and dry environments by a commercially available and novel diamond burnishing tool.

1.10 THESIS ORGANISATION

The outline of the thesis has been divided into the following sections:

Chapter 1

The current unit is associated with the introduction to the surface enhancement techniques, basics of burnishing, its applications in various fields, various cooling methods used in burnishing, difficult to cut materials used, various aspects of sustainable machining processes, significance of cryogenic cooling in machining and burnishing, need for the current investigation, outline of the thesis.

Chapter 2

This chapter presents a thorough literature review on burnishing methods, different cooling techniques used in burnishing, process parameters considered for burnishing, optimization, and modeling of the burnishing process parameters, scope, and objectives of the current study.

Chapter 3

The present division deliberates the detailed information of workpiece material, burnishing tools, methodology, experimental setup, different equipment's used for measuring performance characteristics during diamond burnishing.

Chapter 4

Chapter 4 is focused on the experiments conducted based on the one factor at a time approach (OFATA) by considering burnishing speed, burnishing feed and burnishing force as process parameters under MQL, dry and cryogenic cooling conditions using a commercially available diamond burnishing tool.

Chapter 5

This unit deliberates the experiments conducted based on OFATA by considering burnishing speed, burnishing feed, and burnishing force as process parameters under

sustainable cooling conditions using a novel diamond burnishing tool. Further, the experiments were extended to study the influence of additional process parameters such as the number of tool pass and diamond sphere diameter along with the major process parameters under cryogenic environment.

Chapter 6

The contemporary section discusses the determination of optimal process parameters for a single as well as multi-objective responses under the cryogenic environment using a novel diamond burnishing tool. Single objective optimization was carried out using Taguchi method and multi-objective optimization using Taguchi coupled Grey Relational Analysis (GRA).

Chapter 7

It presents the development of a mathematical model for each response, namely surface roughness and surface hardness using RSM under the cryogenic environment using a novel diamond burnishing tool. Further optimization has been carried out by a multi-objective genetic algorithm (MOGA).

Chapter 8

In this chapter, the conclusions have been drawn from the performance of diamond burnishing process in enhancing the surface integrity of the material. It also deliberates the future scope of work based on the current investigation.

CHAPTER-2

LITERATURE REVIEW

2.1 INTRODUCTION

This chapter presents a thorough review of the burnishing process performed on the widely used materials in various fields of manufacturing. Further, the influence of the control variables on the performance of diamond burnishing under varying working conditions has been defined clearly. Moreover, the effect of variables on the surface integrity characteristics of the material has been reviewed. A brief discussion on the modeling and optimization aspects of the burnishing process under varying lubrication condition has been presented.

2.2 DIFFICULT TO CUT MATERIALS

Based on the previous studies by various researchers, it was found that it is very difficult to classify the materials into difficult to cut materials by using a standard organization. Hence the definition of difficult to cut materials is still vague. However, on the basis of the findings from the literature, Shokrani et al. (2012) has categorized the difficult to cut materials into non-homogeneous materials, ductile materials, and hard materials. These three major classifications can be divided into subcategories, as depicted in Figure 2.1. The advances in manufacturing have led to improved functional characteristics of the materials. In the meanwhile, it also results in the difficulty of machining such kind of alloys. The properties which are responsible for the difficulty in the machining of materials are poor thermal conductivity, high strength, and high hardness (Zhang et al. 2010; Jaffery and Mativenga, 2009; Ezugwu et al. 2003). Another set of difficult to cut materials, namely low carbon steels and polymers exhibits high elongation and ductility. The major problems encountered while machining these kinds of materials are surface finish, geometrical accuracy and chip formation (Hong et al. 1999; Hong and Ding, 2001a; Kakinuma et al.

2008). Because of the short tool life and poor surface quality, composites are also categorized under difficult to machine materials. It is owing to the fact that composites are a combination of a different variety of materials which usually has different properties and also it is neither chemically combined nor homogeneous. Therefore it is difficult to describe the process variables to deal with a composite material during machining. The materials which encounter difficulty in chip formation produces more tool wear and cutting forces are termed as difficult to cut materials. Another major drawback of machining difficult to machine materials is a generation of high cutting temperature at the tool and workpiece interface.

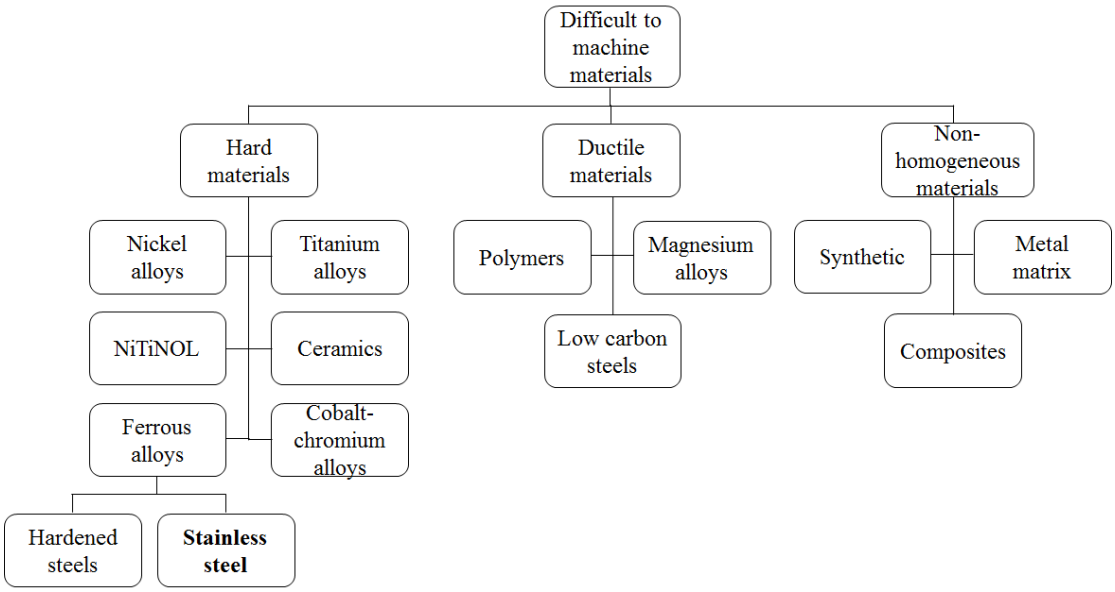

Figure 2.1 Organization of hard to machine materials (Sivaiah and Chakradhar, 2017).

To minimize the difficulties encountered during machining of difficult to machine materials, different kinds of lubricants/cooling techniques have been employed to reduce the temperature generated during burnishing. The effective utilization of coolant at the working zone plays a crucial role in removing the heat generated during burnishing. Proper selection of the lubricant leads to improved surface and subsurface characteristics of the material. The conventional fluids are not feasible for machining of difficult to cut materials. Hence there is a need to explore a better mode of lubrication/cooling method to machine

difficult to cut materials. Machining of difficult to cut material under dry condition has produced more tool wear and poor surface quality of the material (Mohanty et al. 2016). In the present investigation, cryogenic and MQL lubrication/cooling techniques have been employed.

2.3 EFFECT OF COOLING/LUBRICATION ON BURNISHING

The use of the sustainability principle in burnishing has been an emerging trend in the development of a superior quality product. The usage of various kinds of lubricants has been tried by many researchers to minimize the drawback faced by the manufacturers and to improve the productivity (Jawahir et al. 2016; Kaynak et al. 2014). Variety of coolants have been tried during machining to improve the quality of the machined surface. Some of the frequently used lubrication/cooling techniques are flood cooling, gas-based coolants, MQL, cryogenic cooling, etc. In recent years, MQL and cryogenic lubrication/cooling have been widely used due to its ability to mitigate the heat developed in the tool and workpiece interface. Caudill et al. (2018) have examined the influence of control variables on the surface integrity characteristics of the Ti-6Al-4V alloy. Four types of cooling/lubrication conditions such as flood cooling, MQL, LN_2, and hybrid cooling/lubrication (MQL+LN_2) were considered for studying the impact of lubrication on the surface integrity of Ti-6Al-4V alloy. It was proved that lubrication is an essential requirement in enhancing the surface integrity of the material after burnishing. However, improved results were obtained for the specimen which was burnished under hybrid cooling/lubrication condition. Revankar et al. (2014) have attempted to optimize the process parameters of the burnishing process. Ti-6Al-4V alloy was burnished under MQL environment. Taguchi technique was considered to optimize the control factors. The surface finish and surface hardness of the material were improved by 77% and 17% respectively after performing burnishing.

Yang et al. (2015) have attempted to study the surface characteristics of Co–Cr–Mo alloy burnished in the cryogenic environment. It was observed that the favorable phase structure was formed, which substantially increases the wear resistance of the specimen. Small grains which are reduced in size have been formed under the top surface layer, which is a

reason for an enhanced hardness of the material. According to Pu et al. (2011), cryogenic burnishing is a reason for the formation of ultrafine grains on the subsurface layer of the Mg–Al–Zn alloy. It was also revealed that the corrosion resistance of the specimen was enhanced after performing burnishing under the cryogenic environment. Yang et al. (2018) examined the impact of burnishing on corrosion film formation mechanism of Ti-6Al-4V alloy under cryogenic environment. Both burnished and unburnished samples were examined, and it was found that three oxide layer was formed in both the conditions. Burnished sample reveals a thicker subsurface layer in contrast with the unburnished sample. The cryogenic burnishing was concluded to be an efficient method to enhance the corrosion resistance of the material. Huang et al. (2015) proved that refined nano grains were formed during cryogenic burnishing on Al 7050-T7451 alloy. The hardness of the material was increased in a cryogenic environment when compared to a dry environment. It was reported that because of the impingement of LN_2 at the burnishing zone, the grains would be refined and which is a possible reason for the enhancement of hardness of the burnished sample. Pu et al. (2012b) investigated the influence of cryogenic burnishing on AZ31B Mg alloy and confirmed enhancement in corrosion resistance and surface hardness of the material. The surface characteristics of Ti-6Al-4V alloy was explored in a study conducted by Tang et al. (2017). The cryogenic burnishing was performed to reveal the influence of process parameters on the output responses. It was reported that the corrosion resistance of the material was enhanced by burnishing under cryogenic cooling and also it substantially improved the surface integrity characteristics of the material. Caudill et al. (2014) have conducted a study on the surface integrity characteristics of cryogenic burnished Ti-6Al-4V alloy. The surface finish, hardness, and residual stresses were improved. The grain refinement was also observed due to the impact of cryogenic burnishing.

2.4 EFFECT OF PROCESS VARIABLES ON BURNISHING

The basic requirement of burnishing is a proper selection of process variables for improving the surface quality of the component. It is believed that proper selection of the process variables leads to an improved productivity, which is an important factor to be

considered in the manufacturing industries. Moreover, an inappropriate selection may results in poor surface quality along with the poor surface integrity of the material. During the process, burnishing speed, burnishing feed, burnishing force, diamond sphere diameter, number of tool passes, and coolant/lubrication are used as the process variables. In the current investigation, diamond burnishing process has been performed, and all the process parameters which are mentioned above are considered to improve the performance characteristics of the material. Some of the performance characteristics considered for the present study are surface roughness, hardness, morphology, topography, subsurface microhardness, and residual stresses. Based on the relevant literature on this area of study, the surface integrity characteristics have been studied and are discussed in further subsections.

2.4.1 Influence of process variables on surface roughness

The surface roughness of the component is treated to be one of the most influential surface integrity characteristics. Controlling this parameter will result in improved fatigue life of the product. It is treated to be one of the important aspects in deciding the quality of a part. The effect of process parameters on surface roughness has been described by researchers in the literature by considering numerous materials. The roughness of roller burnished AZ80 magnesium alloy was observed to be decreasing with an upsurge in the burnishing force, and additional upsurge in the force yields a deteriorated surface finish. The burnishing force of 350 N was observed to be efficient in producing a better surface finish of the material (Zhang and Lindemann, 2005). Recently, Saldana-Robles et al. (2018) performed ball burnishing to understand the effect of process parameters on surface roughness and hardness of AISI 1045 steel. The burnishing force was found to have more influence in reducing the surface roughness and enhancing the hardness of the steel sample. The surface roughness was reduced to 0.61 μm, and hardness was enhanced to 236 HB. Okada et al. (2017) have developed a rotary tool which contains a diamond burnisher to burnish a flat or curved surface. It was concluded that surface roughness of 0.07 μm is possible to achieve with the newly developed tool.

In a study conducted by Maximov et al. (2017), surface roughness was analyzed for the variation in the process parameters, namely diamond sphere radius, burnishing force, burnishing feed rate, and burnishing velocity. The analysis was carried out for D16T aircraft aluminum alloy by performing slide diamond burnishing. Figure 2.2 depicts the variation of surface roughness for varying process variables. It was observed that the least surface roughness of 0.05 µm obtained by performing slide burnishing on the D16T aircraft aluminum alloy. Sequera et al. (2014) have conducted a thorough study on the influence of process parameters of ball burnishing on the surface roughness of Inconel 718. The size of the ball and pressure applied to the material were considered to be the significant parameters. It was found that the ball size of 12.7 mm diameter yields an improved surface finish. Whereas, the least surface roughness was recorded for pressure of 17.5 MPa. Further increase in the applied pressure resulted in a deteriorated surface finish of the material. In another evaluation of surface roughness by El-Taweel and El-Axir (2009), it was revealed that the process parameters play a crucial role in minimizing the surface roughness of a brass component by performing ball burnishing technique. It was found that burnishing feed and burnishing force were the major contributors in minimizing the surface roughness. Whereas, burnishing speed and number of tool passes were adjudged to be the insignificant factors in reducing the surface roughness. Further, El-Tayeb et al. (2008) have explored the influence of ball diameter and burnishing speed on the surface roughness of aluminum 6061 alloys. A specially designed tool with an interchangeable adapter for both roller and ball burnishing was used. It was observed that the surface roughness decreased to a minimum value when the burnishing speed was in the range of 160 to 440 rpm. If the burnishing speed was increased from 440 rpm, a deteriorated surface finish was noticed as shown in Figure 2.3. Grzesik and Żak (2014) have studied the state of surface integrity produced on 41Cr4 steel after hard turning and ball burnishing process. It was observed that the burnished sample was able to produce lower roughness in contrast with the hard turned specimen. Bougharriou et al. (2010) have carried out the analytical study and a finite element modeling on burnished AISI 1042. The compressive residual stresses were developed along with the improved surface finish of the sample. It was concluded that

burnishing is a beneficial process in improving the surface quality of the steel sample. Kuznetsov et al. (2015) have performed the numerical and physical modeling of nanostructuring burnishing to reveal the limiting values of the process parameters.

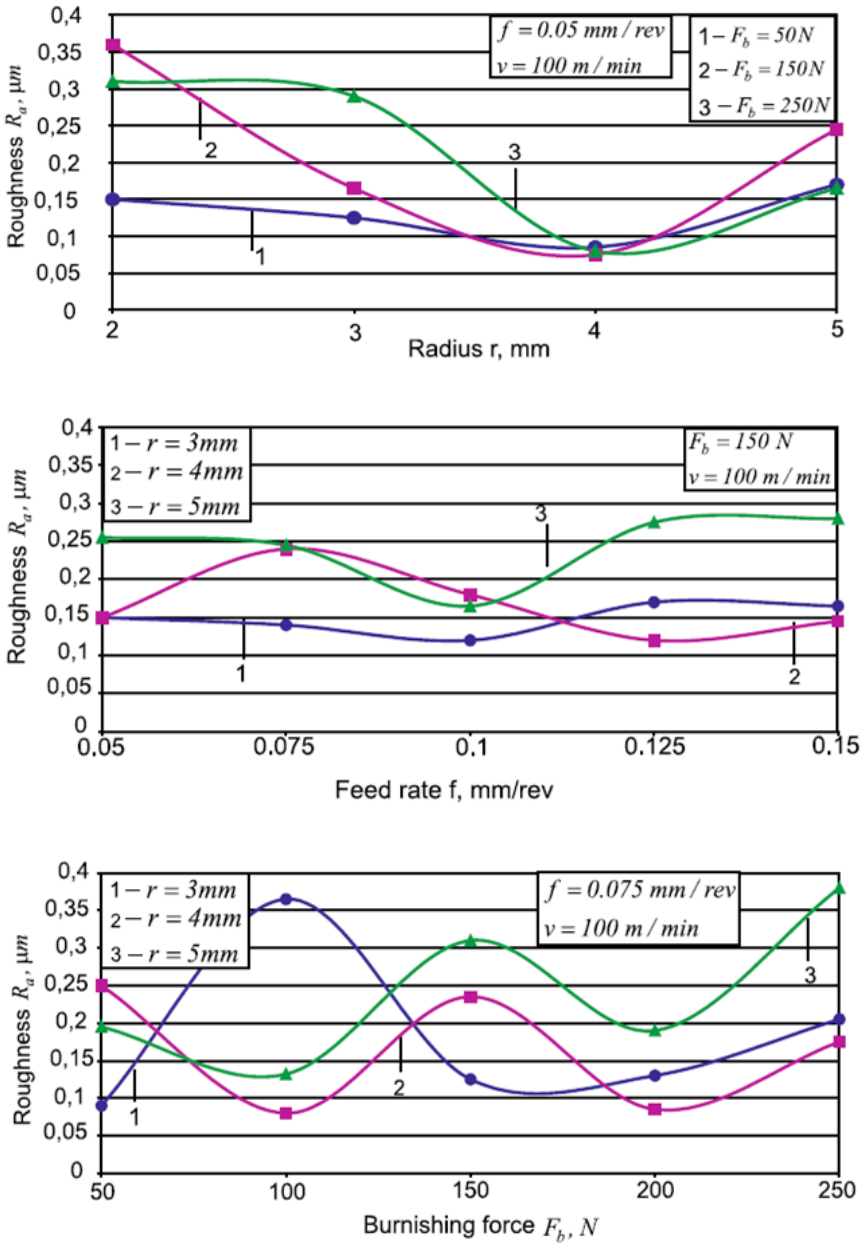

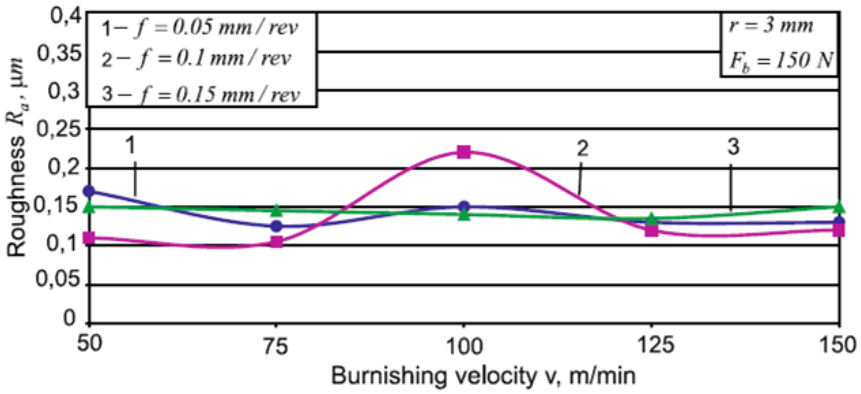

Figure 2.2 Surface roughness at varying process variables (Maximov et al. 2017).

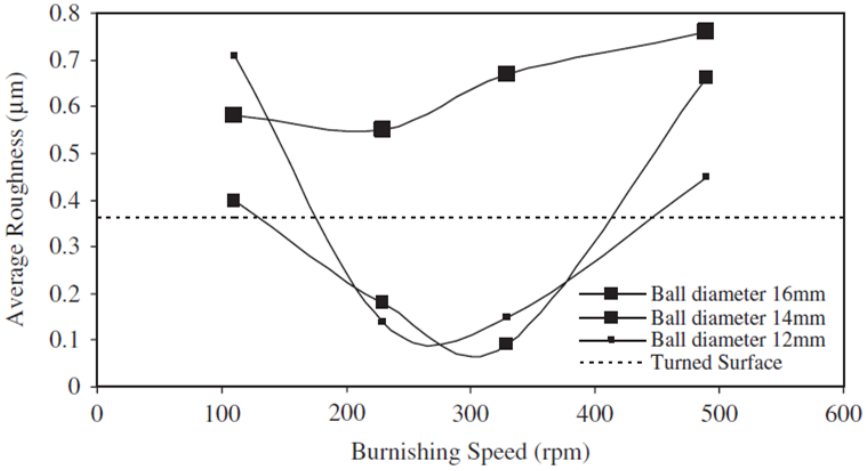

Figure 2.3 Average surface roughness observed at varying burnishing speed and ball diameter (El-Tayeb et al. 2008).

2.4.2 Influence of process variables on surface hardness

The surface hardness is treated to be one of the crucial performance characteristics of a material. In general, the resistance offered by the material to a localized plastic deformation induced by the tool is a measure of surface hardness. In the present study, the surface hardness is treated to be one of the important output response because after performing the burnishing process, the hardness of the material is expected to be improved. It is due to the effect of permanent plastic deformation taking place on the workpiece after performing the burnishing process.

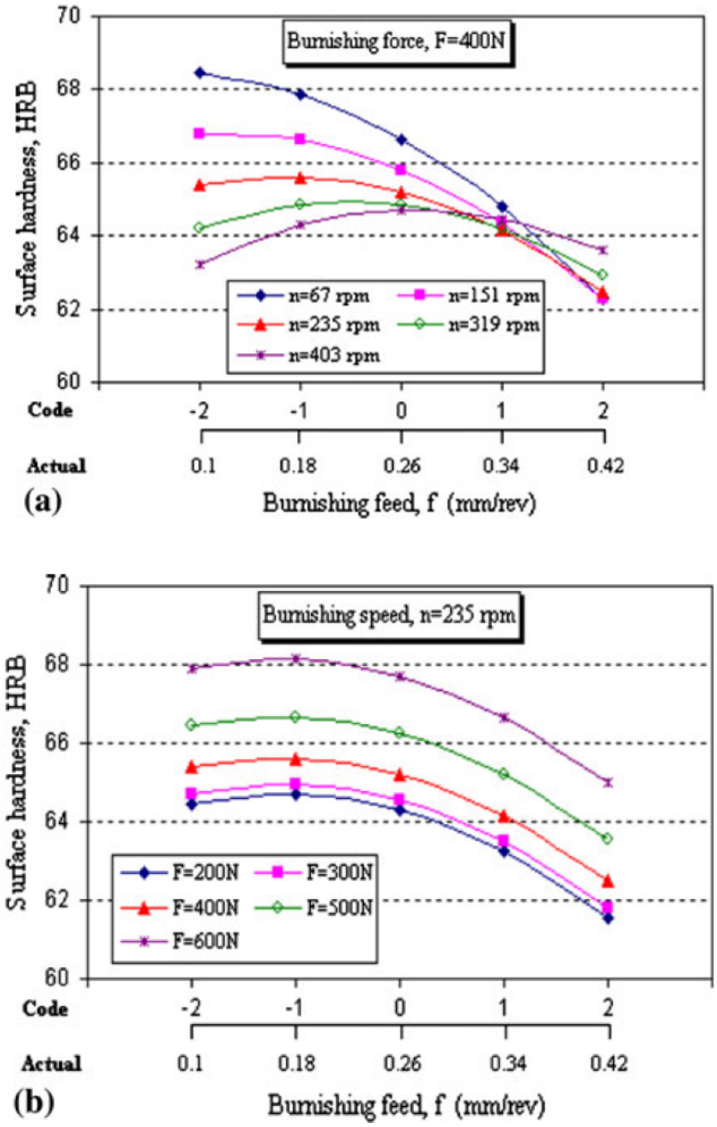

Figure 2.4 Surface hardness observed at varying burnishing feed with (a) constant burnishing force (b) constant burnishing speed (Gharbi et al. 2011).

According to Gharbi et al. (2011), the burnishing feed has an adverse effect on the surface hardness of AISI 1010 steel plates, which was processed by ball burnishing. It was found that the combination of low feed and increase in the burnishing speed substantially decreases the surface hardness. Meanwhile, at a fixed feed rate and increased burnishing force, the surface hardness of the specimen was observed to be increased, as illustrated in Figure 2.4. Hassan (1997b) have conducted ball and roller type burnishing on nonferrous

metals, the number of tool passes was considered as one of the process parameters in the study. It was observed that the surface hardness increases with an increase in the number of tool passes. It is owing to the fact that all metals will have their own considerable limitation for cold working condition.

Further, Al-Qawabeha (2007) carried out diamond burnishing and roller burnishing on carbon steel surfaces. Three different carbon steels such as low, medium, and high, were used. It was pragmatic that the diamond burnishing was able to produce exceptional microhardness in contrast with roller burnished sample. Maximum microhardness was achieved for high carbon steel. Luo et al. (2006) have attempted to study the influence of the process parameters of burnishing by using a cylindrical polycrystalline diamond tool. Aluminum alloy and brass were tested under the same working conditions. It was claimed that up to spindle revolution of 4000 rpm, the surface microhardness of the samples does not change. An increase in the spindle speed from 4000 rpm to 5000 rpm, the surface microhardness was found to be decreasing. According to Yuan et al. (2017), the surface microhardness of TA2 alloy continuously increases along with an increase in the pressure applied during low plasticity burnishing. That's because as the applied pressure rises, the plastic deformation also increases, which result in work hardening.

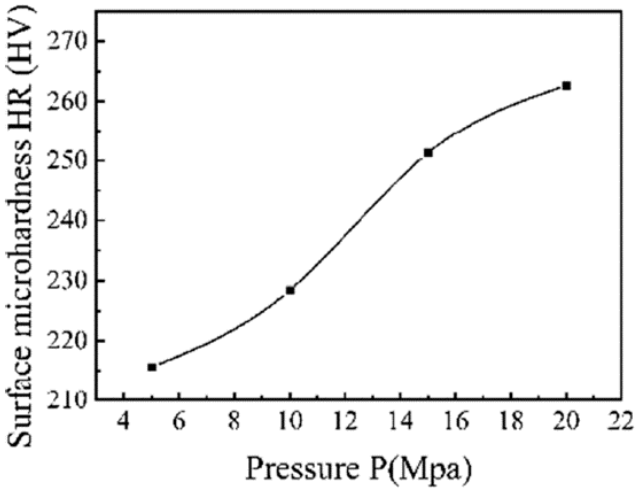

Figure 2.5 Surface microhardness for varying burnishing pressure (Yuan et al. 2017).

Figure 2.5 shows the impact of pressure on surface microhardness of the TA2 alloy. El-Khabeery and El-Axir (2001) have explored the importance of roller burnishing process parameters in improving the surface integrity of 6061-T6 aluminum alloy. It was found that the increase in the number of passes leads to enhanced surface microhardness and whereas, an increase in the burnishing speed causes a drastic decrease in the surface microhardness.

2.4.3 Influence of process variables on surface morphology

The surface morphology plays a dominant role in understanding the influence of burnishing process parameters on the workpiece. It is believed that a uniform surface will be generated on the top surface layer after performing burnishing. The formation of cracks, micro-voids, and feed marks on the specimen can be identified by a thorough analysis of the surface generated after burnishing. This could be achieved by observing the surface of the burnished specimen under a scanning electron microscope (SEM). Gharbi et al. (2012) have examined the top surface layer of the ball burnished specimen. Aluminum 1050A sheet was used to carry out ball burnishing operation. The surface morphology analysis was carried out for various process parameters to understand its effect on the work material. It was concluded that the application of high burnishing force has led to excess plastic deformation of the material and the traces of the ball was also identified from the SEM images shown in Figure 2.6. It depicts the formation of plastic deformation and ball traces on the surface of the material after performing ball burnishing.

Further, Amdouni et al. (2017) have compared the surface morphology generated by the machining and burnishing of 2017A-T451 aluminum alloy. It was pragmatic that the burnished surface was free from material tearing and scratches in contrast with the unburnished surface. The surface hardening was also observed, and the traces of the machining was removed while performing burnishing. Low and Wong (2011), have carried out ball burnishing on polyoxymethylene and polyurethane. The surface morphology results revealed that pile up and bulged edges were formed on the surface of the polymers after performing burnishing.

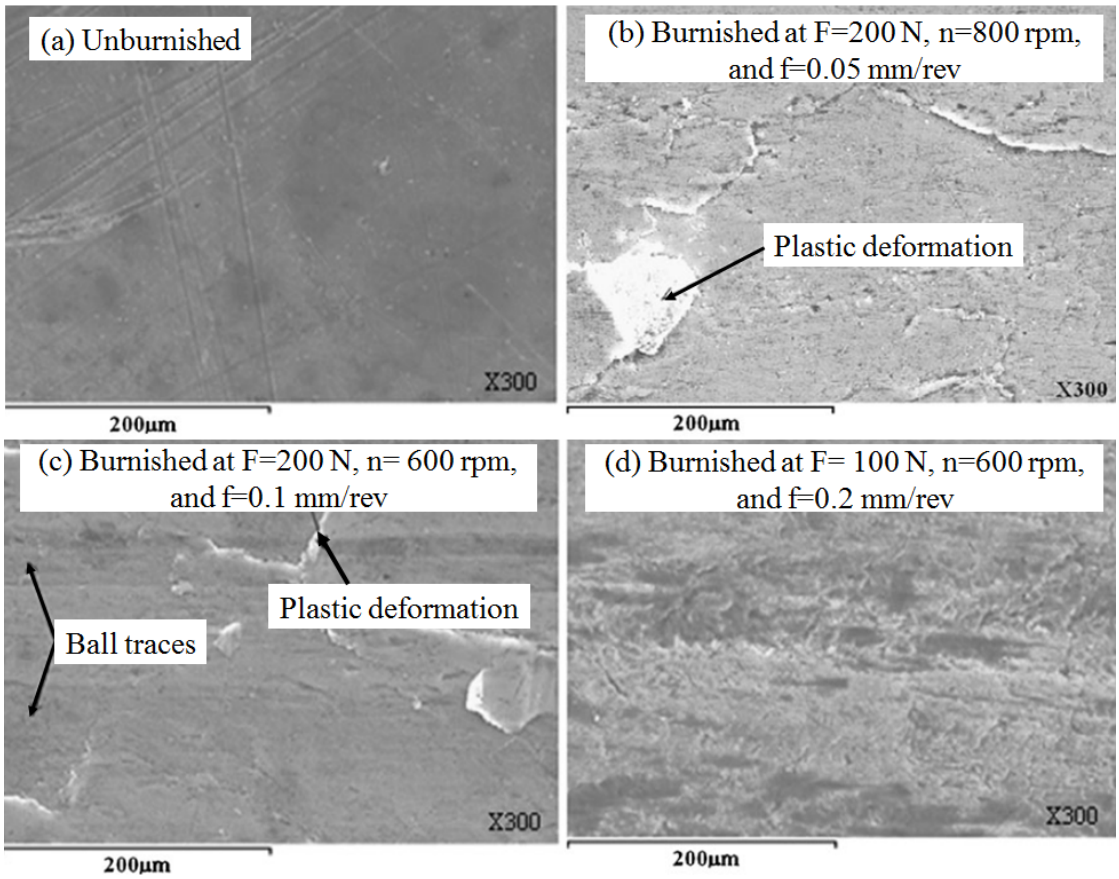

Figure 2.6 Surface morphology of ball burnished aluminum 1050A sheet (Gharbi et al. 2012).

The surface roughness of the specimen after burnishing was reduced to 0.44 µm in polyoxymethylene and 0.46 µm in polyurethane. Revankar et al. (2014) have exposed the influence of control factors while burnishing Ti–6Al–4V alloy. The surface morphology of the burnished surface was compared with a turned surface. It was concluded that rough texture characterized marks, profound grooves, sharp ridges, and feed marks were present over the turned surface. However, the sharp asperities were plastically deformed after performing burnishing, and the uniform surface was achieved. In another study conducted by El-Tayeb et al. (2008) shows that the ball burnishing of aluminum 6061 can remove feed marks, which will be generated after turning, as shown in Figure 2.7. The burnishing process was observed to be superior to turning process because it can plastically deform the material and in the meanwhile, due to this plastic deformation the scars can be removed.

It was also reported that among three different ball diameters such as 12 mm, 14 mm and 16 mm, the largest diameter produces deteriorated surface because of excessive plastic deformation of the material.

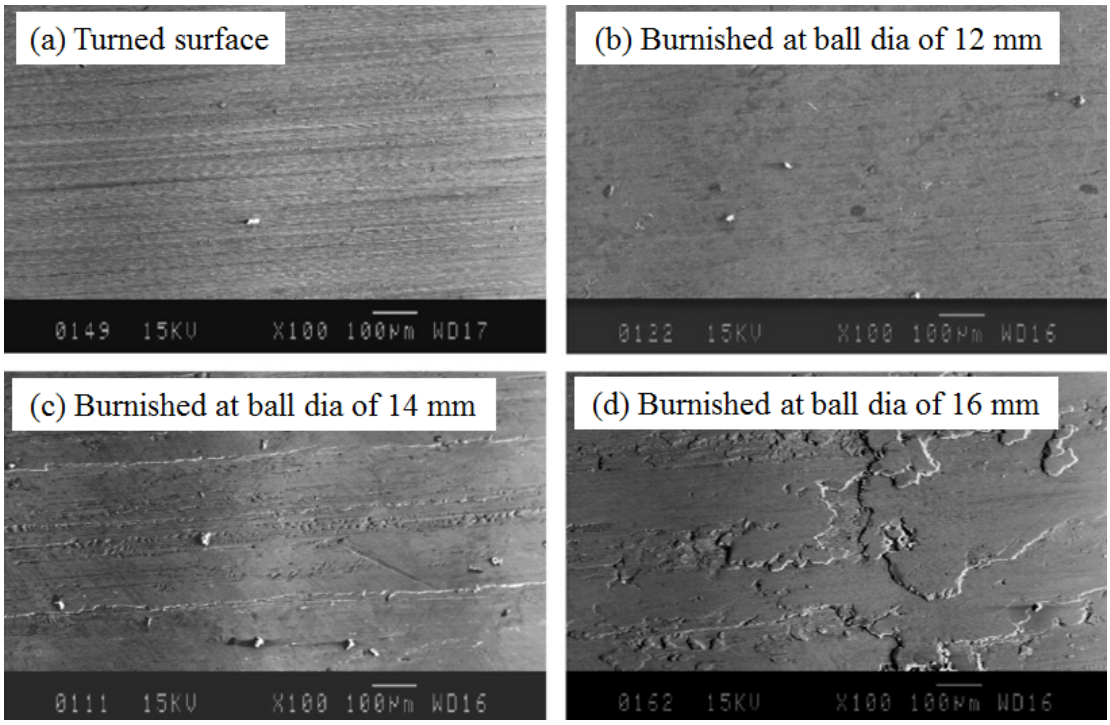

Figure 2.7 Surface morphology of ball burnished aluminum 6061 (El-Tayeb et al. 2008).

2.4.4 Influence of process variables on surface topography

The surface topography analysis has become increasingly important in tribology, machine condition monitoring, and materials. The surface topography analysis reveals the surface irregularities present over the diamond burnished surface. The surface topography of the burnished surface substantially affect the properties of the material. Recently, Denkena et al. (2017) have examined the surface topography of the hardened steel after burnishing and machining. After burnishing the surface intensity of the material was reduced in contrast with the machined surface. Hence it was concluded that burnishing is a better choice to improve the tribological properties of the hardened steel and also the surface roughness was drastically reduced after performing burnishing. The most affecting process parameter was observed to be burnishing pressure, overlap factor, and topography of the surface. In

a research work conducted by Zhang and Liu (2015) on Ni-based stainless steel have produced an improved surface topography of the specimen after performing low plasticity burnishing. Burnishing feed was optimized to improve the surface topography of the material. The rough surface was generated after performing turning operation with the conventional and wiper inserts. The burnishing process was able to produce a uniform surface with less peak to valley height when compared to turning. It is owing to the fact that after burnishing operation the material will be subjected to plastic deformation which results in the displacement of the material from peak to valley. Figure 2.8 shows the surface topography images obtained at four different conditions.

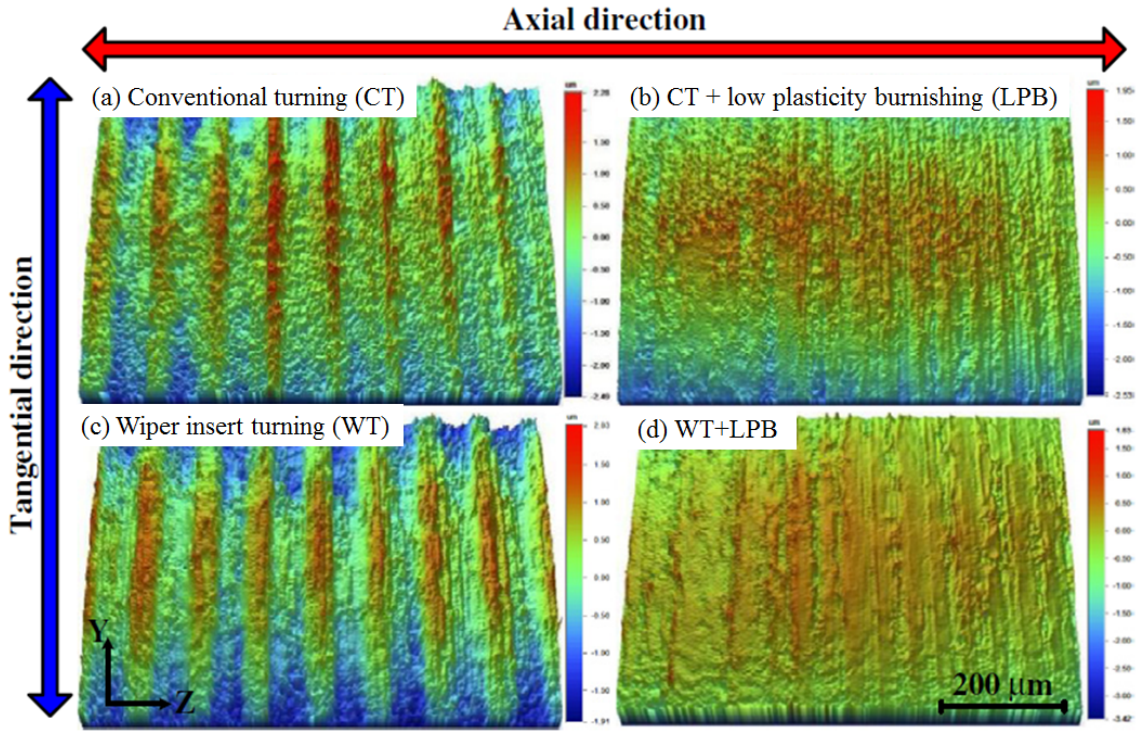

Figure 2.8 Surface topography observed for Cr–Ni-based stainless steel (Zhang and Liu, 2015).

Also, Swirad (2011) have investigated the influence of diamond burnishing process parameters on the surface topography of 42CrMo4 steel. It was perceived that the surface topography height was reduced due to the diamond burnishing process. The amplitude

parameter values were observed to be in the range of Sa=0.0497 to 0.185 µm, St=0.532 to1.84 µm, Sz=0.49 to 1.71 µm. The highest height observed for a small tool diameter of 4 mm was in the range of Sa=0.132 to 0.185 µm. Yuan et al. (2016) explored the impact of roller burnishing variables on TA2 alloy. Burnishing speed was observed to be the most influencing parameter followed by burnishing depth and burnishing feed. The optimization studies showed that the surface irregularities were reduced during burnishing at the optimal process parameters. Figure 2.9 demonstrates the surface topography obtained before and after optimization of the process parameters.

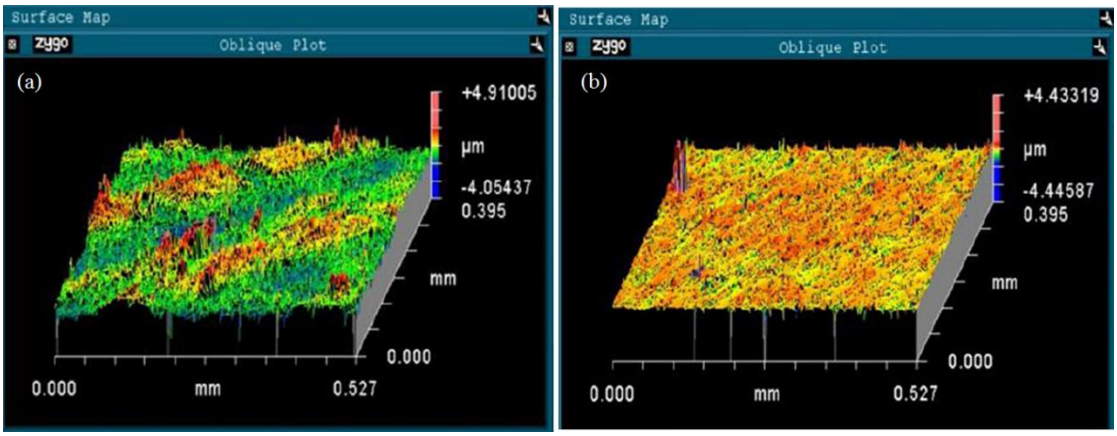

Figure 2.9 Surface topography observed (a) Before optimization and (b) After optimization (Yuan et al. 2016).

Recently, Korzynski et al. (2018a) have explored the importance of diamond burnishing in improving the surface texture of the valve stems made of 317Ti steel. Based on the results, it was stated that diamond burnishing is a better technique to form a surface texture of increased bearing capacity. Steep pits and protrusions were reduced after performing the diamond burnishing process. The flattened surface was also obtained with reduced surface peaks. Nestler and Schubert, (2015) have worked on slide diamond burnishing of aluminum alloy AA2124 as a matrix material and SiC particles with a volume proportion of 25%. The diamond sphere radius and burnishing feed were considered as the most important process parameters. The wavy surface structure with rounded valleys was observed due to the diamond burnishing. Burnishing feed of 0.05 mm/rev and a diamond

sphere radius of 1 mm was proved to be essential to obtain a regular surface in contrast with a premachined surface.

2.4.5 Influence of process variables on subsurface microhardness

While performing burnishing, the appropriate selection of the burnishing control variables plays a vital role in inducing an improved surface and subsurface hardness of the material. It is believed that the application of burnishing process parameters at a significant level produces the repeated plastic deformation of the material which also results in work hardening. It was also proved by most of the researchers that the grains beneath the top surface layer of the material would be affected and the reduction in the grain size could be observed due to the repeated plastic deformation. It might be the reason for the microhardness improvement at the subsurface layer up to a particular depth from the top surface layer (Babu et al. 2011). Recently, Maximov et al. (2017) have studied the influence of the number of passes on the microhardness of the D16T aircraft aluminum alloy. Two working schemes were tried by the authors to understand the influence of the number of passes on subsurface microhardness of the material. One way scheme has produced maximum microhardness after the first pass, whereas in two way scheme the microhardness was found to be increasing with an increase in the number of passes. It was due to the fact that in one way scheme the softening effect was observed to be more pronounced. In another work conducted by Yuan and Li (2017) showed that the burnishing process carried out on TA2 alloy could improve the subsurface microhardness of the specimen. It was observed that the highest microhardness was observed just beneath the top surface layer of the specimen. The microhardness variation observed was due to the fact that the heat and the strain effects are neutralized for the bulk material. This is the evidence for the formation of a compressive layer and a work hardened surface after performing burnishing. Yang et al. (2011) compared the subsurface microhardness of Co-Cr-Mo biomedical alloy after performing burnishing under dry and cryogenic conditions. It was observed that the subsurface microhardness followed a decreasing trend in both the environments as depicted in Figure 2.10. It was proved that 87% improvement of

subsurface hardness was possible to achieve under cryogenic burnishing in contrast with the dry condition.

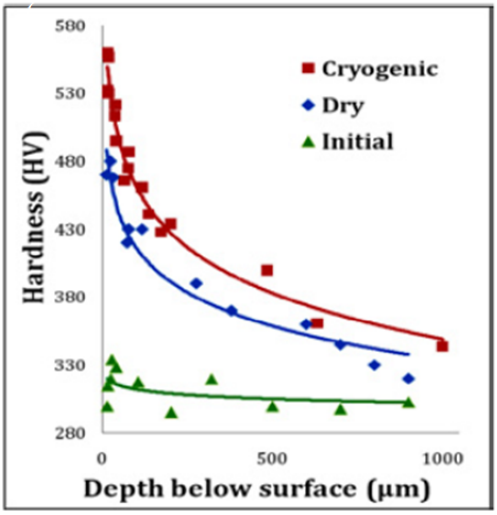

Figure 2.10 Subsurface microhardness observed at the initial, dry, and cryogenic conditions (Yang et al. 2011).

In an evaluation of the burnishing process on ultrasonically assisted ball burnishing of AA6061-T6 alloy performed by Teimouri et al. (2018) showed that the burnished sample yields improved subsurface hardness just beneath the burnished surface. A comparison was made between the conventional and ultrasonic assisted burnishing. It was proved that ultrasonic burnishing had produced improved hardness when compared to conventional burnishing as portrayed in Figure 2.11. Sai and Lebrun, (2003) have compared the performance of burnishing and grinding on surface characteristics of duplex stainless steel. It was noticed that the burnished sample was able to yield improved subsurface hardness along the depth in contrast with a ground sample, it was because of the effect of work hardening. Also, it was observed that the depth of penetration of grinding was 35 µm, whereas it was 75 µm in the case of burnishing. Caudill et al. (2014) have performed a study on burnishing of Ti-6Al-4V alloy under the cryogenic, flood, and dry conditions. One of the important process parameter, namely preload, was considered for the study, and it was varied by keeping all other parameters as a constant. It was seen that a preload of

2500 N under the cryogenic environment had produced improved subsurface hardness of the Ti-6Al-4V alloy.

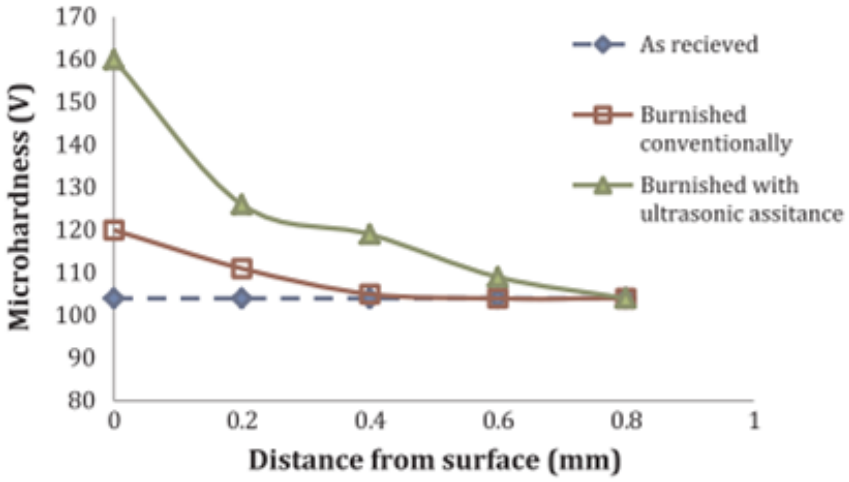

Figure 2.11 Subsurface microhardness observed at the initial, dry, and cryogenic conditions (Teimouri et al. 2018).

2.4.6 Influence of process variables on residual stress

Residual stress analysis is important because the fatigue life of the component depends on its inducement. The functional performance of a component can be substantially determined by the physical state of the surface, and the distribution of residual stress near the burnished surface is treated to be one of the significant parameters. Recently, sequential turning and burnishing process was carried out on a cold spray 17-4 PH stainless steel by Sova et al. (2017). It was found that the cold spray sample which was subjected to turning and burnishing has produced compressive residual stresses. Whereas, the turned sample was able to produce tensile residual stresses. Chomienne et al. (2016) have studied the influence of burnishing on surface integrity characteristics of 15-5 PH martensitic stainless steel. The residual stresses were measured in axial and tangential directions, as depicted in Figure 2.12. It was observed that the sequential turning and burnishing had produced compressive residual stresses in both directions. It was concluded that the burnishing velocity does not influence the formation of residual stresses. However, feed and number of passes have a limited effect on the formation of residual stress. An exclusive study was

conducted by Radziejewska and Skrzypek, (2009) on slide burnishing of laser alloyed and burnished steel. It was noticed that the multiple path laser alloying treatment was able to produce tensile residual stress of 500 MPa at the surface. Multiple alloying with burnishing has produced compressive residual stress of -600 MPa at the surface. Hence, the slide burnishing was proved to be essential to obtain compressive residual stresses at the surface.

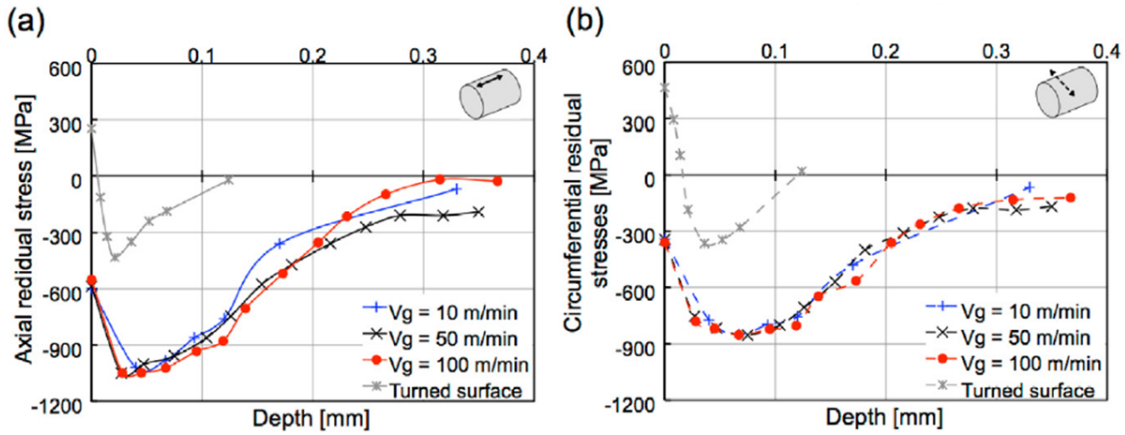

Figure 2.12 Effect of burnishing velocity on residual stress in (a) Axial (b) Circumferential directions (Chomienne et al. 2016).

Further, Pu et al. (2012a) have examined the influence of lubrication/cooling on residual stress of AZ31B Mg alloy during burnishing. The axial residual stresses were found to be more compressive than circumferential residual stresses. It was perceived that the application of more burnishing pressure resulted in the formation of tensile residual stresses. In the case of cryogenic burnishing, forces will be small, which led to the largest compressive residual stress inducement, as shown in Figure 2.13. Aviles et al. (2013) showed the inducement of compressive residual stresses during the burnishing of medium carbon AISI 1045 steel. It was confirmed that the compressive residual stress of -600 MPa was induced in the longitudinal direction and -300 MPa in the tangential direction. Salahshoor and Guo, (2011) performed burnishing on MgCa alloy to study the influence of process parameters on residual stress. Four process parameters such as pressure, feed, speed, and pattern were considered for the study. It was observed that among all the process parameters, pressure plays a key role in inducing maximum residual stress. Further, Prevey

and Cammett, (2001) have explored the influence of burnishing in improving the fatigue strength of the aluminum alloy 7075-T6. It was proved that the formation of compressive residual stress during burnishing would be able to improve the fatigue strength of the material. Hence it was suggested to use burnishing as a secondary finishing process to obtain compressive residual stress of the material.

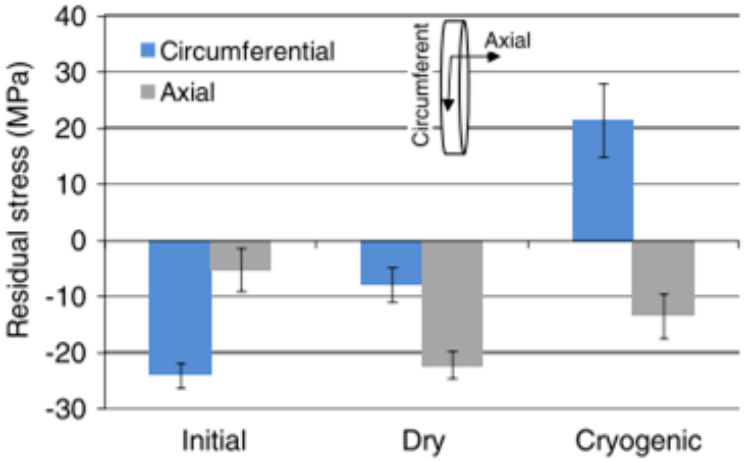

Figure 2.13 Effect of lubrication/coolant on residual stress (Pu et al. 2012a).

2.5 INFLUENCE OF BURNISHING TOOLS

It is believed that the most influencing factor during burnishing is the selection of a suitable tool for enhancing the productivity of a component. The size, shape, radius of the ball, the spring actuation mechanism, and the material used are the important factors to be considered while designing a burnishing tool. There are three major kinds of burnishing tools available, they are ball burnishing, roller burnishing, and slide/diamond burnishing tool. Most of the research work performed on burnishing shows that the burnishing tool plays a significant role in improving the surface integrity characteristics of the material. The present investigation focuses on slide/diamond burnishing of 17-4 PH stainless steel. Recently, Hiegemann and Tekkaya, (2018) have developed a new rotating ball burnishing tool which can perform burnishing at a constant applied burnishing force even on wavy edges, as shown in Figure 2.14. When compared to the conventional tool, improved surface

characteristics of the material was achieved. It was also revealed that working at high velocities resulted in better finishing of the surface of the material.

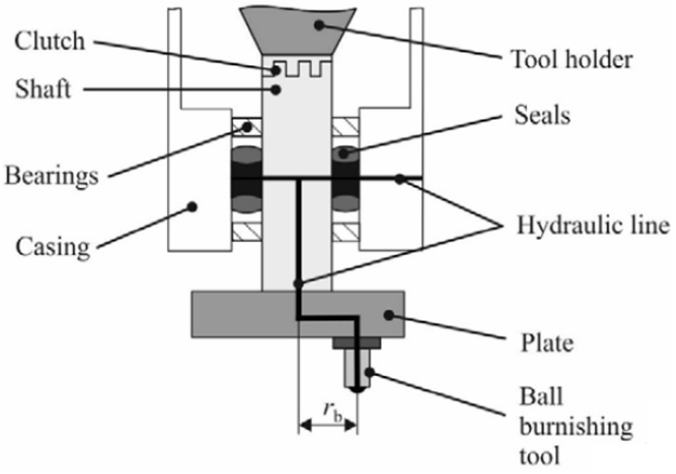

Figure 2.14 Rotating ball burnishing tool (Hiegemann and Tekkaya, 2018).

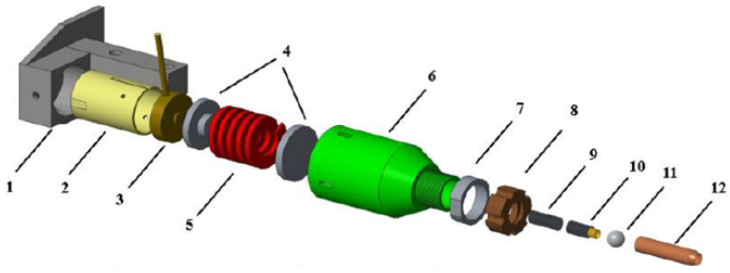

1	Tool holder	5	Spring	9	Push rod
2	Inner cover	6	Outer cover	10	Ball holder
3	Load cell	7	Collect chuck (L)	11	Burnishing ball
4	Spring block	8	Collect chuck (R)	12	Ball cover

Figure 2.15 Newly designed ball burnishing tool (Shiou et al. 2017).

Yu and Wang, (1999) have deliberated the influence of process variables on the surface roughness of an aluminum alloy which was undergone burnishing using a spherical surfaced polycrystalline diamond tool. It was observed that the new tool was successfully implemented to reduce the feed marks on the material after turning process, and the surface roughness was reduced to 0.026 µm. Further, Travieso-Rodríguez et al. (2015) have

performed ball burnishing on aluminum A92017-T4 alloy. The tool was made to vibrate with a new vibrating module attached to the ball burnishing tool. It was found that the vibration assisted tool was successful in reducing the surface roughness of the specimen, along with a reduction in the processing time. John and Vinayagam, (2011) have designed a new ball burnishing tool which has a facility to interchange the springs. Tool steel T215Cr12 was tested to check the adequacy of the newly designed tool. It was noticed that the surface roughness was reduced to 0.055 µm, and surface hardness was enhanced to 46.69 HRC.

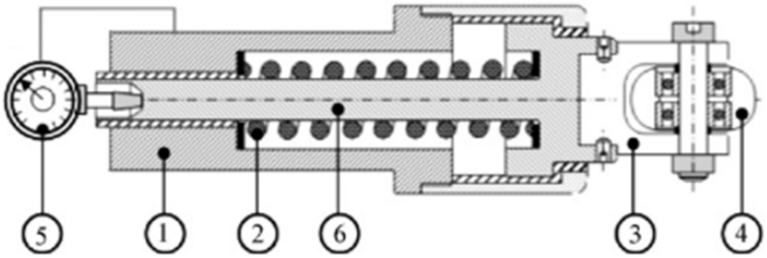

1	Shank	4	Roller
2	Spring	5	Dial gauge
3	Roller adapter	6	Spring guide

Figure 2.16 Detailed sectional view of roller burnishing tool assembly (El-Tayeb et al. 2007).

In a study conducted by Shiou et al. (2017) on SUS420J2 stainless steel showed an improvement in the surface finish from 1.1 to 0.025 µm and hardness from 51 to 52.5 HRC. A new ball burnishing tool was developed, as shown in Figure 2.15. A load cell was embedded within the tool to measure the applied thrust force. Okada et al. (2015) have used a novel roller burnishing technique which can perform simultaneous rolling and slide burnishing to substantially enhance the material properties. It was proved that thrust force and feed rate are the most influencing process parameters on the surface integrity of aluminum-based alloy, ASTM 2017 and carbon steel, ASTM 1055. In another recent work performed by Okada et al. (2017) shows the effectiveness of the diamond burnishing process with a rotary tool. It was designed in such a way that the flat and curved surfaces

were easily burnished to achieve a superior surface quality of the materials. It was concluded that a high-quality surface, uniform profile, and high glossiness could be possibly achieved with ease even for hard materials.

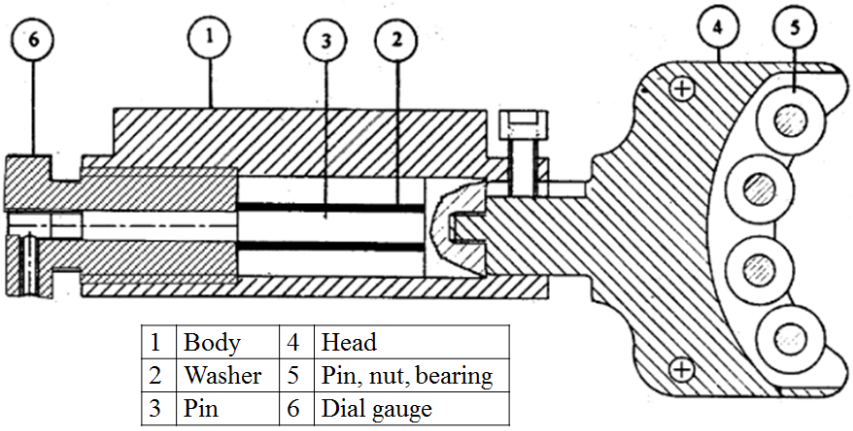

1	Body	4	Head
2	Washer	5	Pin, nut, bearing
3	Pin	6	Dial gauge

Figure 2.17 Four roller burnishing tool (El-Axir and El-Khabeery, 2003).

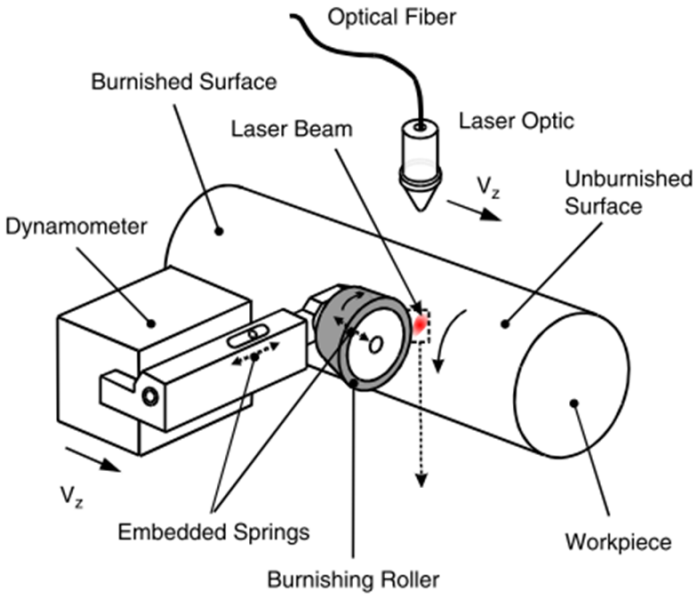

Figure 2.18 Experimental setup of laser-assisted burnishing (Tian and Shin, 2007).

In a study conducted by Shiou et al. (2017) on SUS420J2 stainless steel showed an improvement in the surface finish from 1.1 to 0.025 µm and hardness from 51 to 52.5 HRC. A new ball burnishing tool was developed, as shown in Figure 2.15. A load cell was

embedded within the tool to measure the applied thrust force. Okada et al. (2015) have used a novel roller burnishing technique which can perform simultaneous rolling and slide burnishing to substantially enhance the material properties. It was proved that thrust force and feed rate are the most influencing process parameters on the surface integrity of aluminum-based alloy, ASTM 2017 and carbon steel, ASTM 1055. In another recent work performed by Okada et al. (2017) shows the effectiveness of the diamond burnishing process with a rotary tool. It was designed in such a way that the flat and curved surfaces were easily burnished to achieve a superior surface quality of the materials. It was concluded that a high-quality surface, uniform profile, and high glossiness could be possibly achieved with ease even for hard materials. Further, El-Tayeb et al. (2007) developed a roller burnishing tool to burnish Aluminum 6061 workpiece as represented in Figure 2.16. Figure 2.17 shows a new four roller burnishing tool which was designed and fabricated to study the surface characteristics of the Aluminum 2014 and brass components by El-Axir and El-Khabeery, (2003). Tian and Shin, (2007) proposed a novel roller burnishing tool and experimental investigation was performed to reveal the influence of laser-assisted burnishing on AISI 4140. The experimental set up is as framed in Figure 2.18. It was proved that the tool was successful in yielding improved surface finish, higher surface hardness and similar compressive residual stress compared to its conventional counterpart.

2.6 ADVANCEMENT IN BURNISHING

Over the last few decades, burnishing has been emerged as an excellent superfinishing technique in manufacturing industries. Diamond burnishing is a new technology in the field of superfinishing method, which has the capability of finishing even the hard materials to obtain superior surface quality. Hence the researchers all over the globe are exploring the importance of using burnishing in the manufacturing industries. Recently, Salahshoor et al. (2018) developed a synergistic cutting-burnishing set up to enhance the corrosion resistance of MgCa0.8 alloy. The surface integrity properties such as surface finish, hook-shaped compressive residual stress, strain hardening, and grain size were improved after performing burnishing. Toboła and Kania, (2018) used slide/diamond burnishing as a pre-

nitriding treatment on sverker 21 and Vanadis 6 tool steel. The experimental findings proved that slide burnishing significantly alters the phase composition of the surface layers of both the materials. Another work presented by Nestler and Schubert, (2018) showed an improvement in surface finish and compressive residual stress after performing roller burnishing on particle-reinforced aluminum matrix composites. Korzynski et al. (2018a) have worked on the equilibrium surface texture of valve stems. It was observed that the improved surface characteristics of the component were achieved after performing slide burnishing.

Also, Avilés et al. (2019) have compared the effect of low plasticity burnishing and shot peening on the fatigue strength of 34CrNiMo6 steel. The surface roughness of low plasticity burnishined sample was 0.08 µm, and after shot peening, it was observed to be 1.41 µm. It was also seen that improved surface texture was observed for low plasticity burnished sample in contrast with a shot peened sample. Further, Hemanth et al. (2018) designed and fabricated a new roller burnishing tool to improve the performance characteristics of aluminum 6061. Surface finish and surface hardness of the material was enhanced with minimum time. Jerez-Mesa et al. (2018) developed a new vibration assisted ball burnishing tool to modify the surface integrity of Ti-6Al-4V alloy. The impact of vibration was proved to be essential to improve the surface texture of the material. The preload and number of passes were determined to be important process parameters in modifying the surface integrity properties. In another research work performed by Korzynski et al. (2018b) on 317Ti stainless steel by slide diamond burnishing have revealed the possibility of obtaining an improved surface texture of the material. The influence of process parameters on surface texture was investigated by using regression analysis. It was concluded that slide burnishing is a better technique to improve the surface texture of the 317Ti stainless steel.

2.7 MODELING AND OPTIMIZATION OF BURNISHING PROCESS

The burnishing process is treated to be highly nonlinear because of the deformation, material, and the boundary conditions involved in the contact region of the tool and the

workpiece. Hence, it is essential to develop a correlation model between the output responses and the process parameters to understand the mechanism involved in burnishing. To obtain an improved performance characteristic, it is also necessary to perform optimization of the burnishing process parameters. Researchers have optimized the control factors of the burnishing using various optimization techniques and performed mathematical modeling to predict the output responses. Quality and productivity are the two major factors which have to be considered seriously in the production sectors. Proper selection of the control variables leads to a good quality product. One of the scientific techniques which have been effectively used to solve the multi-objective optimization problem is TGRA. In recent times, Sachin et al. (2018a) have optimized the control variables of diamond burnishing performed on 17-4 PH stainless steel. It was observed that at the optimized control factors improved surface hardness and surface finish was obtained. Thorat and Thakur, (2018) have optimized the process parameters during roller burnishing of aluminum 6061. GRA was used to optimize the process parameters. The significance of the process parameters was analyzed by ANOVA. Further, Banh and Shiou, (2016) have investigated the influence of ball burnishing process parameters such as step over, number of passes, lubricant, speed, and force on STAVAX material. The optimal process parameters were obtained using GRA.

The performance index used in the burnishing process significantly gets affected by the input parameters. Hence there is a need to develop a correlation model between them. One of the most commonly used statistical technique is RSM. Hassan et al. (1998) have established a correlation model between force, and the total number of tool passes with surface roughness by RSM. El-Axir et al. (2008) have designed the experiments using RSM with central composite design (CCD) to investigate the surface finish of 2014 aluminum alloy using ball burnishing technique. El-Taweel and Ebied, (2009) have developed a novel method to increase surface microhardness and reduce roundness error in roller burnishing and the optimum control factors in burnishing were obtained by RSM method. El-Khabeery and El-Axir, (2001) have explored the optimal process parameters of roller burnishing on the base of RSM with CCD. Yuan et al. (2016) have performed modeling of process

parameters and their responses in roller burnishing of TA2 alloy using RSM. The technique was successfully implemented to obtain an improvement in the performance of the component. Recently, Patel and Brahmbhatt, (2017) have used the CCD of RSM to carry out the optimization of roller burnishing control factors on Aluminium alloy 6061. Further, Kumar and Sait, (2017) have used CCD design to perform optimization of machining factors. Regression analysis was also performed to find the relation between input parameters and the responses. Suresh and Venkateswara, (2005) have incorporated RSM to predict the surface finish of the mild steel during machining and optimized the empirical model to attain the required surface roughness of the material.

The stochastic nature of burnishing can lead all the conventional techniques of optimization to produce a local optimum solution to a problem. Hence some of the evolutionary algorithm namely GA, differential evolution, particle swarm optimization, teaching learning-based optimization, and artificial bee colony have been successfully implemented to avoid some of the drawbacks faced by the conventional optimization techniques. GA is also one among the broadly used technique, which is a computer-based search algorithm and is the most suitable in optimizing different functions. GA is known to be an effective tool in locating global optima with multiple runs. It is a cost-effective method, and also minimum knowledge is sufficient to attain the optimum values. Surface roughness reduction (Kilickap et al. 2011; Mahesh et al. 2015), minimizing burr height during the drilling process of steel alloys (Kilickap et al. 2010), titanium alloy machining (Çolak, 2014) is the common instances where GA was successfully implemented in industries. Khan et al. (1997) explored the importance of GA in optimizing the machining conditions and determined that it is an efficient, reliable, and accurate tool to perform the optimization of machining parameters. Recently, Santhanakrishnan et al. (2017) have performed a study on the constraints of the machine in analyzing the temperature rise using GA. Liu and Wang, (1999) have optimized the milling process parameters by using modified GA. The performance was improved by the successful implementation of the modified GA.

2.8 MOTIVATION AND SUMMARY

From the previous studies, it has been observed that few researchers have focused on the comparison of performance characteristics of diamond burnishing under cryogenic, MQL and dry environments and also inadequate literature is available on surface integrity investigation under all the three environments. In continuation with the need of investigation shown in P-18-19, so it is very much essential to implement a broad study on the diverse machinability perspectives. To date, limited research effort has been stated on the influence of control factors on surface integrity of 17-4 PH stainless steel under cryogenic, MQL, and dry environments using diamond burnishing. Hence an individual investigation on the effect of each process parameters on diamond burnishing under cryogenic, MQL, and dry environments have to be carried out. There is scope for the improvement of performance characteristics by developing a new diamond burnishing tool. To the author's knowledge, not many kinds of literature are available on diamond burnishing process with a newly designed tool.

It has also been observed that only a few researchers concentrated on the optimization of process parameters of the diamond burnishing process under different lubricating media. Hence there is a scope to carry out the optimization studies of diamond burnishing process to enhance the surface integrity properties of the material by using conventional optimization techniques. Some of the important process parameters which need to be optimized to obtain improved performance characteristics are burnishing speed, burnishing feed, and burnishing force. Additional process parameters such as the number of tool passes and diamond sphere diameter can also be considered to further analyze its effect on the output responses.

Literature survey reveals that researchers have worked on different modeling methods to understand the significance of the burnishing process parameters on geometric characterization and performance estimation independently. Few of them have also tried to perform modeling and multi-objective optimization of the control factors of the diamond burnishing at varying lubrication conditions. So far, only a few research works have been

reported on modeling and multi-objective optimization of control factors of the diamond burnishing under cryogenic, MQL, and dry environments using RSM and MOGA. Moreover, other conventional techniques yield a local optimum solution because of the discrete experimental design used for the experimentation. However, in reality during experimentation process factors changes continuously. Hence there is a scope to perform modeling and multi-objective optimization using RSM and GA to obtain a feasible solution to a problem.

2.9 OBJECTIVES OF THE RESEARCH WORK

Focusing on the recent developments in the area of burnishing, which has been used in the manufacturing industries to improve the surface characteristics of the material, the following research objectives have been derived:

1. To investigate the effect of control factors on 17-4 PH stainless steel by using a commercially available diamond burnishing tool under cryogenic, MQL, and dry environments.
2. To design and fabricate a novel diamond burnishing tool and analyze its performance.
3. To investigate the effect of a novel diamond burnishing tool on surface characteristics of the material under cryogenic, MQL, and dry environments.
4. To transfer multi-response performance characteristics into single-response by adopting Taguchi's GRA.
5. To develop a correlation model between the control factors and responses by RSM and optimize the control factors by referring to the developed regression equation by MOGA.

CHAPTER-3

EXPERIMENTAL METHODOLOGY

3.1 INTRODUCTION

The current chapter presents an in detail description of the material used, i.e., 17-4 PH stainless steel, it's chemical composition, the cooling/lubrication system used, and the methodology followed in carrying out the experimentation. The experimental plan used to carry out experimentation by GRA, RSM and OFATA have also been discussed. Further, the performance characteristics measurement details have been deliberated. Some of the performance characteristics considered for the present study include surface roughness, surface hardness, surface morphology, topography, subsurface microhardness, and residual stress.

3.2 PRELIMINARY EXPERIMENTATION

To arrive at the feasible range of diamond burnishing process parameters, preliminary experimentation has been carried out. It was noticed that the improper selection of process parameters leads to the poor surface quality of the diamond burnished material. It was observed that higher range of process parameters such as burnishing speed more than 113 m/min, burnishing feed of 0.1 mm/rev and burnishing force of 200N yields deteriorated surface texture. With the help of preliminary experiments performed by the authors, the feasible range of process parameters was selected and considered for further study (Sachin et al. 2018a).

3.3 WORK MATERIAL SELECTION

In continuation with the need of investigation shown in P-18-19, the material under consideration for the present research work is 17-4 PH stainless steel procured in the form

of a cylindrical bar of 32 mm diameter and 150 mm length. The chemical composition of the material is as depicted in Table 3.1. The microstructure and the energy dispersive x-ray spectroscopy (EDS) analysis of as received material is shown in Figure 3.1. The mechanical properties of the material are tabulated in Table 3.2. Scanning electron microscope (SEM) was used to capture the microstructure of the material. For microstructural studies, the samples were polished with different grades of SiC emery papers to remove the scratches.

Table 3.1 Chemical composition of 17-4 PH stainless steel.

Element	Ni	Cr	Cu	Si	C	P	Fe
(%)	4.62	18.53	2.96	0.07	6.03	0.51	Balance

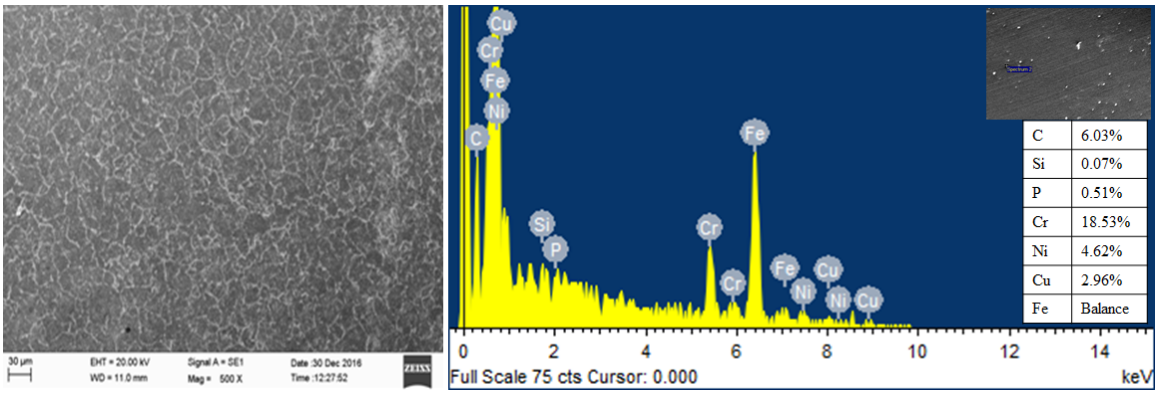

Figure 3.1 Microstructure and EDS analysis of as received 17-4 PH stainless steel.

Diamond polishing was carried out to obtain the mirror finish on the surface. Ferric chloride (10 g $FeCl_3$ + 30 ml HCl +120 ml H_2O) etchant was used to reveal the microstructure of the polished specimen of the material. The etching time of the specimen was kept in the range of 110 to 120 sec. The elemental composition of the as-received material was confirmed by EDS analysis.

Table 3.2 Mechanical properties of 17-4 PH stainless steel.

Ultimate tensile strength (MPa)	Yield strength (MPa)	Elastic modulus (GPa)	Hardness (HRC)	Density (g/cm^3)	Melting point (^oc)	Thermal conductivity (W/m K)
1018	992	199	37	7.79	1300	17.9

3.4 EXPERIMENTAL SETUP

3.4.1 Cryogenic burnishing

The cryogenic diamond burnishing set up used in the present study is as depicted in Figure 3.2. The schematic of the cryogenic diamond burnishing is represented in Figure 3.3.

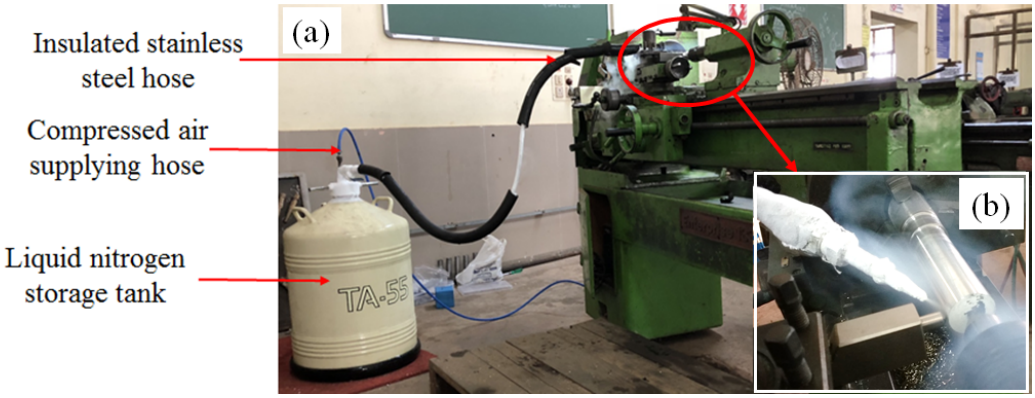

Figure 3.2 (a) Cryogenic diamond burnishing setup (b) Expanded view.

The components of the cryogenic cooling system are 'TA55' model cryocan, compressor, modified stainless steel cap, flow regulator, pneumatic hose, pressure relief valve, braided stainless steel hose, and nozzle. Two stainless steel hose is used to send LN_2 to the burnishing zone and to supply the compressed air to the tank respectively. Cryocan of 'TA55' model has been used for storing the LN_2 at a temperature of -196˚C inside the tank. Compressed air has been supplied to the storage tank at a pressure of 3–4 kgf/cm^2 using an air compressor which produces a jet of LN_2. 2 mm diameter nozzle was connected to the outlet to splash the jet of LN_2 at the burnishing zone. The excessive pressure can be

regulated by the pressure relief valve provided at the outlet of the pipe from the tank. The flow rate of the coolant was controlled by a flow valve.

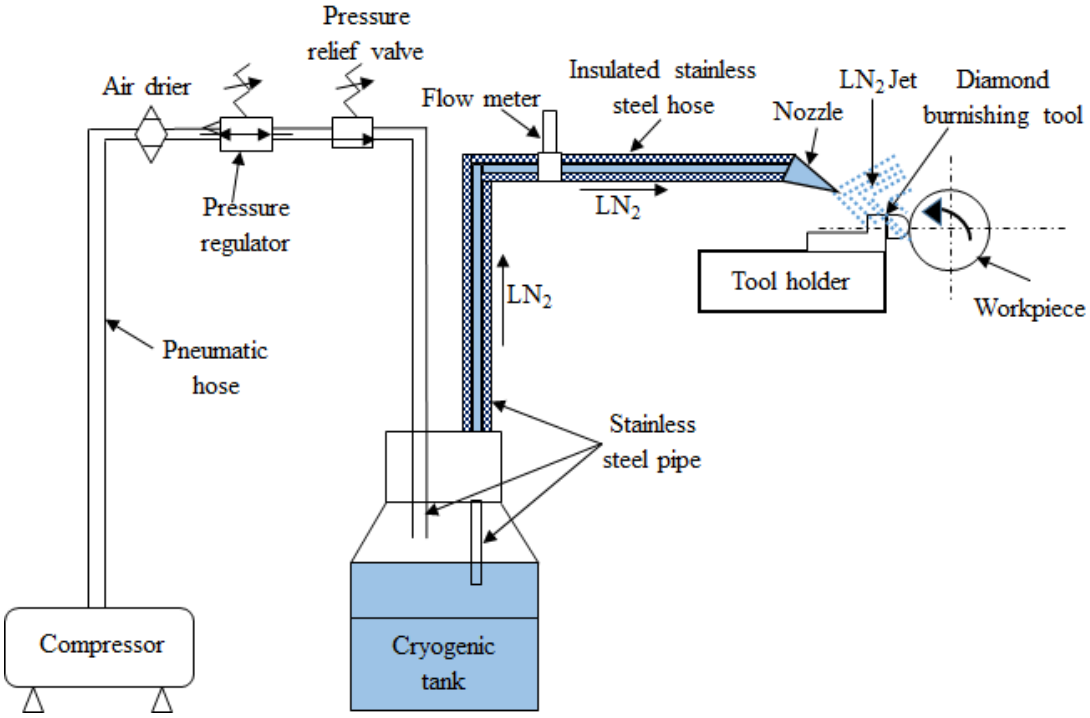

Figure 3.3 Schematic of cryogenic diamond burnishing.

3.4.2 MQL and dry burnishing

The present study has been carried out under the MQL environment, and the setup used is as depicted in Figure 3.4. Coconut oil has been used as a lubricant in MQL set up. The entire setup is comprised of an oil tank of 2 liters capacity and a pneumatic air pump to circulate the compressed air. Electronic timer B1DCA-X has been used to adjust the frequency of the oil piston pump. 0.40 cc/stroke is considered to be the discharge rate of the oil. The flow rate of the oil has been fixed to be 70 ml/hr. To obtain this flow rate, the air compressor has been used to compress the oil inside the tank, and the flow rate was set to be 4 kg/cm^2. An external nozzle has been used to obtain the mist of oil in the burnishing zone. It is flexible, and oil can be easily directed to the required area without altering or affecting the burnishing condition. In dry condition, the burnishing process was performed

in the absence of lubricant. The burnishing zones under various environments during burnishing is depicted in Figure 3.5.

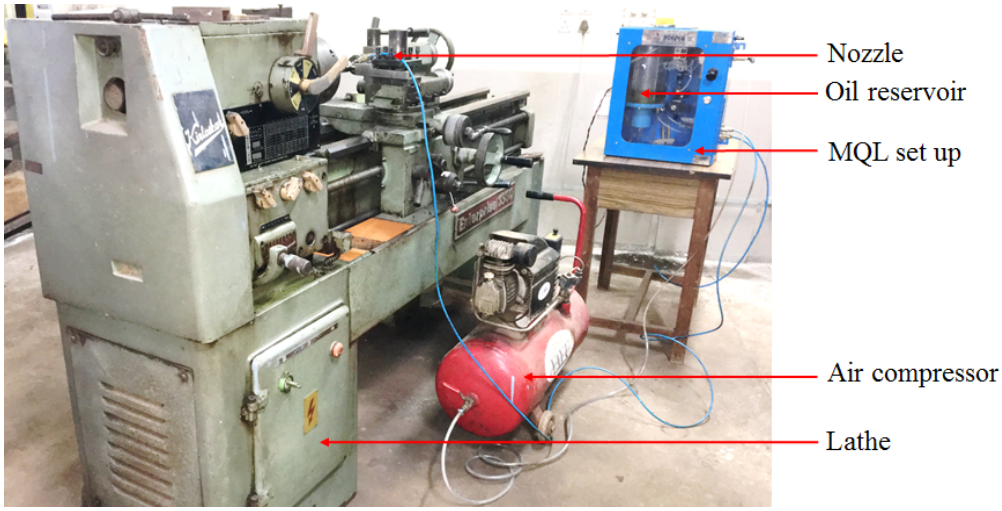

Figure 3.4 Diamond burnishing and MQL set up.

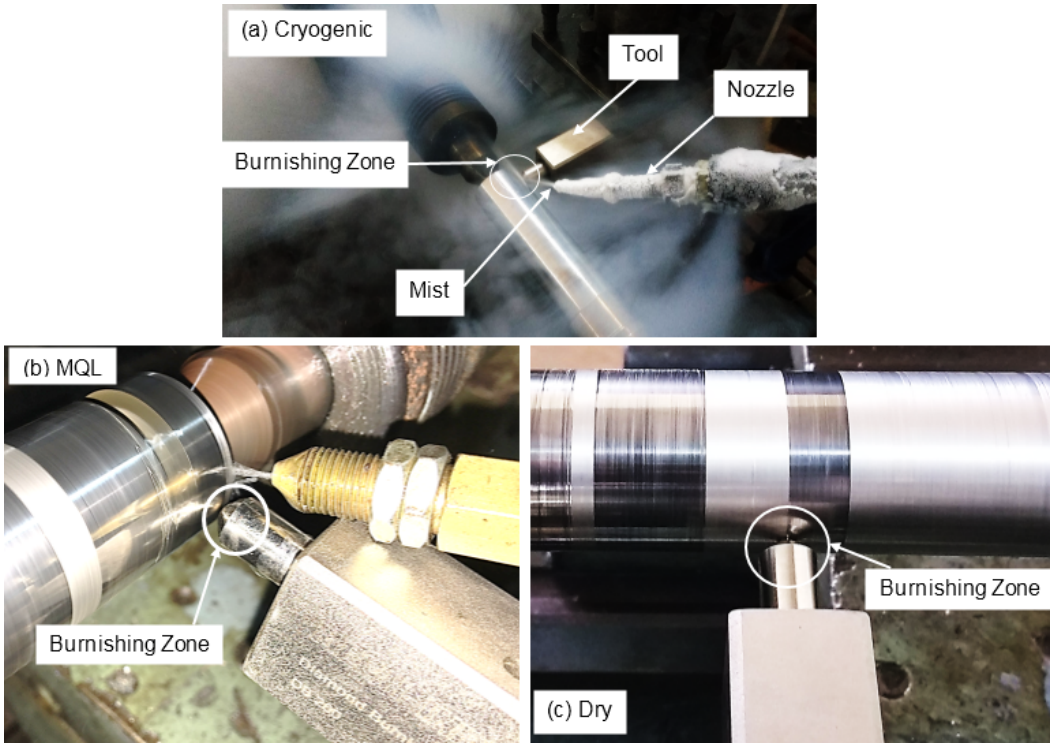

Figure 3.5 Burnishing zone at (a) cryogenic environment, (b) MQL condition and (c) dry diamond burnishing.

3.5 A NOVEL DIAMOND BURNISHING TOOL

To fulfill the requirements of the diamond burnishing process and to overcome the drawbacks faced by the manufacturers while using a conventional tool, a novel diamond burnishing tool has been fabricated and used in the present investigation. Figure 3.6 shows a special tool which has been designed and fabricated for carrying out the diamond burnishing experiments. The tool consists of two major parts: (1) Diamond stem, and (2) Shank of the tool. The stem of the tool contains a spherical diamond tip. The modification has been done in such a way that the stem of the tool can be removed easily from the shank by button head screw without removing the tool from the fixed position. The movement of the stem will compress the spring, which can be used to measure the applied burnishing force. In the novel diamond burnishing tool, heavy duty springs have been used with an increased number of coils, whereas in conventional tool light duty springs have been used. These springs are capable of absorbing any possible vibration induced by the machine bed and also in minimizing the positioning error of the diamond burnishing tool. To transmit the burnishing force of the tool and also for the easy movement of the spring inside the tool, the spring guide has been used. The square shank of the conventional tool has a larger overhang, while the newly designed tool has a better reach with smaller overhang. Attachment to the conventional lathe or CNC machine has become easy because of the extra grip provided with a novel diamond burnishing tool.

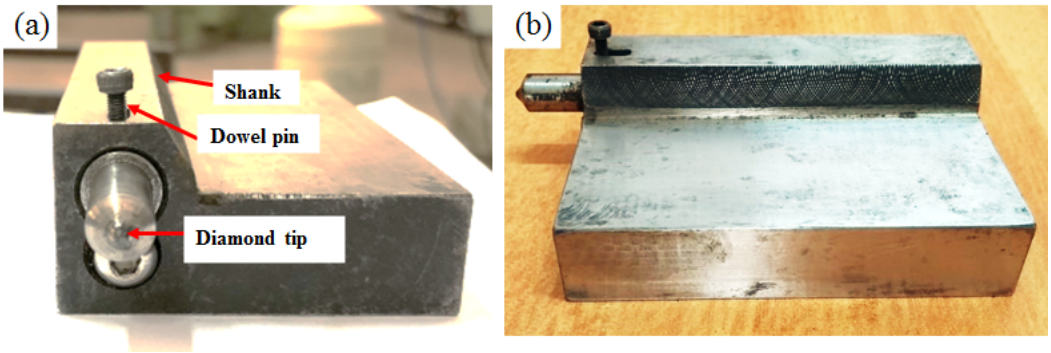

Figure 3.6 A novel diamond burnishing tool (a) Front view, (b) Side view.

Dowel pin has been attached to the tool for the measurement of the deflection of the spring, and it was not present in the conventional tool where the measurement of burnishing force was difficult in contrast with the novel diamond burnishing tool. When the burnishing force is applied to the tool, the deflection readings of the spring was measured by using a dial gauge. Whereas in the conventional tool, the measurement of deflection was difficult due to the absence of a dowel pin. In the preliminary experimentation and from the literature, it was perceived that a spherical diamond tip of the moderate radius would help to improve surface hardness and surface finish of the material. Hence in the present research work, a spherical diamond tip of radius 3.5 mm was used. The length of the tool stem has been reduced to avoid more stress acting on the tool while applying burnishing force.

3.6 EXPERIMENTAL METHODOLOGY

The experiment was performed by a diamond burnishing tool on 17-4 PH stainless steel. The flow chart of the methodology has been illustrated in Figure 3.7. The detailed description of the methodology adopted during the current investigation is presented below:

- Taguchi technique has been used to optimize the process parameters of the diamond burnishing process.
- Diamond burnishing operation was carried out on 17-4 PH stainless steel by using a commercially available diamond burnishing tool under the cryogenic, MQL, and dry environments with OFATA and surface integrity characteristics were analyzed.
- The significant process parameters were selected to study the surface integrity characteristics of the material, namely surface roughness, surface hardness, surface morphology, surface topography, subsurface microhardness, and residual stress.
- A novel diamond burnishing tool was designed and fabricated. Trial experiments were conducted to analyze its performance on the surface characteristics of 17-4 PH stainless steel.

- The influence of process parameters on 17-4 PH stainless steel was analyzed using a novel diamond burnishing tool under cryogenic, MQL, and dry environments.
- OFATA experimental design has been used to know the effect of each control process parameter on diamond burnishing performance characteristics in which one control factor was varied at one time, and other controllable factors were kept as a constant in their respective average level.

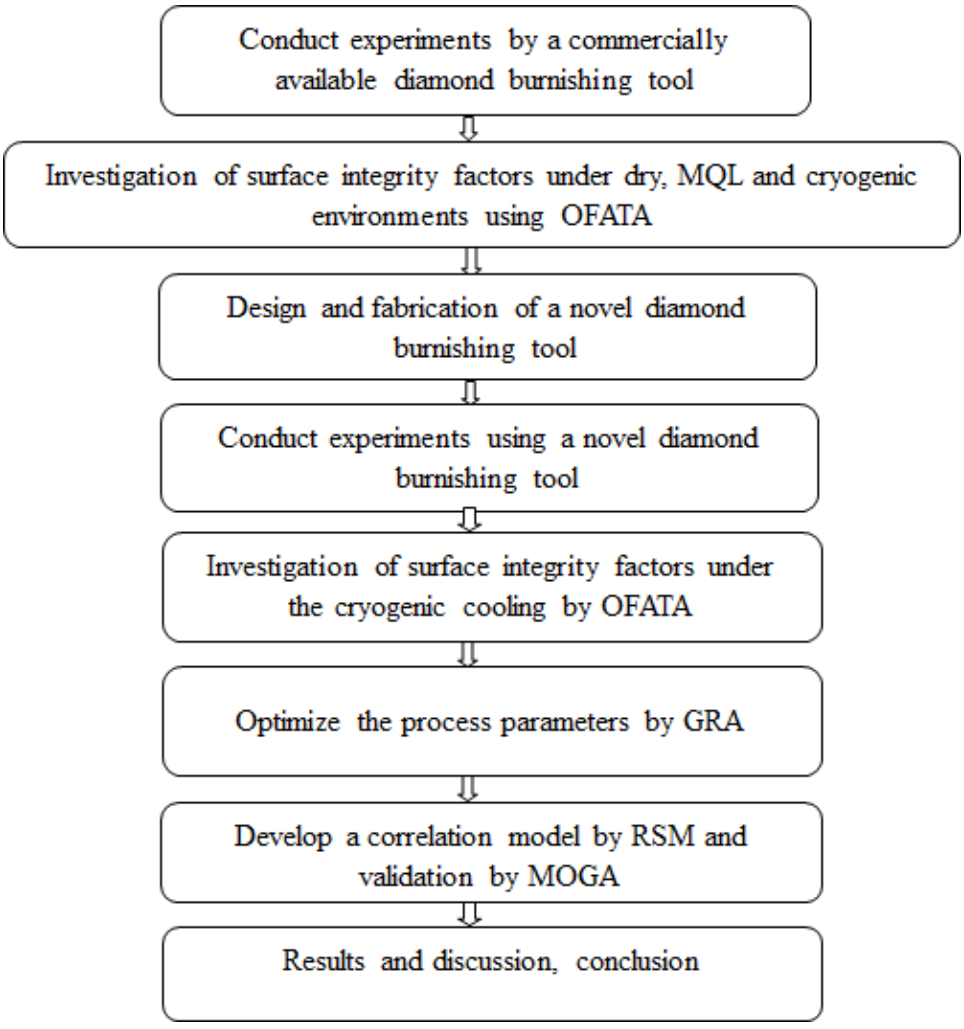

Figure 3.7 Flow chart of the methodology.

- Taguchi based GRA was carried out to optimize the process parameters of a novel diamond burnishing tool in the cryogenic environment.

- The statistical models of diamond burnishing performance characteristics such as surface roughness and surface hardness have been developed using RSM.
- The developed model using RSM was used as a fitness function in GA. To perform multi-objective optimization using GA, a combined objective function was developed by normalizing the surface roughness and surface hardness which satisfies both the objectives.
- The obtained results using RSM and MOGA were validated by performing experiments.

3.7 ONE FACTOR AT A TIME APPROACH

One of the classical engineering technique used for optimization is OFATA. It is a technique where one variable will be varied, and its effect on performance characteristics will be determined by keeping other process parameters as a constant. Therefore it is the most preferred technique to understand the impact of each process variables on output responses. To determine the influence of each control factors on performance characteristics, OFATA has been used in the present investigation. Five input parameters such as burnishing speed, burnishing feed, burnishing force, diamond sphere diameter, and number of passes were considered. All the process parameters were varied up to five levels, at the same time, other parameters were kept as a constant at their average level. Meanwhile, the influence of each process parameter on surface roughness, surface hardness, surface morphology, surface topography, subsurface microhardness, and residual stresses was analyzed.

3.8 GREY RELATIONAL ANALYSIS

GRA is one of the major parts of the grey system theory. A system which contains known and unknown information are collectively called as a grey system (Deng, 1982). GRA provides techniques for achieving a better solution to a problem instead of attempting to find the best solution. To overcome the limitations faced while solving a problem using factor analysis, and multi-attribute method, GRA has been proposed (Moran et al. 2006;

Wen, 2004). It lays a basic foundation for modeling of the performance characteristics, and it is considered as one of the effective tools to perform system analysis. Some of the advantages of GRA are it doesn't need special requirement for independency, and the calculation is simple. To solve a problem which has unique characteristics, GRA is proved to be an accurate and simple tool (Tsai et al. 2003). Grey relational grade (GRG) is a ranking system used in GRA, which rank the order of the relationship among the independent and dependent variables. It is used for selecting the significant process parameters involved in the time series and GRG will be arranged as per the order of their magnitude. These selected process variables will be considered as a foundation for further data mining. GRA will select most and least significant parameters which effect the performance characteristics. In the present study, GRA has been performed to establish GRG. Taguchi's L_9 orthogonal array has been used to carry out the experiments. Two performance characteristics, such as surface roughness and surface hardness, have been considered.

3.9 RESPONSE SURFACE METHODOLOGY

Response surface methodology is a well-known statistical tool which is used to arrive at a quadratic, linear, and squared models. It explores the relationship between explanatory variables and the output responses. It is employed to increase the production of a substance optimization of the operational process parameters. To understand the influence of explanatory variables on the output response factorial experiment will be used. It is possible to optimize and predict the responses by generating a regression equation, and also, it is possible to represent independent control variables in quantitative form as:

$$Y = f(X_1, X_2, X_3 \dots\dots\dots\dots\dots\dots\dots\dots\dots X_n) \pm \in \qquad (1)$$

Where Y - response, f - response work, $\in$- trial errors, $X_1, X_2, X_3 \dots\dots\dots\dots\dots\dots\dots\dots\dots X_n$- independent variables. The response surface can be obtained by plotting the response of Y. RSM performs an approximation of 'f' using a lower arrange polynomial in the area of free factors (Reddy et al. 2018).

Different experimental runs can be designed as per Box and Behnken, CCD, and full factorial design in RSM. It is one of the methods to achieve the best possible result by reducing the time required for production. To evaluate the second-degree polynomial model, the CCD design can be implemented. CCD design is the most appropriate method to develop a second order surface model. The design consists of three sets of experimental runs they are: (a) a factorial design, (b) a set of center points, experimental runs whose values of each factor are the medians of the values used in the factorial portion. (c) A set of axial points, experimental runs identical to the center points except for one factor, which will take on values both below and above the median of the two factorial levels, and typically both outside their range. In the present investigation, face-centered CCD design was used to perform experiments. Twenty experimental runs have been performed by considering three input parameters and two performance characteristics. By this method, the two-way interaction effect of two process parameters on output responses can be determined easily.

3.10 GENETIC ALGORITHM

GA is a basic tool which works on the principle of natural selection and genetics. It is an adaptive heuristic search algorithm which is preferred to solve unconstrained and constrained problems to obtain an optimal solution with high probability (Çolak, 2014; Kumar and Sait, 2017). Multiple solutions can be obtained by different persons, which helps in achieving the best feasible solution for a problem. Compound problems involving displaces feasible seats, multimodality, discontinuity, and loud role estimation is possible through GA. Primarily, a set of a feasible solution to a particular problem is maintained. Based on fitness, two individuals will be selected. The individuals who have higher fitness have a chance of being selected among the others. Chromosomes are the initial set of a solution with which the process starts. Mutation, reproduction, and crossover are the genetic operators on which the convergence depends. To select good strings, the process starts with a step called reproduction. Splitting and combining one half of each chromosome with the other pair is performed in a crossover. The flipping of chromosomes is done by mutation. From the current population, GA uses individuals in random, which

is known as parents and children will be produced for the next generation (Kumar, 2018). An optimal solution of the population will be achieved from this generation. The best fitness criteria are achieved by repeating the same process. Proportional selection, ranking, and tournament selection are the most popular selection procedures used in GA.

3.11 MEASUREMENT OF OUTPUT RESPONSES

3.11.1 Surface roughness

The surface roughness measurement of diamond burnished specimen was examined by surface roughness tester of model Surftest SJ-301 Mitutoyo, Japan. The surface roughness tester was used in the present study is depicted in Figure 3.8. The measurement is carried out by using a diamond stylus. The radius of the stylus tip is 2 µm, and a suitable force of 0.75 mN will be applied on the specimen to measure the surface roughness. The speed of stylus is 0.25 mm/sec, and a sampling length of 4 mm was used. For all the specimen average of three readings will be considered as the final roughness value. However, in the present study, only the average roughness value has been considered for further study.

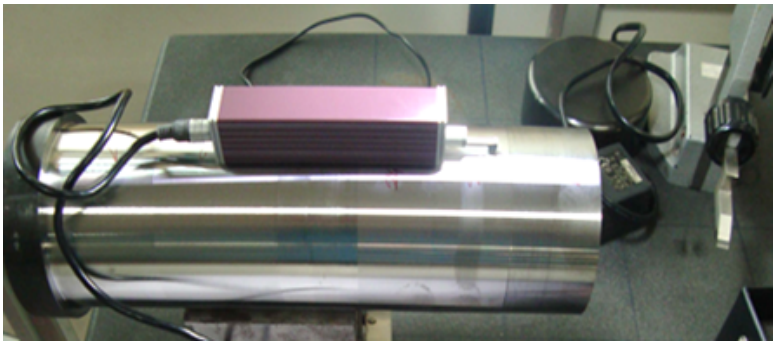

Figure 3.8 Surface roughness tester.

3.11.2 Surface hardness

Vickers hardness tester model ‘VM-120’ was used to measure the surface hardness, which is depicted in Figure 3.9. The surface hardness was measured along the length and periphery of the workpiece. The surface hardness tester is confirmed to IS 1754 – 2002. A dwell time of 15 sec and an indentation load of 30 kgf was used to measure the surface

hardness of the specimen. Average of three readings have been considered as the final surface hardness value of the sample.

Figure 3.9 Vickers hardness testing machine.

3.11.3 Surface morphology

Diamond burnished surface morphology was studied by 'JEOJSM-638OLA' model SEM as shown in Figure 3.10.

Figure 3.10 Scanning electron microscope.

The diamond burnished surface images were directly taken at different resolutions to identify the surface defects after performing diamond burnishing. The images were taken at different locations on the burnished surface. The maximum resolution and magnification of the equipment is 3 nm and 3,00,000 X, respectively. The secondary electron images were captured at an acceleration voltage of 20kV and aperture size of 30 µm. High vacuum mode was used to estimate the surface morphology of the samples.

3.11.4 Surface topography

The surface topography of the burnished surface has been observed and recorded by 'LESTOLS4100' model confocal laser 3D surface tester. Figure 3.11 illustrates the 3D laser microscope used in the present research work to measure the surface topography. It uses a laser scanning system to measure the surface peaks and valleys of the diamond burnished sample. The laser spot diameter of the microscope is 0.4 µm. A scanning area of 1.28 mm × 1.28 mm was used to perform a topographic evaluation of the diamond burnished sample.

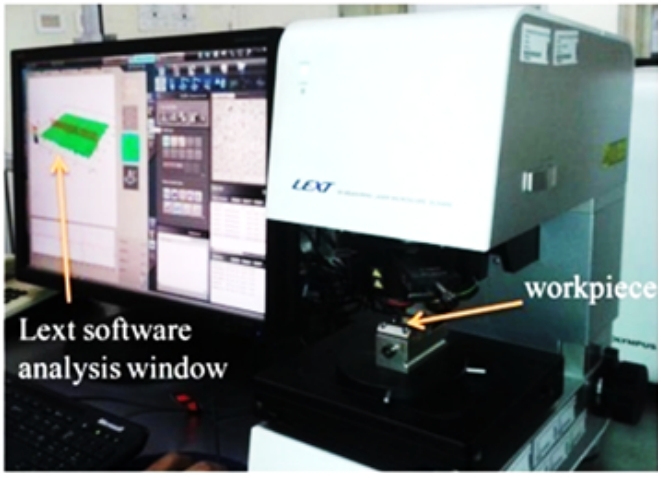

Figure 3.11 Laser optical confocal microscope.

3.11.5 Subsurface microhardness

Figure 3.12 presents the Vickers microhardness tester used in the present investigation to measure the subsurface microhardness of the diamond burnished sample. Vickers microhardness tester type 'OMNI TECHMVHS-AUTO' was used to measure the

subsurface microhardness. Initially, the specimen was cold mounted using acrylic powder and self-curing liquid. Further, the specimen was subjected to polishing and ultrasonic cleaning. For the measurement of subsurface microhardness, dwell time of 15 sec, and a load of 10 kgf was considered.

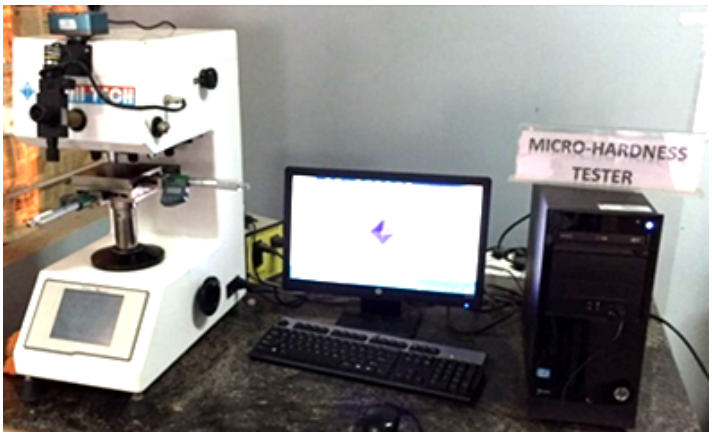

Figure 3.12 Vickers microhardness tester.

3.11.6 Residual stresses

After diamond burnishing, the compressive residual stresses will be induced on the surface of the material. The residual stress measurement was carried out using a stress measurement system, as demonstrated in Figure 3.13.

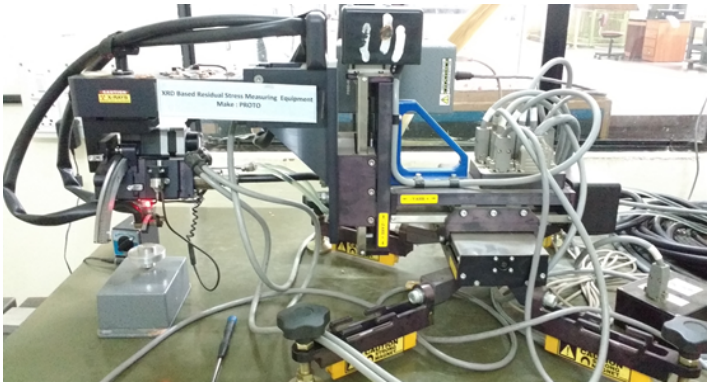

Figure 3.13 Residual stress testing machine.

Residual stress has been measured by X-ray diffraction with MGR40P stress measurement system make ‘PROTO’, Canada. The measurements were carried out by setting the

parameters in accordance with the details of the test sample. The gain is set to the optimum level for better results. The input parameters used are as follows: Braggs angle -155.10, peak shift - (1/2)S2:5.67 E-6 MPa, S1:1.20 E-6 MPa, D spacing - 1.17 Angstroms.

3.12 SUMMARY

In this chapter, the material used and their properties have been demonstrated. The experimental details, the cooling/lubrication system, experimental methodology, have been described. A novel diamond burnishing tool was designed and fabricated to improve the performance characteristics of the material under consideration. The detailed description of the novel diamond burnishing tool used in the study has been discussed. Further, the performance characteristics used in the present research work namely surface roughness, surface hardness, surface morphology, surface topography, subsurface microhardness, and residual stress measuring equipment and method have been demonstrated. Enough care has been taken while measuring performance characteristics to obtain more accurate and precise results. During the measurement of each output responses, the deviation observed in the readings were negligible.

CHAPTER-4

EXPERIMENTAL INVESTIGATION ON CONVENTIONAL DIAMOND BURNISHING TOOL

4.1 INTRODUCTION

The current chapter presents an in detail description of an experimental evaluation of the output responses using a conventional diamond burnishing tool. Three different cooling/lubrication methods such as cryogenic, MQL, and dry conditions were considered for the study. The experiments were performed by adopting OFATA. Five different control factors and their levels were finalized for further study based on the author's preliminary research work carried out on 17-4 PH stainless steel. The chapter also discusses the effect of each process variables on the performance characteristics such as surface roughness, surface hardness, surface morphology, surface topography, subsurface microhardness, and residual stress.

4.2 EXPERIMENTAL METHOD

Based on the preliminary investigation of diamond burnishing, process parameters such as burnishing feed, burnishing speed and burnishing force and their levels have been selected, which is as shown in Table 4.1. 'Kirloskar' make lathe machine has been used to carry out the burnishing process. 17-4 PH stainless steel was used as the workpiece, in the cylindrical rod form of 150 mm length and 30 mm in diameter. Before burnishing, the turning process has been carried out by using Kennametal make AlTiN coated KC5010 tungsten carbide inserts. The pre-machined average surface roughness of the workpiece before burnishing was found to be in the range of 1.20-1.25 μm, and the average surface hardness was found to be 340 HV. Diamond burnishing tool used in the present study consists of a spherical diamond tip which has been supported by the spring and radius of the diamond tip is 6 mm.

The burnishing force was applied by deforming the spring with linear behavior, which is located in the tool. Burnishing process carried out under different environments such as cryogenic, MQL, and dry. Factors such as burnishing feed, burnishing speed, and burnishing force were considered. The surface integrity characteristics such as surface hardness, surface roughness, surface topography, subsurface microhardness, and residual stresses were investigated under cryogenic, MQL, and dry environments.

Table 4.1 Experimental information.

Process Parameters	**Units**	**Levels**				
		Level 1	Level 2	Level 3	Level 4	Level 5
Burnishing speed (S)	m/min	21	30	47	73	113
Burnishing feed (f)	mm/rev	0.048	0.055	0.065	0.079	0.096
Burnishing force (F)	N	20	50	90	120	150

4.3 EFFECT OF BURNISHING PARAMETERS AND CRYOGENIC COOLING ON SURFACE ROUGHNESS

4.3.1 Burnishing speed

The surface finish of the components is of outmost importance in the aerospace and medical fields. The variation of surface roughness concerning burnishing speed is depicted in Figure 4.1(a) and it represents the surface roughness attained at a constant burnishing feed = 0.055 mm/rev, burnishing force = 90 N and varying burnishing speed under different cooling environments. It was pragmatic that the surface roughness decreases from burnishing speed of 21 m/min to 47 m/min and a further increase in the burnishing speed from 47 m/min to 113 m/min results in the deteriorated surface finish of the material. This is because at the lower range of burnishing speed, the diamond tip used in the burnishing tool will have more time and chances of clearing out the irregularities present over the surface of the material. This is possible to achieve only up to a certain limit of burnishing speed. Moreover, at lower burnishing speed, the temperature generated at the tool-workpiece interface will be low. As there is an increase in the burnishing speed to a higher range, the temperature generated during diamond burnishing increases. Due to high

burnishing speed, chattering also will be initiated. This causes the surface roughness to increase at higher burnishing speed.

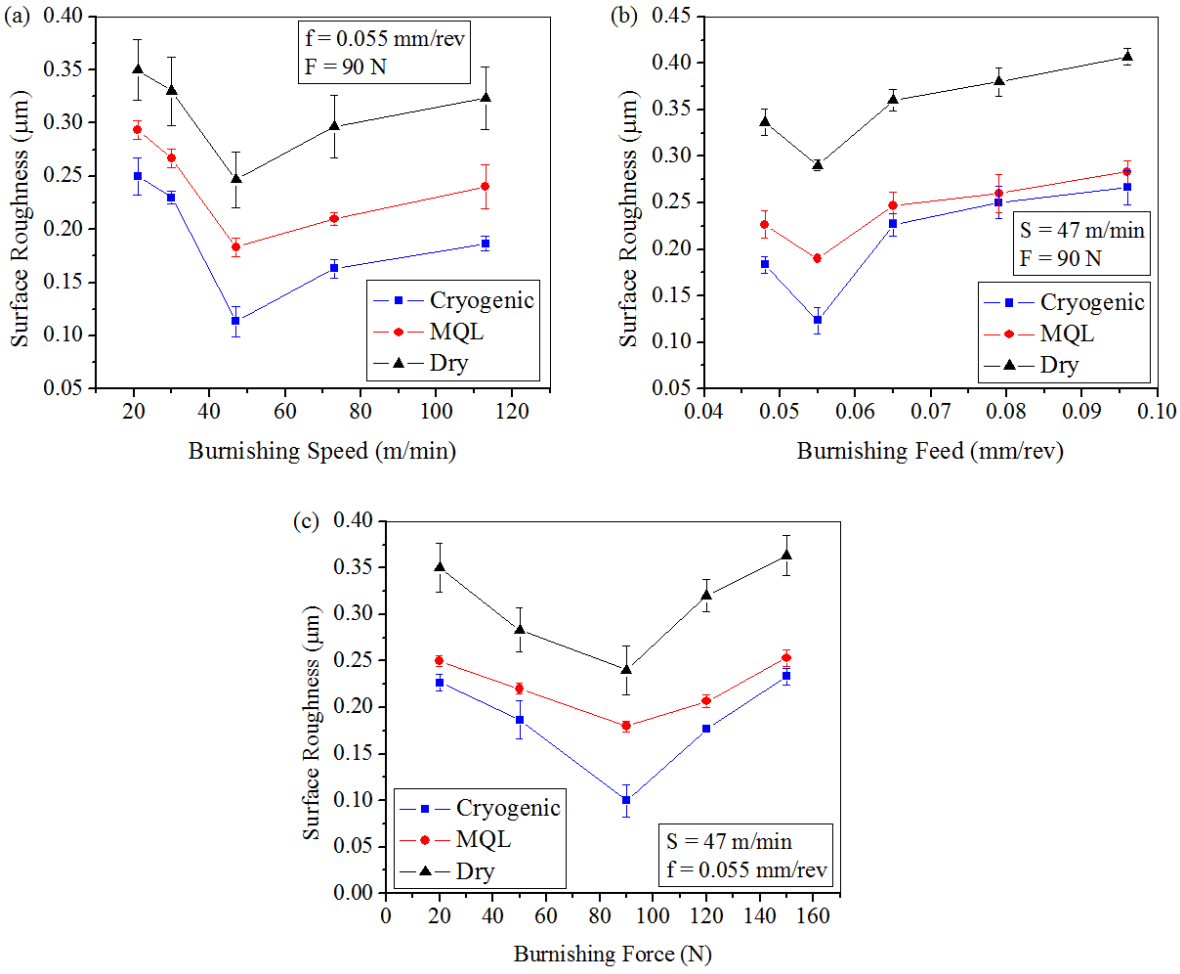

Figure 4.1 Surface roughness at varying (a) burnishing speed, (b) burnishing feed and (c) burnishing force.

Furthermore, at higher burnishing speed, the transformation of the material takes place between the tool tip and the workpiece (Sachin et al. 2019a). This might be another reason for the increased surface roughness at high burnishing speed. Figure 4.1(a) shows that surface roughness was observed to be minimum in the cryogenic environment in contrast with MQL and dry environments. That's because the simultaneous application of LN_2 reduces the temperature developed in the burnishing zone. Lower friction will be generated

between the tool and workpiece even while working with higher burnishing speed. In the present work minimum surface roughness of 0.11 µm, 0.18 µm, 0.24 µm was obtained under cryogenic, MQL and dry environments respectively at burnishing speed = 47 m/min, burnishing feed = 0.055 mm/rev, burnishing force = 90 N. Surface roughness reduction found in the cryogenic environment was 39% and 54% respectively over MQL and dry environment.

4.3.2 Burnishing feed

Figure 4.1(b) shows surface roughness observed at burnishing speed = 47 m/min, burnishing force = 90 N and varying burnishing feed under all the environments. As depicted in Figure 4.1(b), surface roughness decreases when burnishing feed increases from 0.048 mm/rev to 0.055 mm/rev. Further, increase in the burnishing feed from 0.055 mm/rev to 0.096 mm/rev results in an increase in the surface roughness. It is owing to the feed marks generated during the diamond burnishing process. At lower burnishing feed, the distance between the consecutive traces of the diamond tip is less. Minimum feed marks will be generated at lower burnishing feed, which causes a reduction in the surface roughness. At higher range of burnishing feed, the distance between the consecutive traces of the diamond tip becomes more. Hence more feed marks will be generated on the surface of the material, which is a reason for the increased surface roughness at a higher range of burnishing feed (Nemat and Lyons, 2000). A similar result has been observed in the SEM images of the diamond burnished surface as depicted in Figure 4.2(b) and (c) for MQL and dry environments, respectively. In the cryogenic environment, the uniform surface was observed because of the reduced feed marks generated as a reason of constant splashing of the LN_2 at the burnishing zone. Also, a lower coefficient of friction will be generated due to the effect of cryogenic cooling. It was also observed that the effect of vibration induced during diamond burnishing was found to be reduced because of the use of a cryogenic environment, which leads to reduced feed marks on the surface of the material. Minimum surface roughness was observed at a burnishing feed of 0.055 mm/rev under all the three environments. In the cryogenic diamond burnishing, a reduction in the surface roughness of 37% and 59% was noticed contrasted with MQL and dry environments respectively.

4.3.3 Burnishing force

The burnishing force plays a vital role in improving the surface finish. Figure 4.1(c) signifies surface roughness attained at burnishing feed = 0.055 mm/rev, burnishing speed = 47 m/min and varying burnishing force under different cooling environments. It can be seen from Figure 4.1(c) that the surface roughness of the specimen decreases to a minimum value when there is an increase in the burnishing force from 20 N to 90 N. Additional increase in the burnishing force from 90 N to 150 N causes an increase in the surface roughness. It is seen that surface roughness decreases from 0.22 µm to 0.10 µm in cryogenic, 0.25 µm to 0.18 µm in MQL and 0.35 µm to 0.24 µm in dry environments, when burnishing force was increased from 20 N to 90 N. As burnishing force increases from 90 N to 150 N, surface roughness was observed to be 0.23 µm, 0.25 µm and 0.32 µm under cryogenic, MQL and dry environments respectively. The reason being, during the diamond burnishing process, the bulge formed in front of the diamond tip increases in size at a higher range of burnishing force. Also, the zone of plastic deformation widens at this condition. Nevertheless, if the area of plastic deformation on the diamond burnished surface layer increases, it causes severe damage to the surface, which leads to a deteriorated surface finish. Whereas, at lower burnishing force the area of plastic deformation becomes low because of the application of the lower burnishing force on the surface of the material by the diamond burnishing tool (Nemat and Lyons, 2000; Hassan, 1997a). At this condition, the surface roughness decreases to a minimum value. Hence the best possible surface finish was achieved at the medium level of burnishing force in all the three environments. It was observed that the surface roughness in the cryogenic environment is minimal when compared to all other environments. The spraying of LN_2 at the burnishing zone prevents the chemical and mechanical degradation of the burnished surface. Hence improved surface finish was possible to achieve by the cryogenic environment in contrast with MQL and dry environments.

4.4 SURFACE MORPHOLOGY OF DIAMOND BURNISHED SURFACE

The SEM images of the surface produced have been acquired at burnishing speed of 47 m/min, burnishing feed of 0.055 mm/rev and burnishing force of 90 N is depicted in Figure 4.2(a-c). The surface roughness observed for the specimen at the above-mentioned condition was 0.10 µm, 0.18 µm and 0.24 µm under cryogenic, MQL and dry environments respectively. In the cryogenic environment as shown in Figure 4.2(a), a uniform surface was observed because of the constant cooling effect of the LN_2 at the interface of the tool-workpiece. During the diamond burnishing process under cryogenic environment, the metal which is accumulated at the top surface layer of the material starts flowing because of the constant pressure of the LN_2 supplied at the burnishing zone. This causes the easy flow of the material. Some of the micro voids present over the surface will be filled because of the flow of the metal and also while flowing over the surface layer of the material, the metal occupies the space on the mico voids instantly (Revankar et al. 2014). Hence uniform surface will be generated because of the combination of diamond burnishing process and cryogenic cooling effect. In the previous discussion on surface roughness under varying burnishing feed condition [Refer Figure 4.1(b)] reveals that the mechanism behind the surface roughness increase at a higher range of burnishing feed was due to the generation of feed marks. A similar observation was made in this study of surface morphology. It can be observed that the presence of feed marks have been noticed in Figure 4.2(b) and (c) for MQL and dry environments respectively. Also, the presence of micro voids has been observed in the MQL and dry environments. It is due to the fact that in the MQL environment, at the applied levels of diamond burnishing process parameters considered in this study and the amount of lubrication splashed at the burnishing zone may not be sufficient to cause the uniform flow of the metal over the surface of the workpiece. Hence the micro voids have not been filled completely in the case of MQL environments. Whereas in the dry environment, the deteriorated surface was observed at the similar diamond burnishing condition. In the dry environment, the absence of lubrication causes an increase in the temperature generated in the burnishing zone. The plastic deformation on the surface layer also increases because of the sudden increase in the temperature generated. However,

the effect of excessive plastic deformation was minimized because of the presence of the cooling effect of LN_2 and the presence of lubrication respectively under cryogenic and MQL environments.

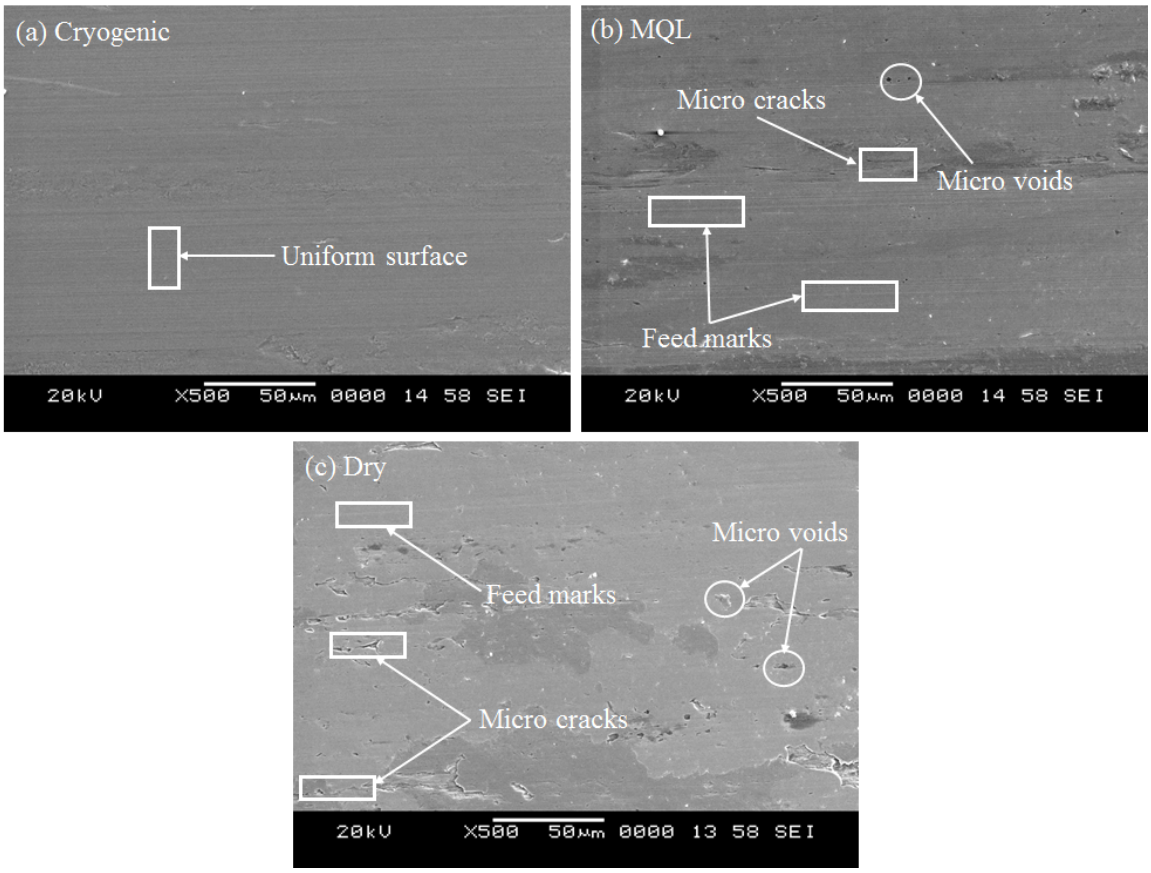

Figure 4.2 SEM images of the burnished surface under (a) Cryogenic, (b) MQL, and (c) Dry environments.

4.5 SURFACE TOPOGRAPHY

The burnishing operation leaves characteristic topographic features on the surface of the components. The surface topography analysis is essential in understanding the deviation of the surface produced from a flat surface. In the previous discussion about the surface morphology in all the three environments, it was observed that the cryogenic environment yields a better result in comparison with MQL and dry environments. Figure 4.3 depicts the 3D surface topography observed at a constant burnishing speed of 47 m/min, burnishing

feed of 0.055 mm/rev and burnishing force of 90 N. The surface topography observed for the cryogenic environment is better than the remaining two environments. The surface topography images are analyzed based on the peak intensity height produced on the diamond burnished surface. Low peak intensity was observed for the cryogenic environment in contrast with MQL and dry environments.

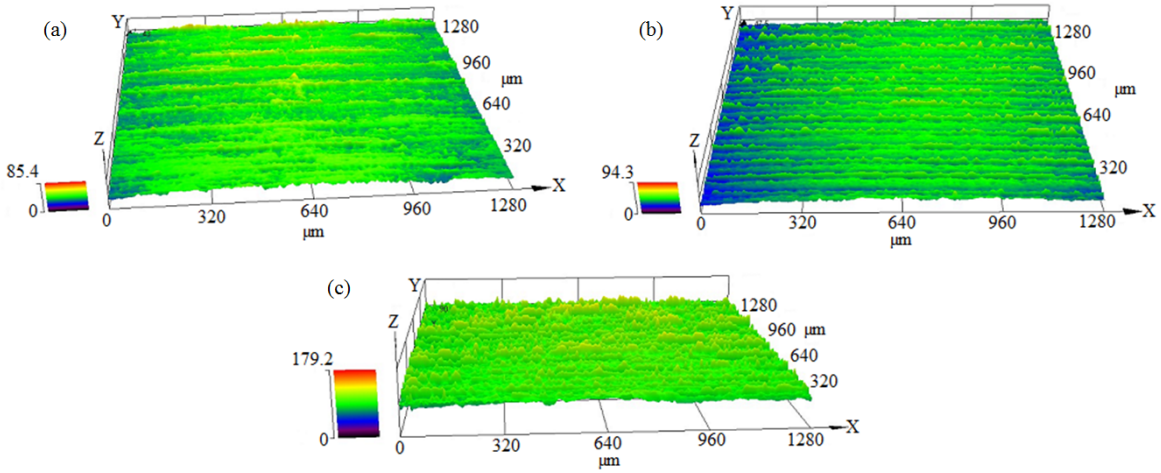

Figure 4.3 Surface topography of the burnished surface under (a) Cryogenic, (b) MQL, and (c) Dry environments.

Uniform surface was observed in the cryogenic environment. Whereas in MQL and dry environments, surface defects have been observed. However, the surface defects were minimized in the cryogenic environment. The presence of the cryogenic environment during diamond burnishing reduces the temperature generated at the tool-workpiece interface. Also, the thermal distortion produced on the diamond burnished surface will be reduced due to the spraying of the LN_2 at constant pressure to the tool-workpiece interface. It can be seen that the peak intensity height was higher in MQL and dry environments in comparison with the cryogenic condition. In MQL environment the lubrication effect may not be sufficient to reduce the temperature developed at the burnishing zone. Hence the peak intensity was observed to be high. Similarly, in a dry environment, the absence of the lubrication during diamond burnishing increases the temperature generated at the tool-workpiece interface which leads to higher peak intensity when compared to cryogenic and

MQL environments. From the surface topography study, it was observed that cryogenic environment yields a favorable surface topography in contrast with the other two environments and hence it is believed that cryogenic environment is a better mode of lubrication to improve the performance characteristics of the material.

4.6 EFFECT OF BURNISHING PARAMETERS AND CRYOGENIC COOLING ON SURFACE HARDNESS

4.6.1 Burnishing speed

Surface hardness testing is one of the major aspects of machining which is used to determine the characteristics of a material and its suitability for a given application. Variation of surface hardness is depicted in Figure 4.4(a) which has been observed at burnishing feed = 0.055 mm/rev, burnishing force = 90 N and varying burnishing speed under different cooling environments. From Figure 4.4(a), it is evident that if burnishing speed increases from 21 m/min to 47 m/min, surface hardness decreases. As the burnishing speed increases from 47 m/min to 113 m/min, the surface hardness was found to be decreasing. The mechanism behind this drastic decrease in the surface hardness could be attributed to the temperature generation at the higher level of burnishing speed. At the lower range of burnishing speed, the temperature generated at the tool-workpiece interface will be low which does not allow the recovery of the work hardened surface layer of the material at this point (Sachin et al. 2018a). When the burnishing speed was increased from a lower range to a higher range, the temperature at the interface increases to the maximum extent. When the temperature is high, the work hardened surface layer of the material will be recovered at this condition which could be highlighted as the reason for the decrease in the surface hardness at a higher range of burnishing speed. However, the primary reason for the reduction of surface hardness at higher burnishing speed may be partly due to the possible chatter induced at the tool-workpiece interface (El-Taweel and El-Axir, 2009). It could be observed that among all the environments, cryogenic cooling yield improved surface hardness of the material. This behavior could be explained by the fact that the effective cooling of the burnishing zone with LN_2 mitigates the thermal softening effect

which plays a dominant role in MQL and dry environments. Figure 4.4(a) shows that, at burnishing speed of 21 m/min, burnishing feed = 0.055 mm/rev, burnishing force = 90 N, a maximum surface hardness of 388 HV, 377 HV, and 359 HV were observed under cryogenic, MQL and dry environments respectively.

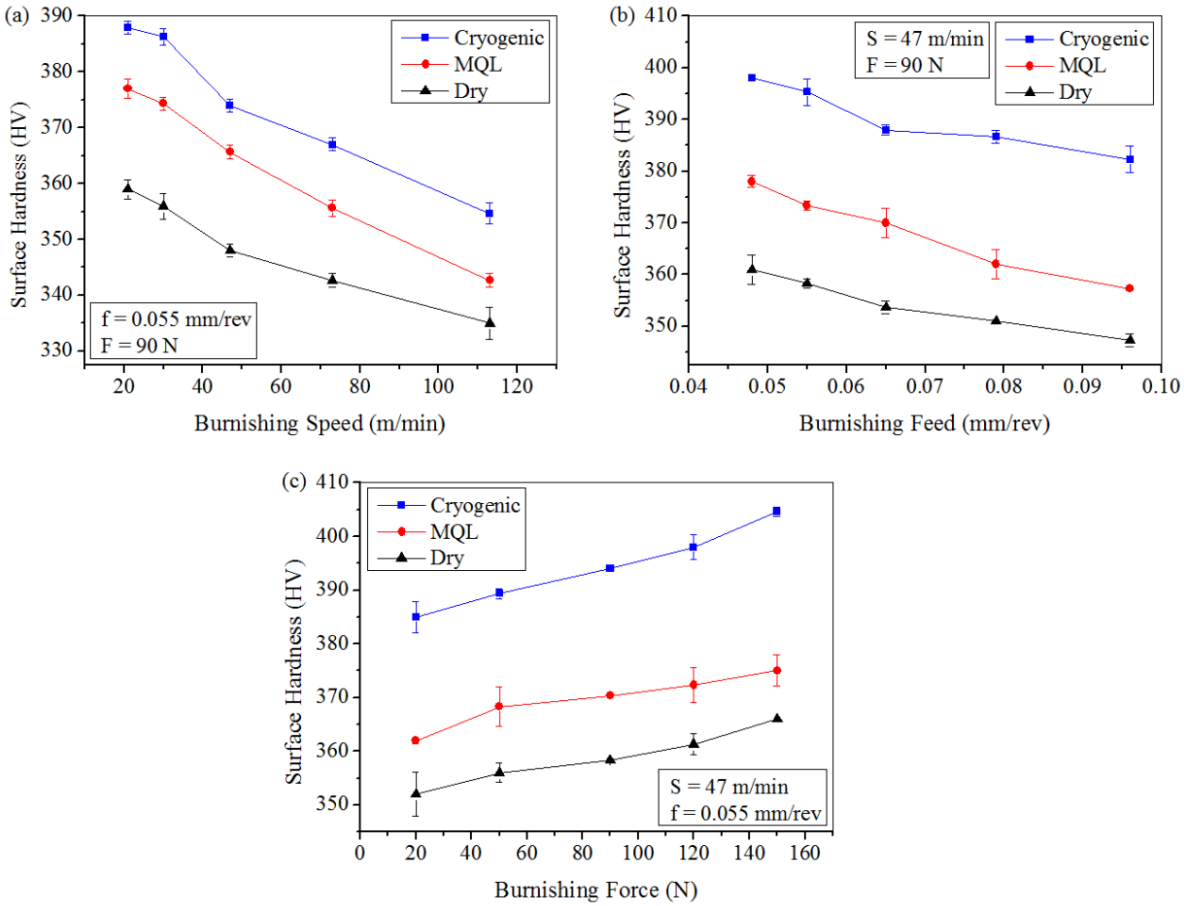

Figure 4.4 Surface hardness at varying (a) burnishing speed (b) burnishing feed and (c) burnishing force.

4.6.2 Burnishing feed

Figure 4.4(b) exemplifies the effect of burnishing feed on surface hardness at burnishing speed = 47 m/min, burnishing force = 90 N and varying burnishing feed under all the three environments. In all the three environments, a decreasing pattern was noticed for surface hardness when burnishing feed increases from 0.048 mm/rev to 0.065 mm/rev. A further

increase in the burnishing feed from 0.065 mm/rev to 0.096 mm/rev causes a reduction in the surface hardness. The reason for this trend might be due to the fact that at lower burnishing feed, the repeated movement of the tool on the workpiece will be low because of the lower feed provided to the diamond burnishing tool. At this condition, the plastic deformation of the material will be high which in turn lead to the maximum surface hardness at lower burnishing feed. But if the burnishing feed was increased from a lower range to the higher range, the tool movement on the workpiece will be repetitive. The total plastic deformation of the workpiece decreases because of the repeated movement of the tool on the workpiece surface and also the tool will move forward quickly due to the higher burnishing feed provided to the diamond burnishing tool (Hassan and Al-Bsharat, 1996). Hence the surface hardness decreases continuously whenever there is an increase in the burnishing feed. Similar to the varying burnishing speed condition, the maximum surface hardness was recorded at lowest burnishing feed under the cryogenic environment followed by MQL and dry environments. It is owing to the strain hardening effect observed in the cryogenic environment because of the continuous cooling effect of the LN_2. As per the objective of this research work, an enhancement in the surface hardness was achieved after performing diamond burnishing under cryogenic environment. It was noticed that an enhancement of surface hardness was found to be 5% and 10% respectively in cryogenic diamond burnishing when compared to MQL and dry environment.

4.6.3 Burnishing force

Variation of surface hardness concerning burnishing force is presented in Figure 4.4(c) and was observed at burnishing feed = 0.055 mm/rev, burnishing speed = 47 m/min and varying burnishing force. It is a crucial parameter which has to be considered seriously to enhance the surface hardness of the material after performing diamond burnishing. As shown in Figure 4.4(c), the surface hardness was found to be increasing with an increase in the burnishing force from 20 N to 90 N. As the burnishing force was advanced from 90 N to 150 N, the surface hardness was found to be increasing continuously. It is believed that whenever there is an increase in the burnishing force, it results in the application of more pressure by the diamond burnishing tool on the workpiece surface. It could be seen that if

the pressure applied on the workpiece is higher, the amount of plastic deformation on the surface layer of the material also increases which results in work hardened surface. Also, as the plastic deformation increases, the inducement of compressive residual stresses on the surface layer of the specimen also increases (Nemat and Lyons, 2000; Sachin et al. 2019c). All these combinations lead to the maximum surface hardness at the burnishing force of 150 N. In the cryogenic environment, improvement in surface hardness was observed when compared to the other two environments. That's because cooling the burnishing zone with the help of LN_2 leads to the grain refinement that results in small grain formation which substantially increases the surface hardness of the material. The grain refinement also takes place due to the effect of severe plastic deformation of the material induced by the application of burnishing force on the workpiece (Pu et al. 2011). A maximum surface hardness of 388 HV, 398 HV, and 404 HV respectively was observed at varying burnishing speed, burnishing feed and burnishing force under cryogenic environment.

4.7 SUBSURFACE MICROHARDNESS

Fatigue life and wear resistance of the product depends on the surface and subsurface hardness of the material. Figure 4.5(a) represents the microhardness of the specimen which has been measured at burnishing speed of 47 m/min, burnishing feed of 0.055 mm/rev and burnishing force of 90 N under cryogenic, MQL and dry environments respectively and Figure 4.5(b) shows the measurement procedure. The point below the burnished surface has been represented by 0 µm in Figure 4.5(a) and each measurement has been considered at a distance of 10 µm from the previous point. The measurement has been carried out till the depth of 150 µm from the top surface layer of the specimen. At this point, the subsurface microhardness of the specimen reached the bulk hardness of the material. The bulk hardness of the material before diamond burnishing was found to be 340 HV. It was observed that the subsurface microhardness of the material decreases continuously from the top surface layer of the specimen. Further, an increase in depth beneath the diamond burnished surface results in the reduction of the subsurface microhardness of the material. Finally, the subsurface microhardness of the specimen reaches the value of the bulk

hardness of the material. It was also noticed that a similar trend had been observed for all three environments.

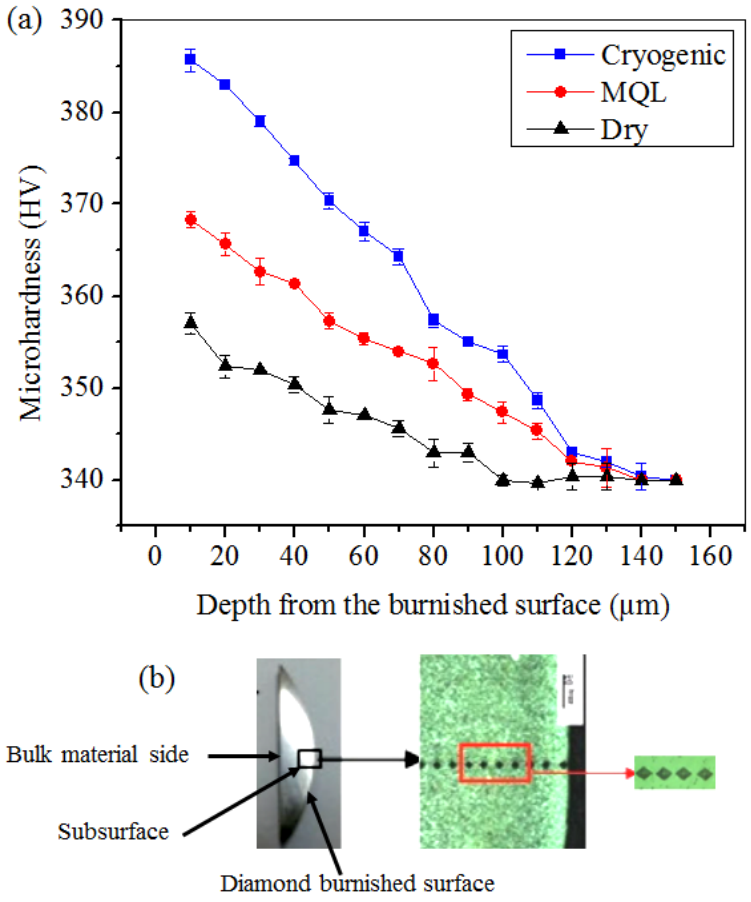

Figure 4.5 (a) Subsurface microhardness of the burnished sample under cryogenic, MQL, and dry environment (b) Measurement method.

The reason behind this variation may be explained by the fact that after performing diamond burnishing under varying lubrication condition, lower strain rate and less shearing will be produced (Sachin et al. 2018b; Revankar et al. 2014). This leads to a reduction in the subsurface microhardness of the material as the depth beneath the top surface layer increases. The cryogenic environment has produced excellent microhardness improvement in contrast with the other two environments, and also the highest microhardness was observed for the cryogenic environment. Based on the maximum subsurface hardness

observed in cryogenic, MQL and dry environment, the improvement attained was calculated. The percentage improvement observed in the case of cryogenic burnishing was 5% and 8% contrasted with MQL and dry environment respectively. The percentage of improvement was observed due to the grain refinement which was promoted by the application of LN_2 (Pu et al. 2011; Pu et al. 2012b). The diamond burnishing process yields grain refinement because of severe plastic deformation. The grains will be reduced in size due to the application of force on the surface layer of the material. Overall, an improvement in the microhardness was observed for the cryogenic environment and hence it is one of the favorable methods to improve the wear resistance and fatigue life of the material when compared to MQL and dry environments.

4.8 RESIDUAL STRESS

It is believed that the residual stresses induced after burnishing have an impact on the tribological properties and fatigue life of the component (Maximov et al. 2019). Hence it is necessary to study the impact of diamond burnishing on residual stress inducement under three different modes of lubrication. XRD is known to be one of the non-destructive techniques by which the residual stresses will be measured. The basic principle of residual stress measurement follows Bragg's law (Mawaad et al. 2011). The present study focuses on the residual stress induced on the surface of the diamond burnished sample. Before measuring the residual stresses induced on the surface of the material, the top surface layer of the material was subjected to electropolishing to minimize the possible modification in the induced stresses. Figure 4.6 depicts the distribution of residual stress under all three environments. The residual stresses were measured at burnishing speed of 47 m/min, burnishing feed of 0.055 mm/rev and burnishing force of 90 N under cryogenic, MQL and dry environments respectively. It was observed that after the diamond burnishing process, compressive residual stresses had been induced on the surface of the 17-4 PH stainless steel under cryogenic, MQL and dry environments respectively. Compressive residual stresses are more favorable in improving the fatigue life of the components than tensile residual stresses. Compressive residual stresses of -345 MPa, -268 MPa, -181 MPa were induced under cryogenic, MQL, and dry environments respectively.

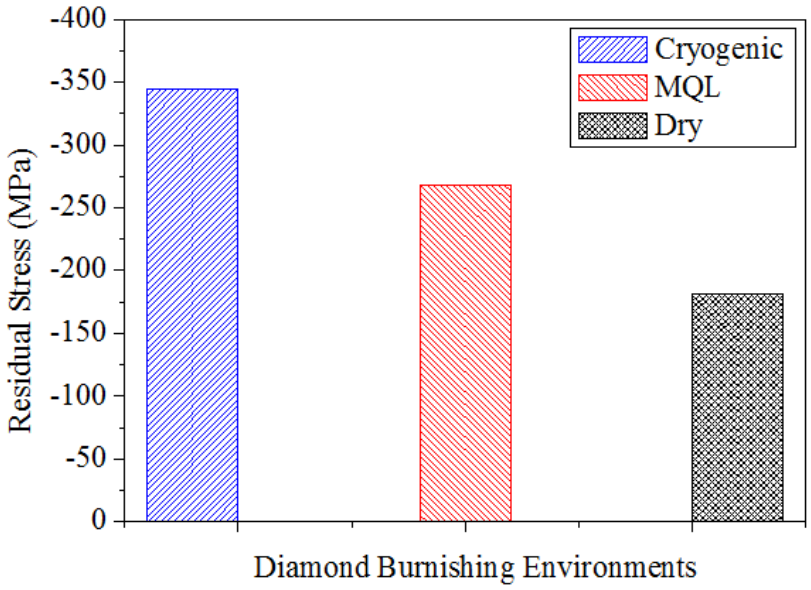

Figure 4.6 Residual stress distribution under varying diamond burnishing environments.

The induced compressive residual stresses on the surface show that cryogenic diamond burnishing is a better mode of lubrication for inducing favorable compressive residual stresses on the surface of 17-4 PH stainless steel. It is to be noted that the inducement of residual stress will be affected by the diamond burnishing process parameters. Hence the careful selection of the burnishing process parameters is essential for achieving improved experimental results. The fatigue strength of the material is expected to be improved since the induced compressive residual stresses retard the formation of cracks which is usually developed after the burnishing process (Nalla et al. 2003). The combination of sever plastic deformation and the splashing of the LN_2 at the burnishing zone is the primary reason for the inducement of maximum compressive residual stresses on the surface of the diamond burnished specimen under cryogenic environment. Overall from the above experimental findings, it has been observed that compressive residual stresses induced on the surface of the material play an important role in improving the fatigue life of the components.

4.9 INFLUENCE OF LUBRICATION ON DIAMOND BURNISHING PROCESS

Development of a new product by sustainability principles has been a major research focus as well as an emerging trend in manufacturing. From previous studies (Dinesh et al. 2017;

Adler et al. 2006), it has been found that exposure to various types of lubricants leads to respiratory diseases, dermatitis, and various types of cancers. Cryogenic burnishing is a better mode of lubrication since it produces a quality product which increases productivity. It does not cause health and environmental pollution because liquid nitrogen quickly evaporates. However, proper care has to be taken while handling LN_2. Continuous exposure of skin to the LN_2 causes serious cold burning. MQL burnishing does not cause environmental pollution, but the operator faces inhalation problems because of MQL mist. Whereas in dry burnishing because of the absence of lubrication, it does not cause health and environmental problems, but the quality of the workpiece will be poor which results in decreased productivity.

The influence of lubrication on surface integrity of 17-4 PH stainless steel is observed to be significant, and it has an impact on the performance of diamond burnishing. In the present investigation, different types of cooling environments have been used, such as cryogenic, MQL, and dry. Surface roughness was observed to be minimized, and surface hardness was increased after diamond burnishing process in all the three environments. In the cryogenic environment, LN_2 has been supplied at the tool and the workpiece interface. By the application of LN_2, surface integrity characteristics such as wear resistance, surface finish, fatigue life, and surface hardness of the components will be improved (Kaynak et al. 2014). Rapid cryogenic cooling reduces the thermal softening of the material (Caudill et al. 2014), and it leads to improved surface hardness. In the previous discussion of surface morphology (Refer Figure 4.2(a-c)), it was observed that the cryogenic environment had produced an exceptional result when compared to the other two environments. From Figure 4.2(a) it can be seen that the cooling effect of the LN_2 supplied at the tool-workpiece interface has led to reduced feed marks on the surface of the material. Uniform surface was produced due to the filling of the micro voids on the surface of the material. The constant metal flow during the cryogenic diamond burnishing is the reason for filling of these micro voids present over the surface. Whereas in MQL and dry environments, the uniform surface was not noticed, and the presence of the feed mark was observed as shown in Figure 4.2(b and c). In MQL environment because of the presence of lubrication, minimum feed marks

were noticed on the surface which is shown in Figure 4.2(b). It was proved from the investigational results that surface hardness and surface finish obtained were better when compared to the dry environment. The presence of lubrication reduces the effect of thermal softening, thereby reducing the temperature at the interface of tool-workpiece while burnishing, which leads to reduced feed marks. From the experimental results of surface roughness and surface hardness, it was observed that the effect of MQL has impact on diamond burnishing process. While working under the MQL environment, low quantity of lubricant in the form of mist will be sprayed at the burnishing zone. This process reduces the developed temperature in the burnishing zone. It results in the improved surface finish and surface hardness of the material when compared to a dry environment. In a dry environment, lubrication will not be used which results in temperature rise at the tool-workpiece interface. Another major issue is that friction will be more at the contact point, and also the thermal softening effect will deteriorate the surface of the material. A similar effect has been observed in Figure 4.4(a-c), where thermal softening effect leads to reduced surface hardness under dry condition. Experimental results prove that under the cryogenic environment, better results have been acquired when compared to MQL and dry environment.

Overall, from the previous investigational outcomes, it can be observed that the cryogenic environment was proved to be the best lubrication technique compared to MQL and dry environments. By the effective use of cryogenic lubrication in the production sectors, the fundamental issues faced by the manufacturers can be minimized. This chapter presents an improved surface integrity characteristics of the material by the effective use of lubrication at the burnishing zone. Diamond burnishing was proved to be the promising secondary finishing process to simultaneously enhance the surface finish and surface hardness of the difficult to cut material. The dimensional accuracy and productivity can be improved by the integration of diamond burnishing process and cryogenic cooling condition.

4.10 SUMMARY

The effect of diamond burnishing on the surface integrity of 17-4 PH stainless steel was studied under cryogenic, MQL, and dry environments. A conventional diamond burnishing tool was used to perform experiments. The effect of process factors on surface integrity characteristics of the material was studied. As per the findings from the present research work, the following conclusions were drawn:

- A maximum surface hardness of 388 HV, 398 HV, and 404 HV respectively was observed at varying burnishing speed, burnishing feed and burnishing force under cryogenic environment.
- Reduction in the surface roughness observed in the cryogenic environment at varying burnishing force, burnishing speed and burnishing feed was 44%, 39%, and 37% respectively in contrast with MQL environment.
- Similarly, surface roughness was reduced by 59%, 58%, and 54% respectively at varying burnishing feed, burnishing force, and burnishing speed under cryogenic environment when compared to dry environment.
- The enhancement of surface hardness was found to be maximum in case of the cryogenic environment with an increase of 3% to 8%, 5% to 10%, and 8% to 10% compared to MQL and dry environments respectively at varying burnishing speed, burnishing feed and burnishing force.
- An improvement in the microhardness of 5% and 8% has been achieved in cryogenic burnishing when compared to MQL and dry environment respectively.
- Compressive residual stresses of -345 MPa, -268 MPa, -181 MPa were induced under cryogenic, MQL and dry environments respectively.

CHAPTER-5

INFLUENCE OF NOVEL DIAMOND BURNISHING TOOL ON SURFACE CHARACTERISTICS

5.1 INTRODUCTION

This chapter describes the investigation on the impact of process parameters on the output responses using a novel diamond burnishing tool. The experiment was carried out under cryogenic, MQL, and dry environments. The OFATA methodology was adopted to examine the importance of process parameters on the performance characteristics. A novel diamond burnishing tool was designed and fabricated to improve the surface integrity characteristics of the 17-4 PH stainless steel. Based on the authors trial experiments performed on the 17-4 PH stainless steel, five different control factors and their levels were confirmed for further study. The performance characteristics such as surface roughness, surface hardness, surface morphology, surface topography, subsurface microhardness, and residual stress were studied.

5.2 EXPERIMENTAL METHOD

The material under consideration for the present research work is 17-4 PH stainless steel procured in the form of a cylindrical bar of 32 mm diameter and 150 mm length. A novel diamond burnishing tool was designed and fabricated to improve the performance characteristics of the material. The novel diamond burnishing tool consists of the following parts such as heavy duty spring, smaller overhang of the shank with better reach, extra grip provided to attach it on CNC or conventional lathe, and dowel pin which makes it novel in contrast with the conventional burnishing tool. The detailed information on the novel diamond burnishing tool was discussed in the previous chapter-3. The burnishing zones of three environments are framed in Figure 5.1. The experiments have been carried out based

on OFATA. ‘Kirloskar’ conventional lathe has been used in the present investigation to perform diamond burnishing. The surface roughness after burnishing purely depends on the surface roughness before burnishing (Hassan, 1997b; Li et al. 2012). Hence the top layer of the cylindrical rod has been removed, and its size has been reduced to 30 mm diameter and whereas the length remains the same. AlTiN PVD coated KC5010 tungsten coated carbide insert was used for turning operation with a constant depth of 0.25 mm, cutting velocity of 73 m/min and feed rate of 0.1 mm/rev.

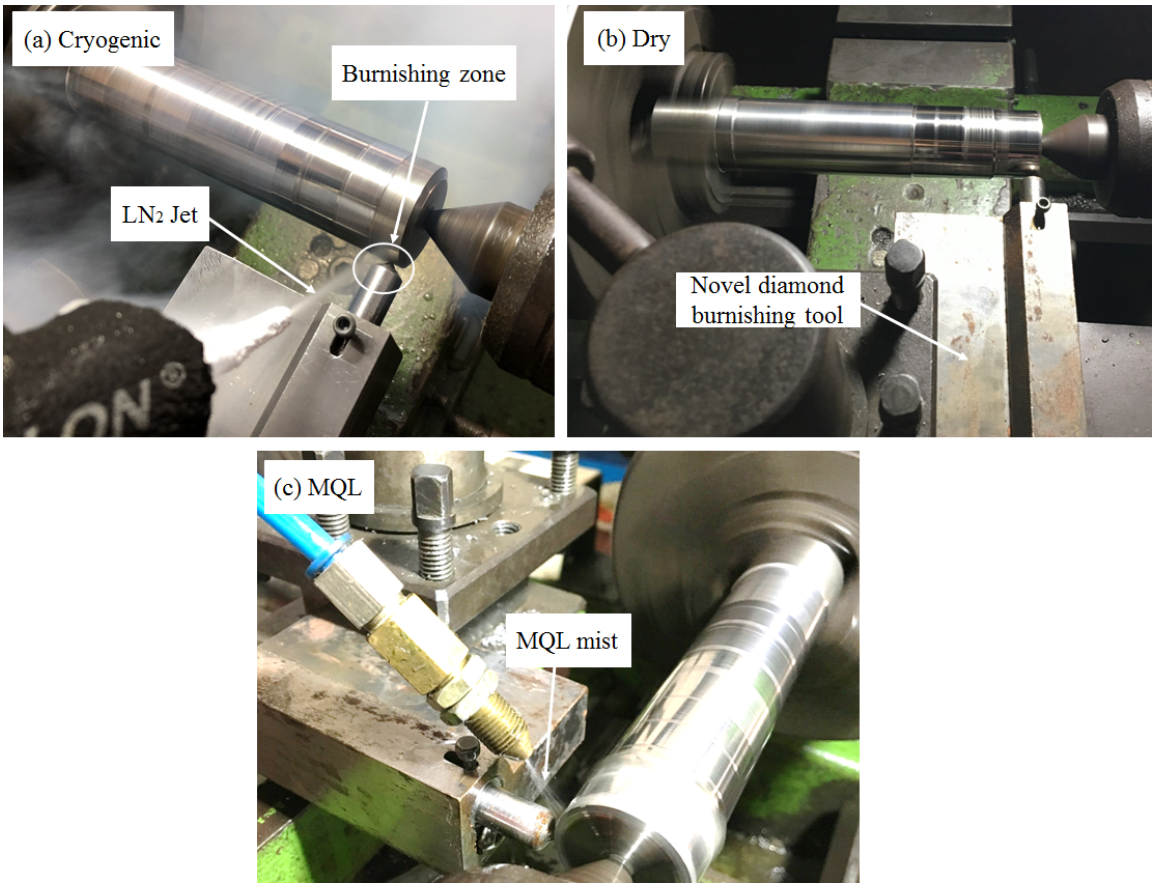

Figure 5.1 Different burnishing zones (a) Cryogenic (b) Dry and (c) MQL environments.

The average surface roughness and surface hardness before diamond burnishing were found to be 1.20 µm and 340 HV, respectively. Based on the preliminary investigation and from the literature review, the diamond burnishing process parameters have been selected. The control factors and their levels are given in Table 5.1. The burnishing process was

performed under cryogenic, MQL, and dry environments. Factors such as burnishing feed, burnishing speed, and burnishing force were considered.

Table 5.1 Experimental details.

Burnishing process parameters		**Levels**				
		1	**2**	**3**	**4**	**5**
Burnishing speed (S)	m/min	21	30	47	73	113
Burnishing feed (f)	mm/rev	0.048	0.055	0.065	0.079	0.096
Burnishing force (F)	N	50	88	125	163	200

5.3 ANALYSIS OF SURFACE ROUGHNESS

5.3.1 Effect of burnishing speed and cryogenic cooling on surface roughness

Performance of the mechanical components mainly depends on the quality of the burnished surface of the material. From Figure 5.2(a), it is noted that the surface roughness decreases from a burnishing speed of 21 m/min to 47 m/min and further increase in the burnishing speed from 47 m/min to 113 m/min leads to an increase in the surface roughness. The reason being, at lower burnishing speed the temperature generated at the burnishing zone will be reduced due to the constant spraying of LN_2 and as the burnishing speed increases the temperature increases which results in possible chattering and hence, the surface roughness increases (Hassan, 1997b). In MQL environment oil mist is sprayed at the workpiece-tool interface which reduces the temperature at the burnishing zone. In a dry environment because of the absence of lubrication, the surface roughness recorded was higher than the other two environments. Also, material transformation takes place between the tool and the workpiece which results in maximizing the surface roughness at higher burnishing speed (Hassan, 1997b). In Figure 5.2(a), all the surface roughness measurements were carried out at a constant burnishing feed of 0.065 mm/rev and burnishing force of 125 N. The variation of burnishing speed was between 21 m/min to 113 m/min. In all the three environments similar trend has been observed for surface roughness. The lowest surface roughness was recorded for a burnishing speed of 47 m/min. An improvement of 33% was observed under the cryogenic environment in contrast with

MQL environment. Similarly, 50% improvement was observed when compared to the dry environment.

5.3.2 Effect of burnishing feed and cryogenic cooling on surface roughness

Figure 5.2(b) indicates that the surface roughness declines with an increase in the burnishing feed up to 0.055 mm/rev. The reason for this decrease could be elucidated by the fact that at a lower burnishing feed, the consecutive traces of the diamond tip on the surface of the workpiece will be small since the tool moves slowly over the workpiece (El-Taweel and El-Axir, 2009; El-Axir et al. 2008).

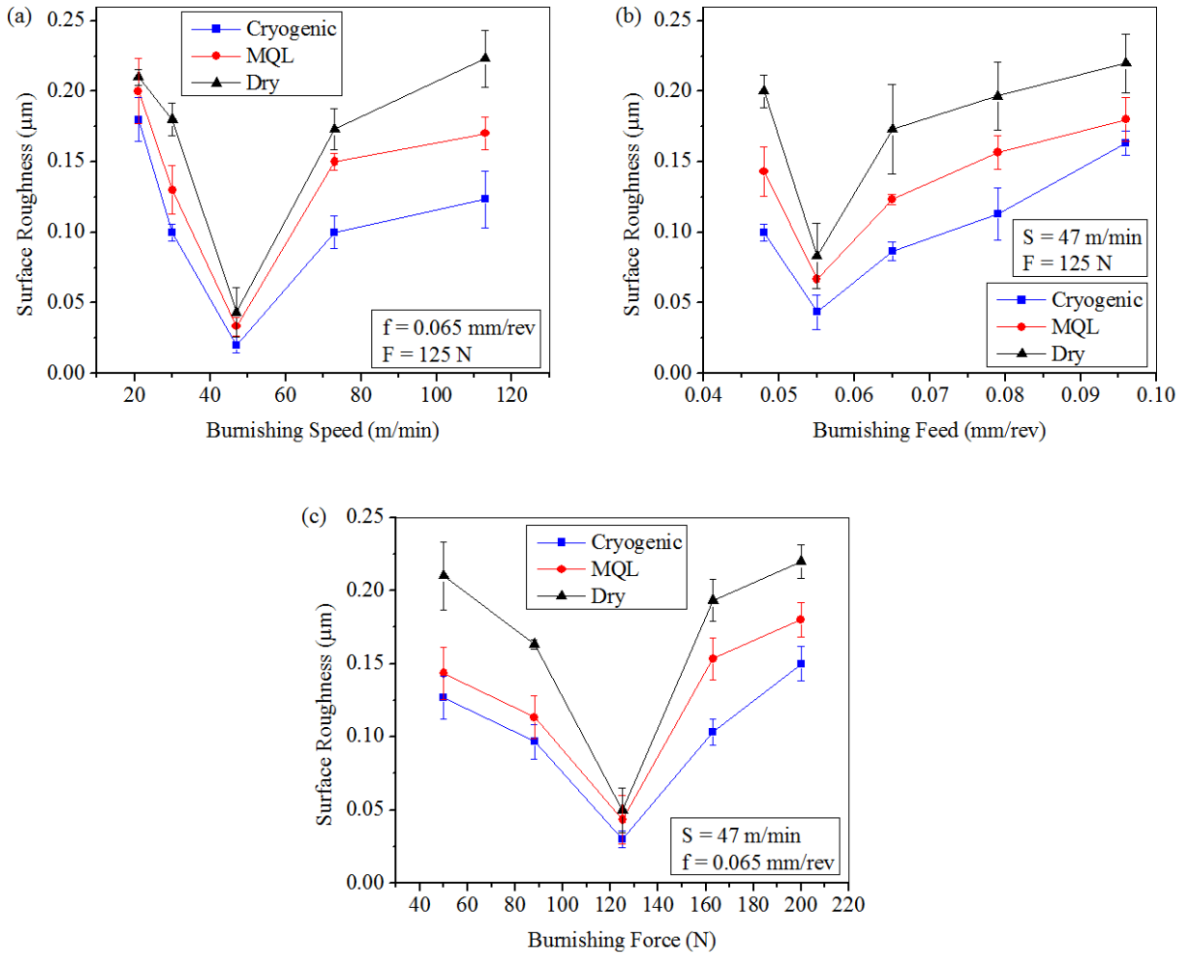

Figure 5.2 Variation of surface roughness for varying (a) burnishing speed (b) burnishing feed and (c) burnishing force under cryogenic, MQL and dry environments.

As there is an increase in the burnishing feed from 0.055 mm/rev, a quick rise in the surface roughness has been observed. The reason being, at upper limits of burnishing feed, the space between consecutive traces of the diamond tip increases. Another reason may be due to the minimum time available to the diamond tip to clear the bulged edges of the successive traces (Lyons and Nemat, 2000). The feed marks have been generated at the higher burnishing feed which can be seen from Figure 5.3. The variation in the cryogenic environment is observed due to the splashing of the LN_2 at the burnishing zone leads to a lower coefficient of friction and also minimum vibration has been observed which leads to minimum feed marks on the burnished specimen. In all the three environments similar trend has been observed. The cryogenic environment has shown the lowest surface roughness when compared to MQL and dry environments. The percentage of reduction in surface roughness was found to be 34% and 51% in contrast with MQL and dry environments, respectively.

5.3.3 Effect of burnishing force and cryogenic cooling on surface roughness

As indicated in Figure 5.2(c), the surface roughness decreases at a lower range of burnishing force and a further increase in the burnishing force from 125 N to 200 N leads to an increase in the surface roughness. The reason for this variation in the surface roughness may be because of the incomplete plastic deformation of the asperities, which leads to decreased surface roughness at the lower burnishing force. The repeated plastic deformation on the surface of the workpiece results in increased work hardening at a higher range of burnishing force which causes flaking on the surface and hence the surface finish deteriorates (Lyons and Nemat, 2000; Klocke et al. 2009). The surface roughness in the cryogenic environment is minimal when compared to all other environments because of spraying of LN_2 at the burnishing zone prevents the chemical and mechanical degradation of the burnished surface. Minimum surface roughness recorded was 0.03 µm at the cryogenic environment. It was found that the surface roughness was reduced by 25% and 40% under the cryogenic environment in contrast with MQL and dry environments respectively.

5.4 ANALYSIS OF SURFACE MORPHOLOGY

The diamond burnished surface morphology has been shown in Figure 5.3(a-c). The SEM images were observed at the burnishing speed of 47 m/min, burnishing force of 125 N and burnishing feed of 0.065 mm/rev. The SEM images of the diamond burnished surface clearly show that uniform surface has been formed after diamond burnishing under the cryogenic environment. The cryogenic diamond burnished surface has the most regular surface in comparison with the MQL and dry environment which has been shown in Figure 5.3(a).

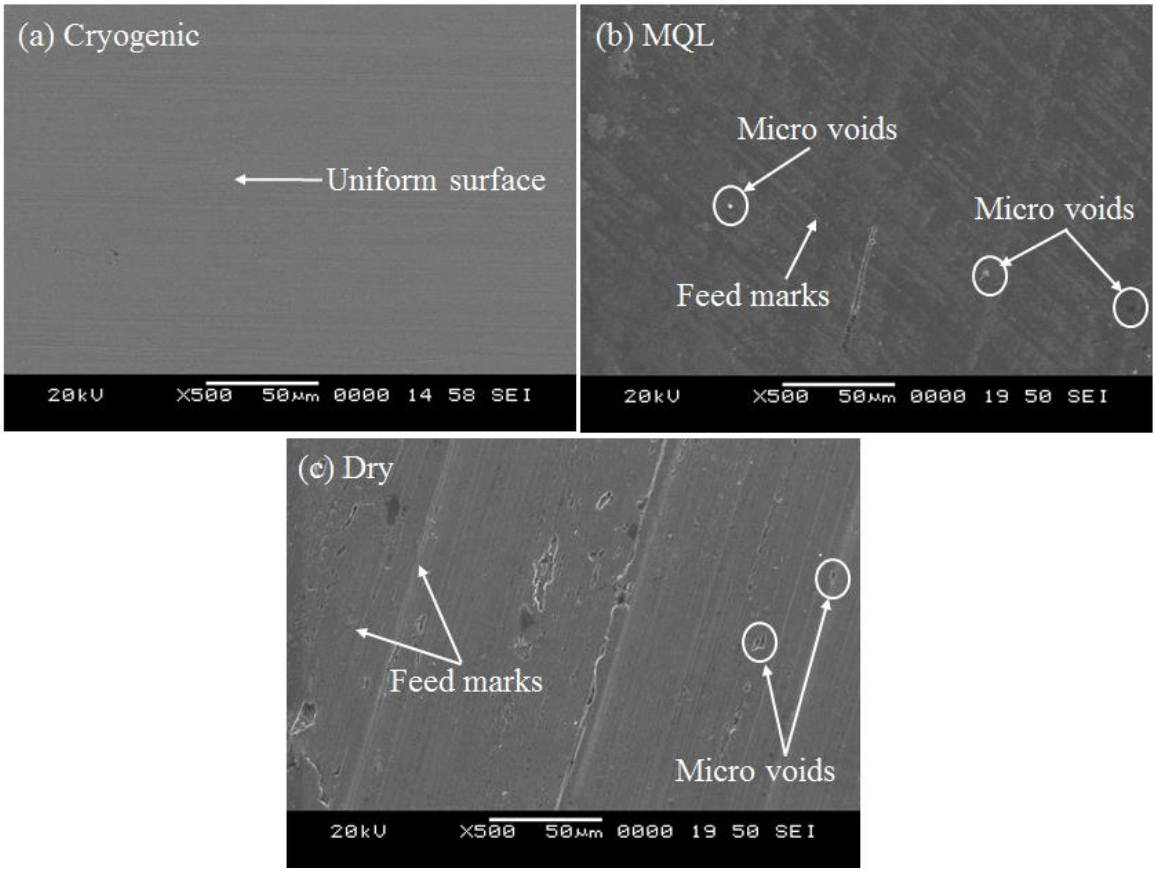

Figure 5.3 Surface morphology of the diamond burnished surface observed at burnishing speed of 47 m/min, burnishing force of 125 N and burnishing feed of 0.065 mm/rev under (a) Cryogenic (b) MQL and (c) Dry environments.

Uniform surface was observed in the cryogenic environment because of the presence of the cooling effect of LN_2 at the interface of the tool and the workpiece. It results in the easy flow of the material and because of which the voids have been filled completely. The effect of feed marks was reduced in the case of cryogenic diamond burnishing due to the cooling effect of the LN_2 at the burnished zone. In the previous discussion about the surface roughness, it was noticed that the surface roughness achieved for the cryogenic environment was minimum in contrast with MQL and dry environments. Similar observations have been made in Figure 5.3(a). It was found that the feed marks have been generated and a similar effect has been observed in the SEM images of MQL environment which can be seen from Figure 5.3(b). Micro voids have been observed in MQL environment because of the improper deposition of the material in the voids and also an easy flow of the metal has been suppressed in MQL environment in contrast with the cryogenic environment. The splashing of the oil mist at the burnishing zone reduces the generation of heat and henceforth the surface roughness has been minimized in comparison with the dry environment. However, because of the absence of lubrication in a dry environment, the presence of feed marks and voids were clearly visible as shown in Figure 5.3(c). Micro cracks have been observed in the dry environment owing to the excess heat produced in the burnishing zone and also due to the absence of lubrication.

5.5 ANALYSIS OF SURFACE TOPOGRAPHY

The 3D surface topography has been measured at the burnishing speed of 47 m/min, burnishing force of 125 N and burnishing feed of 0.065 mm/rev under all the three environments which are as represented in Figure 5.4(a-c). The diamond burnished surface has been considered for the measurement of surface topography. It was observed that in the cryogenic environment, peak to valley height was substantially reduced in contrast with MQL and dry environments. The reason is minimal thermal distortion has been observed on the cryogenic diamond burnished surface because of the constant spraying of LN_2 at the burnishing zone.

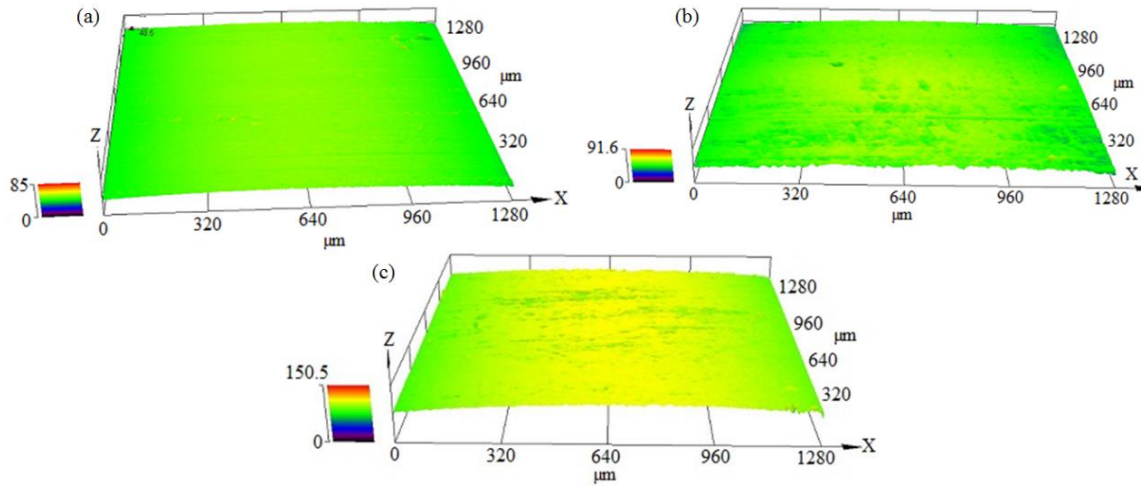

Figure 5.4 The surface topography taken at burnishing speed of 47 m/min, burnishing force of 125 N and burnishing feed of 0.065 mm/rev under (a) Cryogenic, (b) MQL and (c) Dry environments.

Hence the surface roughness observed under cryogenic environment was minimum. However, the other environments have shown increased peak to valley height because of the presence of higher temperature at the burnishing zone. From the results of SEM images and surface topography, it is pragmatic that cryogenic diamond burnishing yields improved surface finish when compared to other environments which help to improve the performance of the product in contrast with other working environments.

5.6 ANALYSIS OF SURFACE HARDNESS

5.6.1 Effect of burnishing speed and cryogenic cooling on surface hardness

The surface hardness variation with respect to varying burnishing speed reveals that the surface hardness of the material decreases continuously when there is an increase in the burnishing speed. The temperature at the tool and workpiece interface increases as the burnishing speed increases, and also at higher burnishing speed, the chattering has been induced due to which the surface hardness decreases (El-Taweel and El-Axir, 2009; Klocke et al. 2009). At a constant burnishing feed of 0.065 mm/rev and constant burnishing force of 125 N, the above trend has been achieved. The variation of the surface hardness with

burnishing speed is represented in Figure 5.5(a). The surface hardness improvement of 5% and 7% was observed under cryogenic environment when compared to MQL and dry environment at a burnishing speed of 21 m/min. An absolute improvement in the surface hardness under cryogenic environment was observed due to the constant spraying of LN_2 at the burnishing zone which reduces the temperature accumulated during the burnishing process.

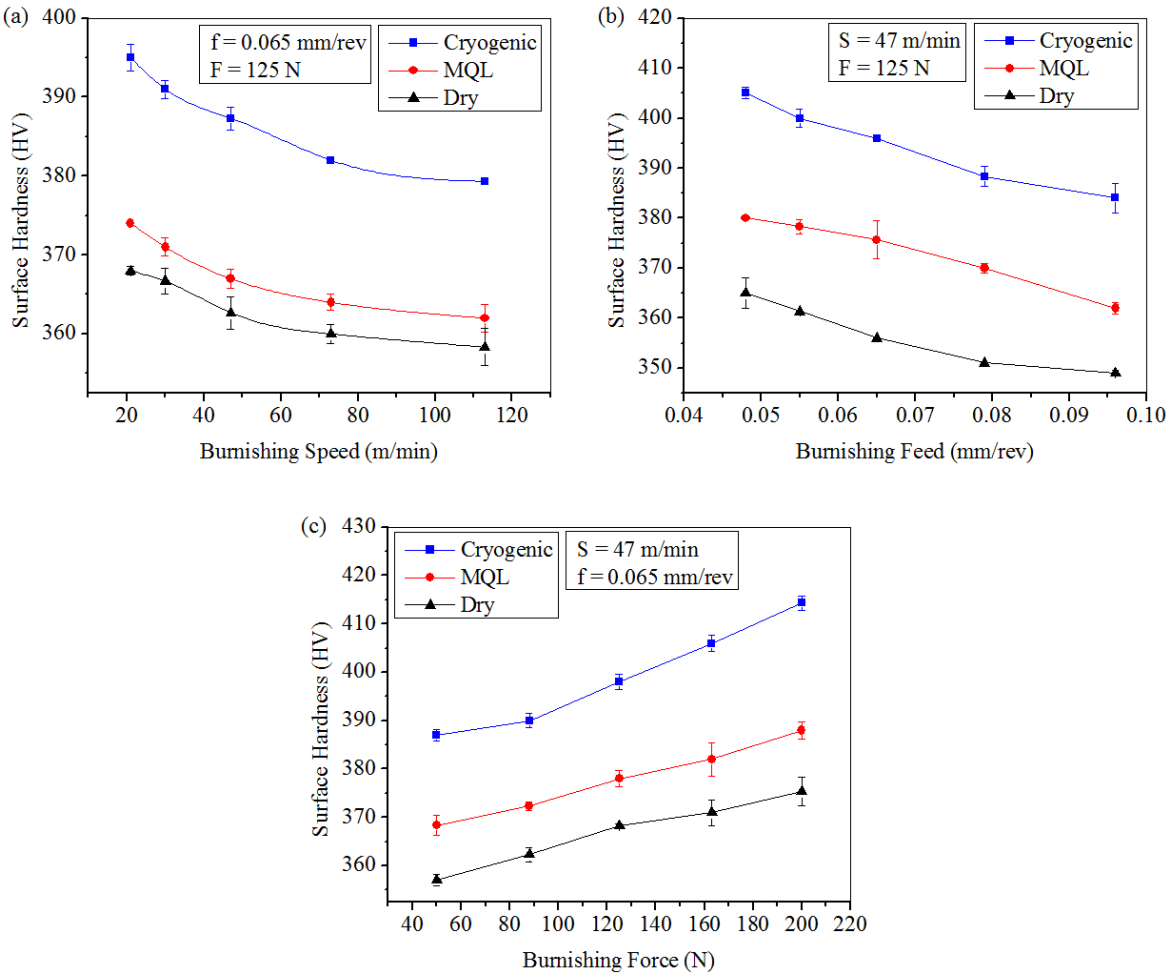

Figure 5.5 Variation of surface hardness at varying (a) burnishing speed (b) burnishing feed and (c) burnishing force under cryogenic, MQL and dry environments.

5.6.2 Effect of burnishing feed and cryogenic cooling on surface hardness

Figure 5.5(b) illustrates the variation of surface hardness with burnishing feed. The decrease in the surface hardness of the material was noted at burnishing speed of 47 m/min, burnishing force of 125 N and varying burnishing feed. The surface hardness of the diamond burnished surface decreases with an increase in the burnishing feed from 0.048 mm/rev to 0.096 mm/rev. That's because an increase in the burnishing feed causes a smaller amount of work hardening on the diamond burnished surface due to the minimum area subjected to plastic deformation (Hassan and Al-Bsharat, 1996). The maximum surface hardness enhancement achieved in the cryogenic environment was 6% and 10% respectively when compared to MQL and dry environments. Maximum surface hardness has been achieved under the cryogenic environment. It is owing to the strain hardening effect observed in the cryogenic environment because of the continuous cooling effect of the LN_2.

5.6.3 Effect of burnishing force and cryogenic cooling on surface hardness

From Figure 5.5(c) it has been observed that the surface hardness constantly increases with an increase in the burnishing force from 50 N to 200 N. This trend has been observed for burnishing speed of 47 m/min, burnishing feed of 0.065 mm/rev and varying burnishing force. Continuous improvement of surface hardness was observed because of the increase in the work hardening and also due to the increased surface deformation during diamond burnishing (Lyons and Nemat, 2000; Hassan, 1997a). The maximum surface hardness of 414 HV was noticed for burnishing force of 200 N under cryogenic environment. The surface hardness of 388 HV and 375 HV respectively was observed under MQL and dry environments. In the cryogenic environment, enhanced surface hardness was observed. It can be explained by the fact that the material becomes stronger and harder due to the impingement of LN_2 at the tool-workpiece interface.

Overall, from the above experimental findings, it was noticed that the effect of MQL has a major impact on the diamond burnishing process. The reason being, during the application of MQL low quantity of lubricant is supplied to the burnishing zone in the form of a mist

which forms a fine spray. At this condition, the temperature at the burnishing zone is minimized. Hence an improved surface finish and surface hardness were achieved by using MQL environment in contrast with the dry environment. In a dry environment because of the absence of the lubrication, the temperature at the tool and workpiece interface increases which causes friction and thermal softening. Hence the surface hardness recorded for the dry environment is less than cryogenic and MQL which has been shown in Figure 5.5(a), (b) and (c) for varying burnishing speed, burnishing feed and burnishing force respectively.

5.7 ANALYSIS OF SUBSURFACE MICROHARDNESS

The subsurface microhardness of the burnished surface was studied to understand the effect of diamond burnishing process parameters on 17-4 PH stainless steel. Previous studies (Revankar et al. 2014; Yang et al. 2011; Huang et al. 2015) related to burnishing shows that the subsurface microhardness of the material decreases as the depth from the surface increases. In the present study, the subsurface microhardness measurement has been carried out at a constant burnishing feed of 0.065 mm/rev, burnishing speed of 47 m/min and burnishing force of 125 N which is as represented in Figure 5.6. The subsurface microhardness of the bulk material was also measured in order to compare the variation of subsurface microhardness before and after diamond burnishing under different cooling environments. From Figure 5.6, it is clear that the subsurface microhardness of the material decreases as the depth from the diamond burnished surface increases. In all the three environments, the trend is observed to be the same. The reason for this may be due to less shearing between the diamond tip and workpiece (Sachin et al. 2018b). And also may be due to the lower strain induced by diamond burnishing (Revankar et al. 2014). As the depth increases beyond 130 microns, a minor difference has been observed and it was also noticed that if the depth from the surface increases, the subsurface microhardness of the material approaches the microhardness of the bulk material. The bulk material microhardness was found to be 340 HV. Beneath the diamond burnished surface, the subsurface microhardness was observed to be maximum because of the work hardening process which has been experienced by the diamond burnished top surface layer of the material. An improvement of 7% and 9% have been attained under the cryogenic

environment contrasted with MQL and dry environments respectively. This impact is because of the viable infiltration of LN_2 at the burnishing zone, creating significant declining of burnishing temperatures, reducing the friction between the contact surfaces (Pu et al. 2011).

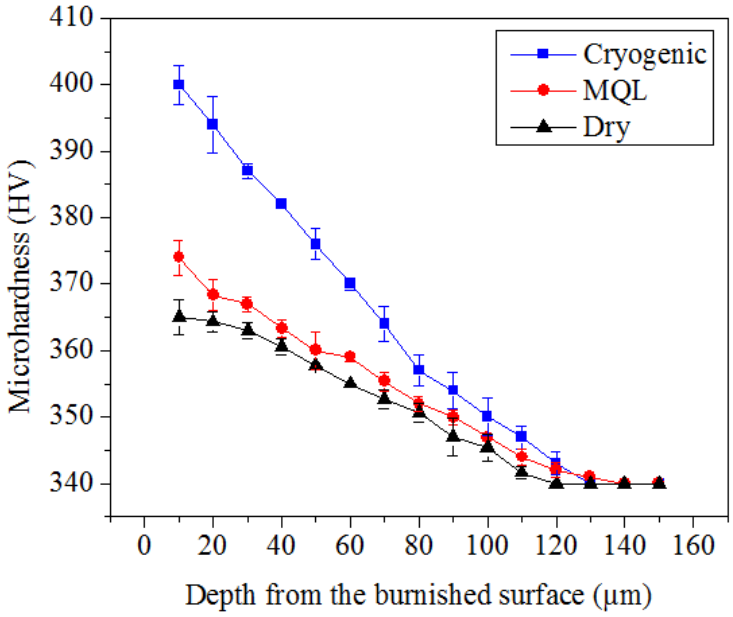

Figure 5.6 Subsurface microhardness found at burnishing speed of 47 m/min, burnishing force of 125 N and burnishing feed of 0.065 mm/rev under cryogenic, MQL and dry environments.

5.8 ANALYSIS OF RESIDUAL STRESS

Residual stress plays a significant role in enhancing the fatigue strength of the component. The residual stresses formed on the surface of the diamond burnished samples were measured using X-Ray diffraction technique. Electrolytic polishing has been carried out to remove the layer of the material before measuring residual stress. The equipment is initialized for about 15 minutes to warm up the system and the X-ray tube is excited to an appropriate level before starting the measurements. The test piece is placed on a suitable fixture & the area where the stress analysis has to be carried out is focused manually in the equipment. The measurements were carried out by setting the parameters in accordance

with the details of the test sample. The residual stress measurement has been performed for burnishing speed of 47 m/min, burnishing force of 125 N and burnishing feed of 0.065 mm/rev. From the previous discussion about the surface roughness, surface hardness, and subsurface microhardness, it was noted that the above-mentioned process parameters yield a better result. Hence these levels of process parameters have been considered for the study.

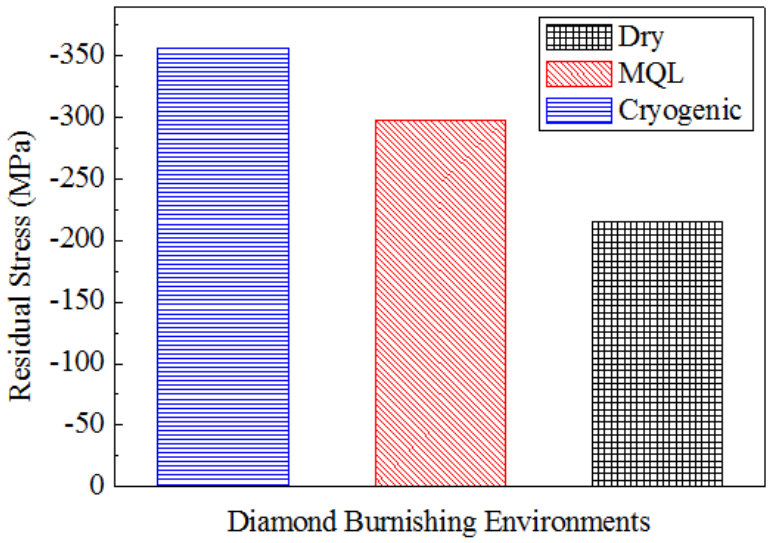

Figure 5.7 Residual stress of the diamond burnished sample taken at burnishing feed of 0.065 mm/rev, burnishing force of 125 N and burnishing speed of 47 m/min for different environments.

Distribution of the residual stress is depicted in Figure 5.7. It has been observed that compressive residual stresses were induced after performing diamond burnishing. The highest compressive residual stress of -356 MPa has been observed for the cryogenic environment. The compressive residual stress of -298 MPa and -215 MPa was observed under MQL and dry environment respectively. The formation of the compressive residual stress enhances the fatigue resistance of the material by retarding the formation and growth of the cracks on the diamond burnished surface (Maximov et al. 2018). Most of the authors discuss that the burnishing force is one of the important parameters which influences the formation of compressive residual stress on the surface. When the applied burnishing force

increases, it leads to increased plastic deformation on the surface layer (Revankar et al. 2014).

5.9 INFLUENCE OF NUMBER OF PASS AND DIAMOND SPHERE DIAMETER ON PERFORMANCE CHARACTERISTICS

This section describes the impact of additional process parameters used in the diamond burnishing process such as number of pass and diamond sphere diameter on the performance characteristics of diamond burnishing process. From the previous discussion, it was observed that the cryogenic cooling condition had produced excellent result in contrast with MQL and dry conditions. Hence, further studies were performed by considering the only cryogenic cooling condition as the mode of lubrication. As discussed in the previous section, a similar experimental setup and a novel diamond burnishing tool was considered for the study. The factors and levels considered are specified in Table 5.2.

Table 5.2 Experimental control factors.

Burnishing factors		**Levels**		
		1	**2**	**3**
Burnishing feed (A)	mm/rev	0.048	0.071	0.090
Burnishing speed (B)	m/min	25	85	132
Tool-tip diameter (C)	mm	6	8	10
Burnishing force (D)	N	65	120	175

The diamond sphere diameter of 6 mm, 8 mm and 10 mm was considered to study the impact of diamond sphere diameter on the performance characteristics. On the basis of the preliminary investigation, the number of pass (E) of ‘2’ was considered to be constant throughout the process for all the set of experiments. The surface integrity characteristics such as surface roughness, surface hardness, surface morphology, surface topography, subsurface microhardness and residual stress were studied.

5.10 ANALYSIS OF SURFACE ROUGHNESS

5.10.1 Influence of burnishing speed and cryogenic cooling

The surface roughness of the component is a fundamental factor in burnishing to determine the interaction of the workpiece with its environment. Figure 5.8(a) clarifies the impact of burnishing speed on surface roughness for dissimilar tool-tip. The surface roughness reduction was found in the range of burnishing speed from 25 to 85 m/min and an additional increase in the burnishing speed beyond 85 m/min causes further increase in the surface roughness for all the tool-tip. The reason being, at a lower speed the temperature generated at the work-tool interface is less and also the chattering of the tool is minimum and as the burnishing speed exceeds 85 m/min the temperature and the possible chattering at the interface increases which causes the material transformation among the tool-tip and the workpiece (Hassan, 1997b). The effect of cryogenic spraying on burnishing speed has been a major factor. The continuous spraying of the LN_2 helps in minimizing the generated temperature at the workpiece-tool interface, because of which the surface finish of the component will be improved. The maximum surface roughness was noticed for a tool-tip diameter of 10 mm, and minimum surface roughness was attained for a tool-tip diameter of 8 mm. This is ascribed to the increased contact area which decreases the contact pressure and also increases the friction coefficient (Hassan and Al-Bsharat, 1996). The optimal burnishing speed was observed to be 85 m/min and the corresponding surface roughness observed was 0.03 µm. Whereas the surface roughness was deteriorated when the burnishing speed was increased from 85 m/min to 132 m/min and the corresponding surface roughness was observed to be 0.08 µm.

5.10.2 Influence of burnishing feed and cryogenic cooling

The tool-tip diameter of 8 mm yields excellent surface finish at all burnishing feed. The trend of the surface roughness attained for varying burnishing feed is demonstrated in Figure 5.8(b). The surface roughness decreases when there is an increase in the burnishing feed from a lower range to 0.071 mm/rev. As the burnishing feed increases from 0.071 mm/rev, a rapid increase in the surface roughness was observed. It is because, at low

burnishing feed, the gap between the successional traces of the tool-tip on the top layer of the material will be small since the tool movement over the workpiece is slow. A large gap will be formed among the successional traces of the tool-tip at higher burnishing feed and hence, less time will be available to deform the material (Nemat and Lyons, 2000). The cryogenic environment has a possible impact on surface roughness. It is owing to the spraying of the LN_2 at the burnishing zone results in a lower coefficient of friction and also minimum vibration has been observed which leads to minimum feed marks on the specimen. The percentage of reduction found in tool-tip diameter of 8 mm was 29% and 44% in contrast with a tool-tip diameter of 6 mm and 10 mm respectively.

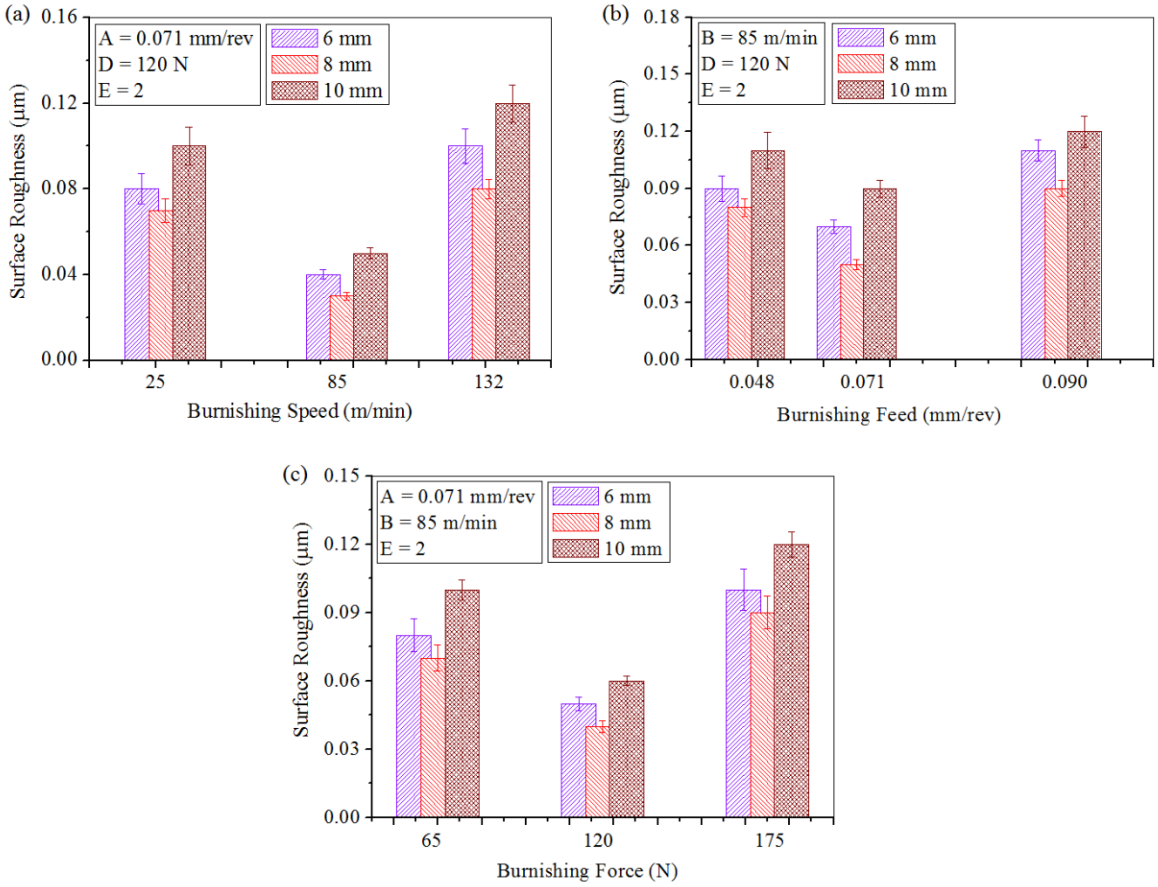

Figure 5.8 Surface roughness observed at varying (a) burnishing speed (b) burnishing feed and (c) burnishing force.

5.10.3 Influence of burnishing force and cryogenic cooling

An adverse impact of burnishing force on the roughness is indicated in Figure 5.8(c). At a lower burnishing force, the surface roughness decreases, and it increases if there is an increase in the burnishing force from 120 N to 175 N. This is due to the incomplete plastic deformation occurring at a lower burnishing force which causes reduced surface roughness. At a higher burnishing force, the repeated plastic deformation on the surface layer increases the work hardening which causes flaking, and it could also be a cause for the deteriorated surface finish (Low and Wong, 2011). Also, the presence of LN_2 in the burnishing zone helps to prevent the chemical and mechanical degradation of the workpiece which helps in improving the surface finish. It was noticed that the minimum surface roughness was recorded for the tool-tip diameter of 8 mm at 120 N burnishing force. It was found that the surface roughness was reduced to 0.04 µm at a tool-tip diameter of 8 mm and a burnishing force of 120 N. At low burnishing force, the surface roughness recorded for 8 mm tool-tip diameter was 0.07 µm.

5.11 ANALYSIS OF SURFACE MORPHOLOGY

The cryogenic diamond burnished surface images were captured by SEM at a burnishing feed of 0.071 mm/rev, burnishing speed of 85 m/min, number of pass of 2 and burnishing force of 120 N at varying the tool-tip diameter of 6 mm, 8 mm and 10 mm which are represented in Figure 5.9. From Figure 5.9, it has been noticed that uniform surface has been generated after cryogenic diamond burnishing operation at varying the tool-tip diameter of 6 mm, 8 mm and 10 mm respectively. Temperature induced at the burnishing zone has been minimized with the help of LN_2 which has been sprayed continuously during burnishing. An easy flow of the material will be initiated soon after performing burnishing and cooling the burnishing zone. Hence, the most regular surface was observed at all the tool-tip diameter. The easy flow of the particles results in the filling of most of the microvoids formed during diamond burnishing. Therefore the surface roughness of the material has been minimized at the above-mentioned burnishing condition. A similar result has been recorded during the analysis of surface roughness in Figure 5.8(a), (b) and (c)

respectively. Feed marks have been generated which is a cause for the deteriorated surface. However, the feed marks were invisible in a tool-tip diameter of 8 mm.

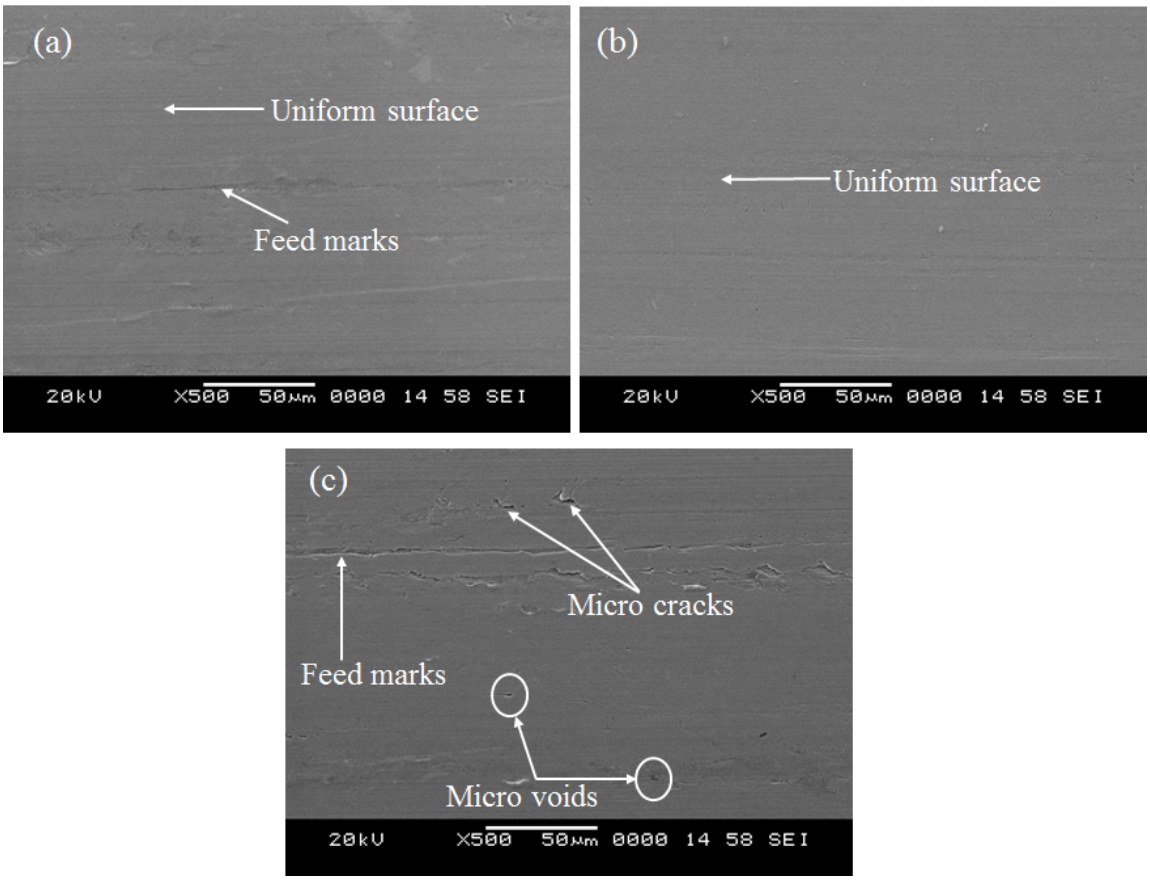

Figure 5.9 Diamond burnished surface observed at diamond sphere diameter of (a) 6 mm (b) 8 mm (c) 10 mm.

It may be because of the pronounced cooling effect of the LN_2 in the burnishing zone. Microvoids and microcracks have been found in the case of a tool-tip diameter of 6 mm and 10 mm, but it was reduced in the case of a tool-tip diameter of 8 mm. The reason for the formation of microcracks is due to the improper cooling in the burnishing zone which retains the heat produced at the interface of the tool and workpiece.

5.12 ANALYSIS OF SURFACE TOPOGRAPHY

The surface topography represents the deviation present over the surface from a regular plane. It is an important investigation which clearly shows the surface texture of the sample. The images were captured on the diamond burnished surface. Surface topography has been measured at the burnishing speed = 85 m/min, burnishing feed = 0.071 mm/rev, number of pass = 2, burnishing force = 120 N and varying tool-tip diameter of 6 mm, 8 mm and 10 mm which is represented in Figure 5.10(a), (b) and (c) respectively.

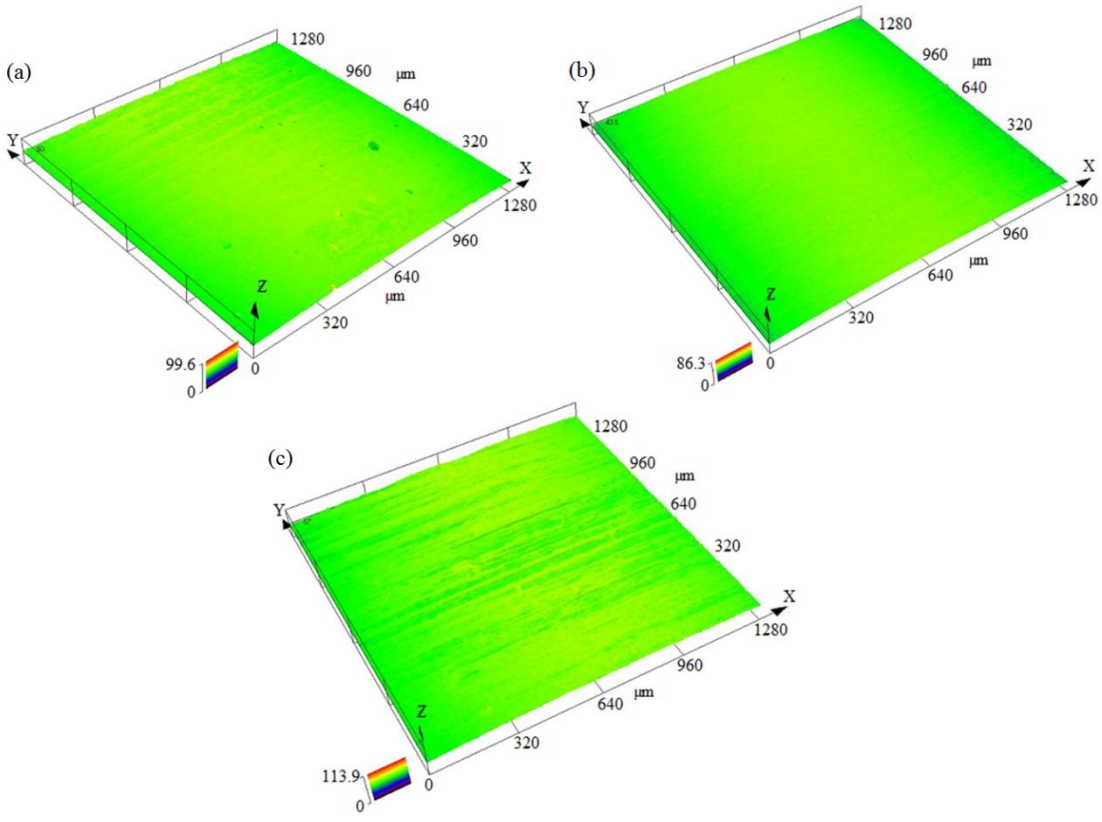

Figure 5.10 Surface topography of the burnished surface observed at diamond sphere diameter of (a) 6 mm (b) 8 mm (c) 10 mm.

The experimental investigation revealed that slight variation had been observed in the topography of the diamond burnished surface at the tool-tip diameter of 6 mm, 8 mm and 10 mm respectively. 10 mm and 6 mm tool-tip diameter produces a slightly rough surface

compared to 8 mm tool-tip. The tool-tip diameter of 6 mm provides a low point of contact, and similarly, the area of contact will be more when the tool-tip diameter of 10 mm was used to burnish the material. Hence, in both cases, a comparatively rough surface was generated. The cryogenic cooling in the burnishing zone causes less distortion which might be a possible advantage of using cryogenic cooling during burnishing to improve the surface texture. In the preceding discussion of morphology, it was seen that the tool-tip diameter of 8 mm had yielded improved surface finish when compared to the other two tool-tip diameters. A similar observation has been made in the surface topography analysis. Hence from the experimental outcomes of surface morphology and topography, it was decided that the improved surface texture can be accomplished for a tool-tip diameter of 8 mm in contrast with the other two spherical tool-tip diameters.

5.13 ANALYSIS OF SURFACE HARDNESS

5.13.1 Influence of burnishing speed and cryogenic cooling

The variation of surface hardness at a burnishing feed = 0.071 mm/rev, burnishing force = 120 N, number of pass = 2 and varying burnishing speed is framed in Figure 5.11(a). It has been observed that a decreasing trend of surface hardness has been achieved at all tool-tip diameters while the burnishing speed range is between 25 m/min to 132 m/min. As the burnishing speed increases, the surface temperature also increases because of plastic deformation. At this point, retrieval of the work hardened material occurs. Hence a decreasing trend of surface hardness has been achieved (El-Taweel and El-Axir, 2009). Working under LN_2 minimizes the temperature generated in the burnishing zone with the cooling effect, which also reduces the heat generation. From Figure 5.11(a) it can be observed that the smallest tool-tip diameter provides excellent surface hardness. The maximum surface hardness noticed in the cryogenic environment was 397 HV.

5.13.2 Influence of burnishing feed and cryogenic cooling

It has been noticed in Figure 5.11(b) that the surface hardness at different tool-tip diameter produces the decreasing trend. The experimental results were observed for 17-4 PH

stainless steel at a varying burnishing feed, a constant burnishing speed of 85 m/min, number of pass of 2, and burnishing force of 120 N. A decreasing trend of the surface hardness was noticed from low to high range of burnishing feed. That's because an increase in the burnishing feed to higher range causes an increment in the succeeding distance between the tool-tip traces. If the distance is more, the extent of plastic deformation decreases (Nemat and Lyons, 2000). The presence of LN_2 increases the strain hardening effect which in turn yields the maximum surface hardness which has to be attained under this cooling environment. Maximum surface hardness observed for a tool-tip diameter of 6 mm was verified to be 406 HV and succeeding surface hardness observed for 8 mm and 10 mm tool-tip diameter was 401 HV and 397 HV respectively for same working condition.

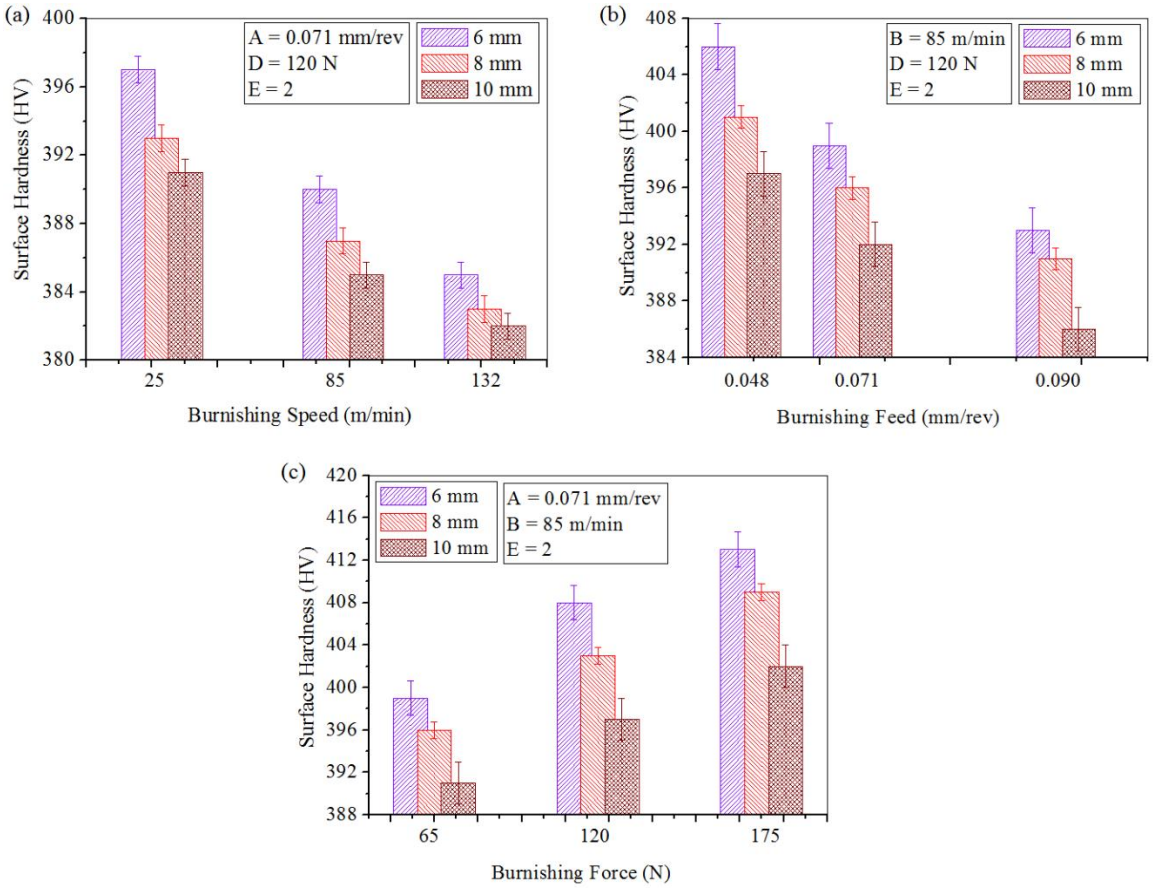

Figure 5.11 Surface hardness at varying (a) burnishing speed (b) burnishing feed and (c) burnishing force.

5.13.3 Influence of burnishing force and cryogenic cooling

As illustrated in Figure 5.11(c), a considerably increasing trend of surface hardness has been observed for all the tool-tip diameters. The burnishing feed = 0.071 mm/rev, burnishing speed = 85 m/min, number of pass = 2, and varying burnishing force were considered. Surface hardness increases as the burnishing force increase from 65 N to the maximum range considered, i.e., 175 N. It is owing to the impact of increased plastic deformation on the workpiece surface. Another reason may be due to the formation of increased internal compressive residual stresses (Hassan, 1997a). The maximum surface hardness recorded was 413 HV, 409 HV and 402 HV respectively for the tool-tip diameter of 6 mm, 8 mm and 10 mm. Working in a cryogenic environment has an advantage in increasing the surface hardness of the specimen. Impingement of LN_2 in the burnishing zone reduces the thermal softening effect which is caused by the sudden increase in the temperature and this considerably maximizes the surface hardness.

5.14 INFLUENCE OF SPHERICAL DIAMOND TIP

From the previous discussion about the surface hardness and surface roughness, the tool-tip proves to have an immense effect on the diamond burnishing process in the cryogenic environment. The larger tool-tip diameter covers a larger contact area amongst the work material and the spherical tool-tip. Hence the penetration of the tool-tip into the work material is smaller in comparison with a smaller tool-tip diameter under a specific applied burnishing force and also the frictional heat developed in the burnishing zone will be higher. The time duration at which the asperities on the surface will be in contact with the workpiece is higher in contrast to the smaller tool-tip diameters (Hassan and Al-Bsharat, 1996; Low and Wong, 2011). In the preceding section, it was observed that the surface finish attained while using 8 mm tool-tip diameter was much improved than it was with 6 mm and 10 mm tool-tip diameter. Under all the working condition, it was predicted that the surface penetration observed while using the 6 mm and 10 mm tool-tip diameter may not be adequate to clean up all the asperities which were accumulated on the surface and hence the surface roughness observed was higher in contrast with the 8 mm tool-tip

diameter. It was also observed that the 6 mm tool-tip diameter yields maximum surface hardness in comparison with the other two tool-tip diameters. It is owing to the deeper penetration of the tool-tip occurring while using 6 mm tool-tip in assessment with 8 mm and 10 mm tool-tip diameter. Overall, it has been perceived that the tool-tip of 8 mm and 6 mm diameter respectively yields improved surface finish and surface hardness in the cryogenic environment.

5.15 ANALYSIS OF SUBSURFACE MICROHARDNESS

The analysis of subsurface microhardness of the diamond burnished specimen is a major aspect because after performing diamond burnishing the subsurface microhardness was expected to be improved, and it is one of the advantages of the diamond burnishing. The variation of the subsurface microhardness of the sample tested at different tool-tip diameter is depicted in Figure 5.12. The variation has been noticed at a burnishing feed = 0.071 mm/rev, burnishing speed = 85 m/min, number of pass = 2, and burnishing force = 120 N. Highest microhardness of the material were recorded for a tool-tip diameter of 6 mm when compared with 8 mm and 10 mm tool-tip diameter. The subsurface microhardness was found to be decreasing for all the three tool-tip diameters. It is owing to a smaller amount of shearing occurring among the diamond tip-workpiece surface and also as a result of low strain inducement (Sachin et al. 2018a; Revankar et al. 2014). Beneath the diamond burnished surface, maximum microhardness was observed and it was found to be 406 HV, 398 HV and 392 HV for 6 mm, 8 mm and 10 mm tool-tip diameter respectively. Maximum microhardness was observed underneath the top layer which is attributed to the effect of work hardening on the surface. The tool-tip diameter of 6 mm has produced maximum microhardness. It is owing to the fact that penetration of the tool-tip is deeper in the case of tool-tip of 6 mm diameter in contrast with the other two tool-tip diameters which results in the work hardened surface. Diamond burnishing in the cryogenic environment is also a key point since it significantly declines the generation of high temperature in the working area which also minimizes the friction at the work-tool interface. The decline in the temperature of the burnishing zone causes strain hardening (Rao et al. 2018; Sachin et al. 2018b). It was observed that as the depth of the measurement point increases from the

diamond burnished surface, the microhardness reaches a point where the microhardness of the material will be the same as that of the bulk material.

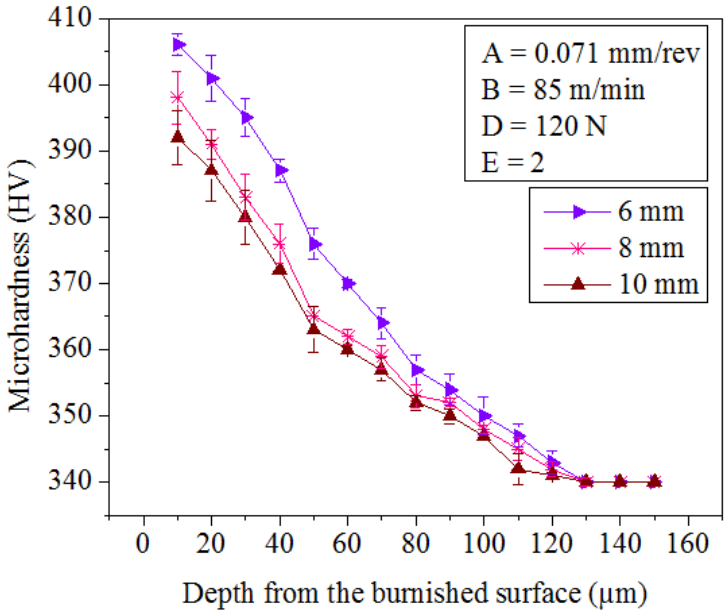

Figure 5.12 Variation of subsurface microhardness.

5.16 ANALYSIS OF RESIDUAL STRESS

The improvement of fatigue life purely depends on the residual stresses induced on the component. Figure 5.13 represents the residual stresses measured for various tool-tip diameters. The measurements were recorded by setting the parameters in accordance with the test sample. The gain is set to the optimum level for better results. All the measurement were performed under an optimum working factor namely a constant burnishing feed = 0.071 mm/rev, varying tool-tip diameters, burnishing speed = 85 m/min, burnishing force = 120 N, and number of pass = 2. The residual stresses induced for the machined specimen was observed to be tensile in nature. However, the introduction of diamond burnishing after performing the turning process has led to the inducement of compressive residual stresses on the top layer of the specimen. It was observed that the residual stresses generated for the tool-tip diameter of 6 mm had produced the highest compressive residual stress of -335 MPa. Whereas, the residual stresses generated after performing diamond

burnishing with a tool-tip diameter of 8 mm and 10 mm was found to be -320 MPa and -305 MPa respectively. It is owing to the deforming anisotropic on account of the cyclic loading of a point from the diamond burnished surface (Maximov et al. 2017). It is one of the major reason for the relaxation of the residual stresses induced on the workpiece. Also, it may be due to the strong deformation of the surface layer taking place at a lower tool-tip diameter and also stress relaxation might have been initiated because of the material fatigue which also results in scaling (Nestler and Schubert, 2015). The residual stress relaxation was found to be increasing as the tool-tip diameter was increasing. Hence from the experimental results, it could be inferred that the tool-tip diameter of 6 mm is a better choice for the generation of maximum compressive residual stress on the surface layer of diamond burnished 17-4 PH stainless steel.

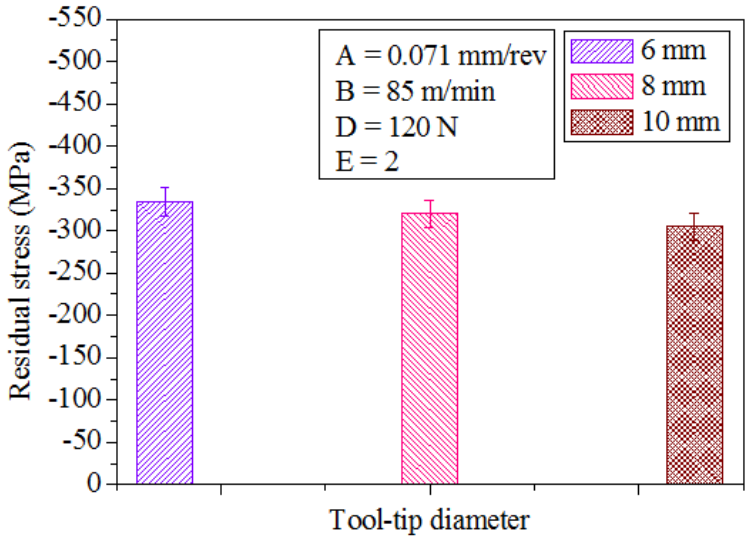

Figure 5.13 Residual stress of the diamond burnished surface.

5.17 SUMMARY

The effect of diamond burnishing on surface integrity characteristics of 17-4 PH stainless steel was studied under cryogenic, MQL and dry environments with a novel diamond burnishing tool. The proposed novel diamond burnishing tool demonstrates a substantial enhancement in the surface and subsurface characteristics of the diamond burnishing

process under the cryogenic environment, which yields an improved performance of the product. As per the findings from the present study, the following conclusions were drawn:

- Surface finish improvement of 33% to 50%, 34 to 51%, and 25 to 40% respectively was observed under the cryogenic environment in contrast with MQL and dry environment at all the levels of burnishing speed, burnishing feed and burnishing force.
- An improvement of 5% to 7%, 6% to 10%, and 6% to 9% respectively were observed in the surface hardness under the cryogenic environment when compared to MQL and dry environment.
- Highest subsurface microhardness was achieved under the cryogenic environment with a percentage improvement of 7% and 9% in contrast with MQL and dry environments.
- Compressive residual stresses of -356 MPa, -298 MPa, and -215 MPa respectively have been achieved under cryogenic, MQL and dry environments.

Two additional process parameters, namely the number of pass and diamond sphere diameter was also considered for the study to understand its influence on the performance characteristics. From the achieved investigational outcomes, the following conclusions were drawn:

- The minimum surface roughness achieved by the cryogenic diamond burnishing at a diamond sphere diameter of 8 mm was found to be 0.03 µm.
- Similarly, at a diamond sphere diameter of 6 mm, the maximum surface hardness was noticed to be 413 HV.
- The surface defect was minimized in a diamond sphere diameter of 8 mm in contrast with 10 mm and 6 mm. Surface intensity of the sample worked under a diamond sphere diameter of 8 mm was reduced after diamond burnishing under the cryogenic environment.
- The percentage enhancement of subsurface microhardness was found to be 2% and 4% respectively for a tool-tip diameter of 6 mm when related to 8 mm and 10 mm.

- Compressive residual stresses were induced on the top layer of all the samples. Highest compressive residual stress attained was -335 MPa for the tool-tip diameter of 6 mm.

CHAPTER-6

GREY RELATIONAL ANALYSIS

6.1 INTRODUCTION

In this chapter, the multi-objective optimization of process parameters under the cryogenic environment was presented. From the discussions of previous chapters, it was found that out of three lubrication/cooling techniques studied, the cryogenic cooling condition provides the best result for the diamond burnishing of 17-4 PH stainless steel. Further, it was also discussed that a novel diamond burnishing tool yields better experimental results in contrast with the conventional diamond burnishing tool. Hence, a novel diamond burnishing tool and the cryogenic cooling condition has been considered for further study. Taguchi based GRA has been used to optimize the process parameters of the diamond burnishing process. The performance characteristics, such as surface roughness and surface hardness were analyzed. ANOVA was also used to find the most significant process parameter.

6.2 EXPERIMENTAL METHOD

Based on the preliminary tests, the diamond burnishing process parameters were determined and the range of the levels was selected by considering the possible minimum, medium and maximum values. The control factors and their respective levels are tabulated in Table 6.1. The experiment was carried out by using a cryogenic cooling condition. A novel diamond burnishing tool was used to perform the experiments. Taguchi L_9 orthogonal array was selected to perform the experiments. The output responses, such as surface roughness and surface hardness were analyzed. The experimental results achieved under the cryogenic cooling condition is tabulated in Table 6.2. The influence of diamond burnishing process parameters on the surface roughness and surface hardness was found from the direct effects plot. Minitab 17.0 software has been used to obtain direct effects

plot. The optimal process parameters were determined from the direct effects plot. ANOVA was performed to understand the effect of each process parameter on the output response and the most significant parameter which influences the diamond burnishing process. Finally, the confirmation test was performed to understand the accuracy of the results attained after performing multi-objective optimization.

Table 6.1 Factors and levels.

Code	Control factor	Level		
		1	2	3
A	Burnishing speed (m/min)	21	73	113
B	Burnishing feed (mm/rev)	0.048	0.065	0.096
C	Burnishing force (N)	50	125	200

Table 6.2 Results for surface roughness, Ra (μm) and surface hardness, H (HV).

Sl. No.	A	B	C	Ra (μm)	H (HV)
1	21	0.048	50	0.12	387
2	21	0.065	125	0.07	383
3	21	0.096	200	0.19	409
4	73	0.048	125	0.03	391
5	73	0.065	200	0.04	409
6	73	0.096	50	0.16	373
7	113	0.048	200	0.1	419
8	113	0.065	50	0.11	367
9	113	0.096	125	0.19	369

6.3 EFFECT OF PROCESS PARAMETERS AND CRYOGENIC COOLING ON THE OUTPUT RESPONSES

6.3.1 Surface roughness analysis

The main effects plot of surface roughness for the cryogenic environment is depicted in Figure 6.1(a-c). In cryogenic diamond burnishing, as the burnishing speed increases from 21 m/min to 73 m/min the surface roughness decreases, and further it increases when the

burnishing speed is increased to 113 m/min as shown in Figure 6.1(a). At lower burnishing speed, reduction in the surface roughness was observed because at this point the diamond tip will have more time to settle down the abnormalities and as the burnishing speed is gradually increased, temperature will also increase at the tool-workpiece interface due to the uneven movement of the tip along the workpiece surface, hence an increased surface roughness was observed (El-Taweel and El-Axir, 2009).

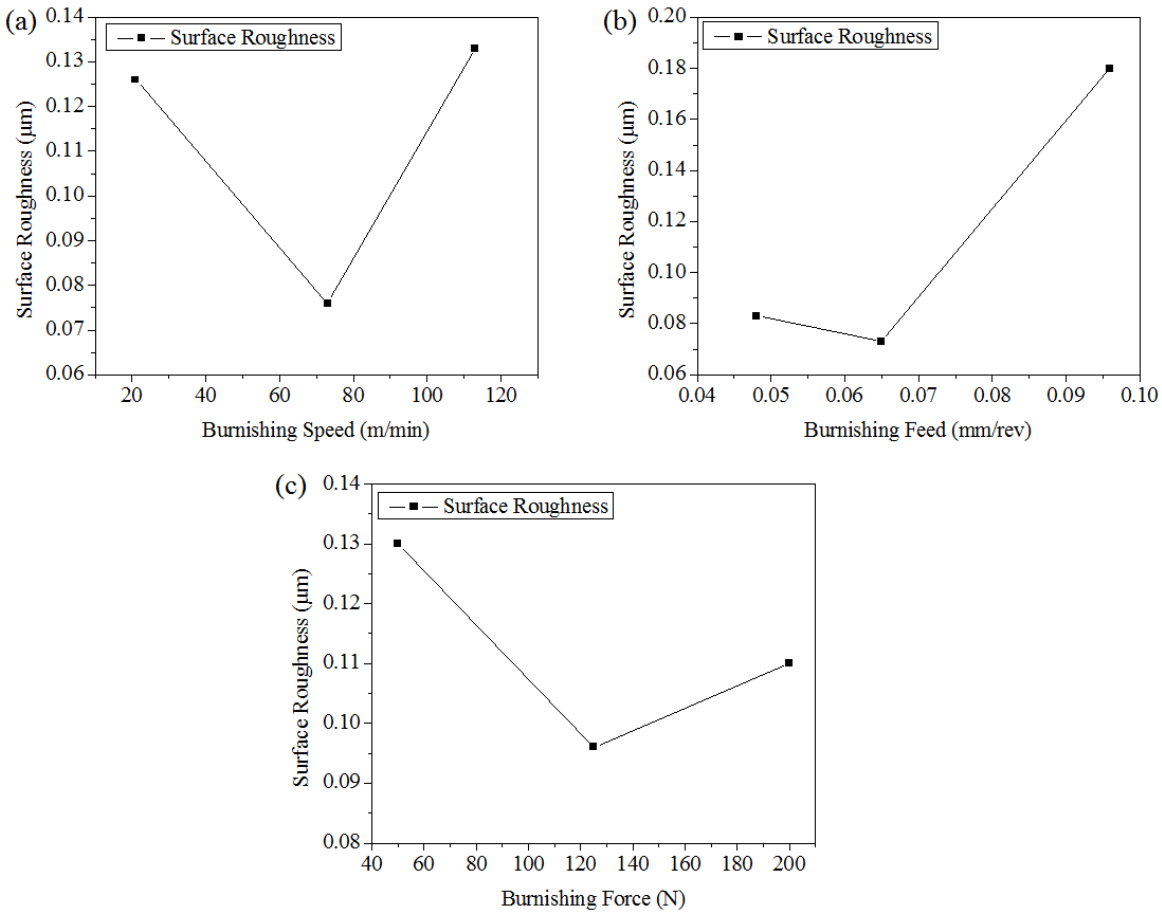

Figure 6.1 Direct effects plot of surface roughness for cryogenic burnishing under varying (a) burnishing speed (b) burnishing feed (c) burnishing force.

As the burnishing feed increases from 0.048 mm/rev to 0.065 mm/rev, the surface roughness decreases and it increases with an increase in the burnishing feed as depicted in Figure 6.1(b). At lower burnishing feed, the distance between the successive traces of the

tool tip is small, hence an improved surface finish can be observed. At higher burnishing feed, the distance between successive traces of the tool-tip will be high hence increased surface roughness can be observed (Deng, 1982). Surface roughness decreases to a minimum value as the burnishing force increases from 50 to 125 N. Further increase in the burnishing force results in an increase in the surface roughness as represented in Figure 6.1(c). It can be explained by the fact that as the burnishing force increases the plastic deformation will be high and which results in the formation of the deteriorated surface (Lyons and Nemat, 2000). The minimum surface roughness of 0.09 µm was observed at burnishing speed of 73 m/min, burnishing feed of 0.048 mm/rev and burnishing force of 125 N. The simultaneous application of LN_2 reduces the temperature developed at the burnishing zone and it also results in lower friction generation which results in the improved surface finish.

6.3.2 Surface hardness analysis

The surface hardness was measured only on the top surface of the material which has been subjected to cryogenic diamond burnishing. The main effects plot of surface hardness for the cryogenic environment is depicted in Figure 6.2(a-c). In cryogenic diamond burnishing, as the burnishing speed increases from 21 m/min to 113 m/min, the surface hardness decreases as depicted in Figure 6.2(a). That's because, as the burnishing speed increases, the increase in the recovery of the work hardened surface takes place due to the increase in the temperature at the tool-workpiece interface (Klocke et al. 2009). In the Cryogenic environment, as the burnishing feed increases from 0.048 mm/rev to 0.096 mm/rev, the surface hardness decreases as shown in Figure 6.2(b). It is because of the increase in the distances between the consecutive traces of the diamond tip (El-Taweel and El-Axir, 2009). As the burnishing force increases from 50 N to 200 N, the surface hardness increases as represented in Figure 6.2(c). It is due to the improvement in the surface deformation taking place because of the increased burnishing force applied (El-Axir et al. 2008). Improvement in surface hardness was observed at all the process parameters that's because cooling the burnishing zone with the help of LN_2 leads to the formation of grain refinement that results in small grain formation which substantially increases the surface hardness of the material.

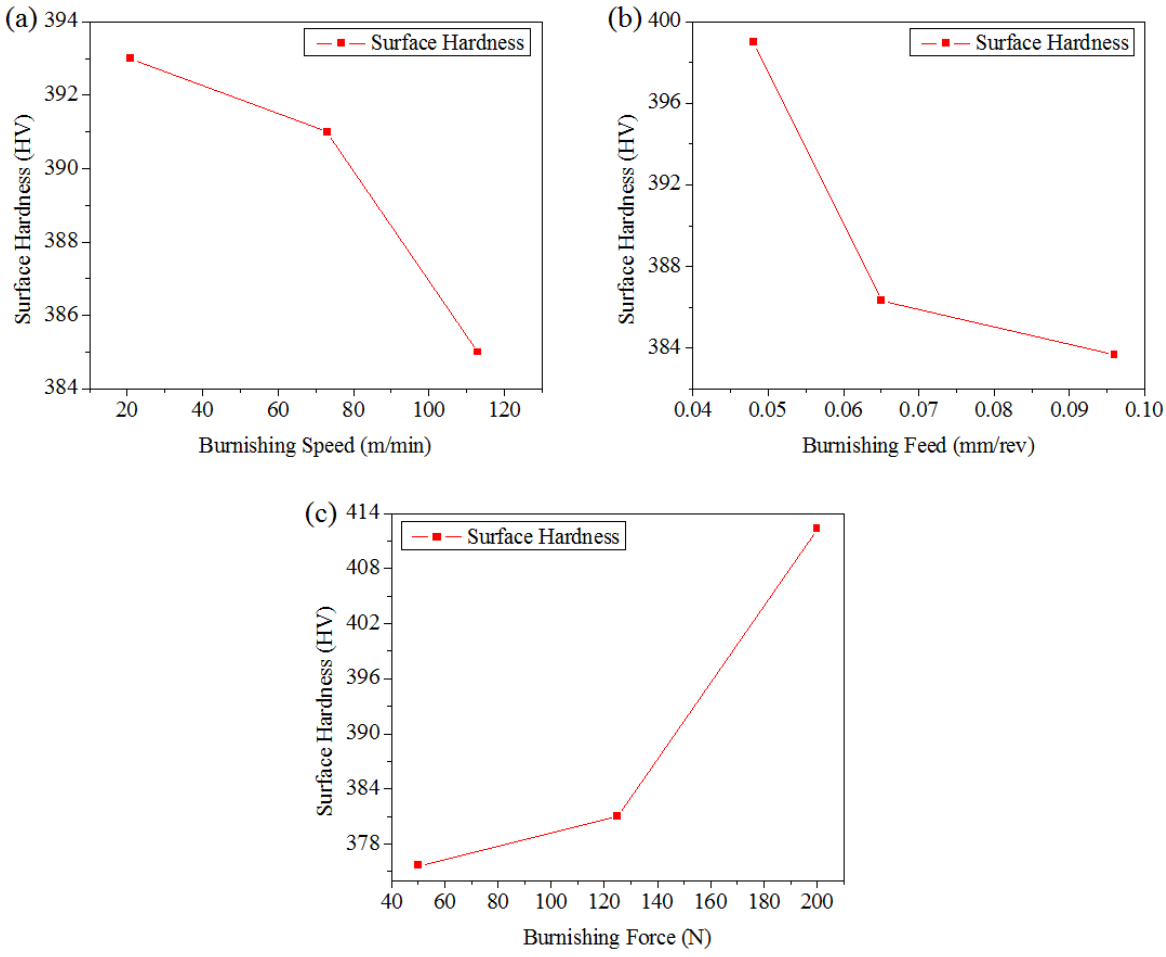

Figure 6.2 Direct effects plot of surface hardness for cryogenic diamond burnishing under varying (a) burnishing speed (b) burnishing feed (c) burnishing force.

6.4 GREY RELATION-BASED TAGUCHI OPTIMIZATION

Grey relation system was proposed by Deng, 1982. It is a tool which is used to analyze the process with multiple performance characteristics. Conversion of actual response values to those values which has been attained by S/N ratios can be found by GRA. This method yields real data based results and also computations are easy to perform. The system which contains the information that is either incomplete or uncertain is called the grey relation system (Sivaiah and Chakradhar, 2017). The multi-objective optimization problems are difficult to solve and with the effective implementation of GRA optimization of performance characteristics can be converted into single optimization with GRG. The

experimental data observed are normalized between the values 0 and 1. Many researchers (Sarıkaya and Güllü, 2015; Goel et al. 2015; Senthilkumar et al. 2014) have incorporated the following steps in TGRA. Flowchart of the grey relation based Taguchi optimization is described in Figure 6.3.

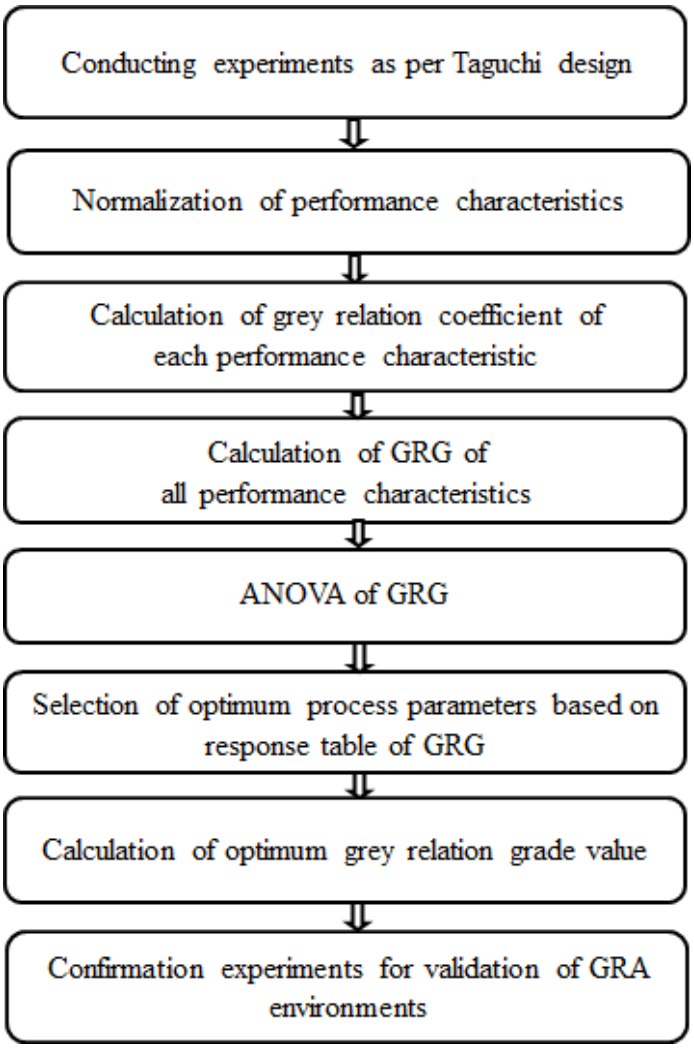

Figure 6.3 Methodology flow chart.

6.4.1 Pre-processing of data

Normalization is defined as a process of converting the original sequence into the comparable data sequence. The raw data from the different factors are normalized on a single scale of dimensions from multi-dimensions scales and are unified. The range of

normalized values has to be performed in the range of zero to one. The normalization process is based on three categories: “the larger the better” for maximization objectives, “the nominal the better” for specific objective expectation and “the smaller the better” for minimization objective.

Table 6.3 Pre-processing and deviation sequence data for surface roughness and surface hardness.

Trial No.	Pre-processing sequence		Deviation sequence	
	Ra (µm)	H (HV)	Ra (µm)	H (HV)
1	0.438	0.385	0.563	0.615
2	0.750	0.308	0.250	0.692
3	0.000	0.808	1.000	0.192
4	1.000	0.462	0.000	0.538
5	0.938	0.808	0.063	0.192
6	0.188	0.115	0.813	0.885
7	0.563	1.000	0.438	0.000
8	0.500	0.000	0.500	1.000
9	0.000	0.038	1.000	0.962

In this research due to minimization and maximization of the objectives “the smaller the better” and “larger the better” normalization function is adapted for surface roughness and surface hardness respectively, which is defined in Equation 6.1 and Equation 6.2 respectively. The normalized data are depicted in Table 6.3.

$$D_i(r) = \frac{max\, E_i\,(r) - E_i\,(r)}{max\, E_i\,(r) - min E_i\,(r)} \qquad (6.1)$$

$$D_i(r) = \frac{E_i\,(r) - min E_i\,(r)}{max\, E_i\,(r) - min E_i\,(r)} \qquad (6.2)$$

Where, $E_i(r)$ is the original sequence, $D_i(r)$ is sequence after data pre-processing, max $E_i(r)$ and min $E_i(r)$ are the maximum and minimum values of the original data respectively.

6.4.2 Grey relation coefficient

The relationship between the investigational and desirable results can be defined by calculating the grey relation coefficient. The grey relation coefficient can be computed by adapting Equation 6.3.

$$\varepsilon_i = \frac{\Delta_{min} + \zeta\Delta_{max}}{\Delta_{0i}(r) + \zeta\Delta_{max}} \quad (6.3)$$

Where $\Delta_{0i}(r)$ indicates absolute sequence deviation of sequence reference $D_0(r)$ and comparability sequence $D_i(r)$, i is the number of characteristics (1, 2, 3, 4) and r is the number of experimental runs (1, 2,……., 9). Hence $\Delta_{0i}(r)$ can be written as:

$$\Delta_{0i}(r) = \left| D_0(r) - D_i(r) \right| \quad (6.4)$$

$$\Delta_{min} = min_i\, min_r\, \Delta_{0i}(r) \quad (6.5)$$

$$\Delta_{max} = max_i\, max_r\, \Delta_{0i}(r) \quad (6.6)$$

The distinguishing co-efficient can have a value $\zeta \in [0, 1]$ and in this study $\zeta = 0.5$ has used to correct the difference of the relation co-efficient (Mia et al. 2017). The computed difference sequence is listed in Table 6.3 and grey relation co-efficient in Table 6.4. Equations (6.4), (6.5) and (6.6) are used to calculate the values of Δ_{0i}, Δ_{min}, *and* Δ_{max}.

Table 6.4 Grey relation coefficient and grades of grey relation.

Trial No.	Grey relational co-efficient		Grey relational grade		
	Ra (µm)	H (HV)	Magnitude	S/N ratio	Order
1	0.471	0.448	0.459	-6.75557	6
2	0.667	0.419	0.543	-5.30383	4
3	0.333	0.722	0.528	-5.55098	5
4	1.000	0.481	0.741	-2.60668	3
5	0.889	0.722	0.806	-1.87809	**1**
6	0.381	0.361	0.371	-8.61178	8
7	0.533	1.000	0.767	-2.30787	2
8	0.500	0.333	0.417	-7.60422	7
9	0.333	0.342	0.338	-9.42888	9

6.4.3 Grey relational grade

Estimation of characteristics of multiple performances is computed by GRG. The means of grey relation coefficient gives the GRG. Equation 6.7 is used to calculate GRG $\gamma_i(r)$ and achieved results along with GRG ranks are tabulated in Table 6.4.

$$\gamma_i(r) = \frac{1}{N}\sum_{i=0}^{n}[\omega_i * \varepsilon_i(r)] = \frac{1}{N}\sum_{i=0}^{n}\varepsilon_i(r) \qquad (6.7)$$

Where

N = is the no. of performance characteristics

ω_i = weights. In the present work, it is assumed that all control factors have equal importance.

Generally, the value should be in the range of 0 to1 ($0< \omega_i <1$). The larger GRG, the closer is the corresponding experimental responses to ideal values. It has been observed that multiple factors are transformed into single factors and preserved as a single-objective optimization problem. The "larger the better" approach is used in obtaining the signal-to-noise ratio for GRG. The signal-to-noise ratio values of GRG are tabularized in Table 6.4, and Minitab 17 software is used to compute the average for each level of control factors and the results are tabularized in Table 6.5. GRG results of each parameter such as burnishing speed, burnishing feed, and burnishing force are depicted in Figure 6.4(a-c) respectively. From the analysis of means, $A_2B_1C_3$ is determined as the predicted optimal factors. The optimum factors are burnishing speed of 73 m/min, burnishing feed of 0.048 mm/rev and burnishing force of 200 N.

Table 6.5 Response table for average GRG.

Control factors	Level 1	Level 2	Level 3	Delta	Rank
A	0.5101	0.6391	0.5070	0.1321	3
B	0.6556	0.5884	0.4122	0.2434	2
C	0.4157	0.5405	0.7000	0.2843	1

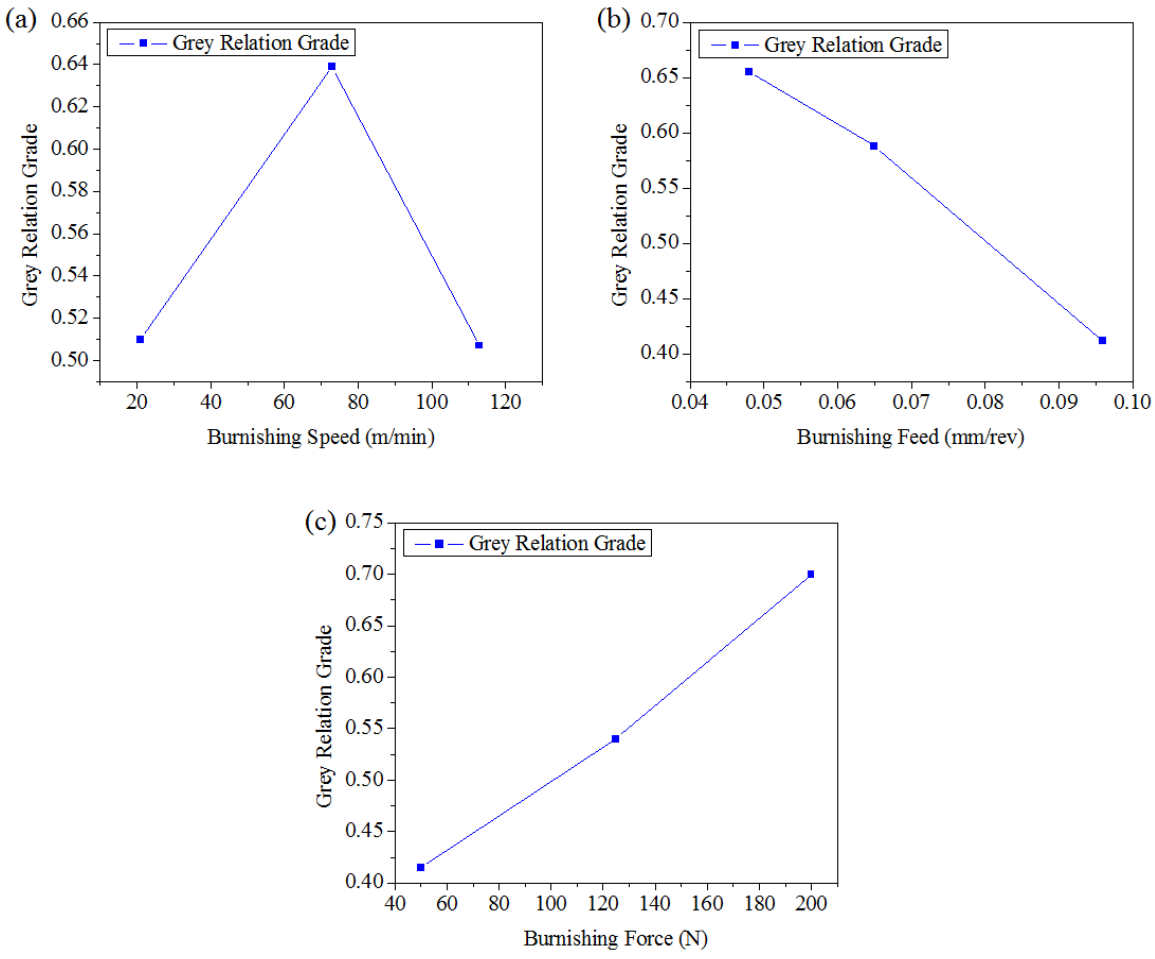

Figure 6.4 Main effects plot of mean of means for GRG at varying (a) burnishing speed (b) burnishing feed (c) burnishing force.

6.5 ANALYSIS OF VARIANCE

To determine the effect of individual process parameters on diamond burnishing performance characteristics, ANOVA has been performed for GRG data. From Table 6.6, it is observed that burnishing force has the highest contribution of 48.29% and is the most influencing parameter on diamond burnishing process. Next, most influencing process parameter is burnishing feed with a contribution of 37.58%. Burnishing feed is directly proportional to the surface roughness. The least possible contribution of 13.52% is observed in burnishing speed.

Table 6.6 ANOVA of GRG.

Factors	Degrees of freedom	Sum of square	Mean square	Factors Contribution (%)
A	2	0.0341	0.0170	**13.52**
B	2	0.0948	0.0474	**37.58**
C	2	0.1218	0.0609	**48.29**
Residual error	2	0.0014	0.0007	0.55
Total values	8	0.2522	-	-

6.6 CONFIRMATION EXPERIMENTS

To validate the perfection of performance characteristics while machining 17-4 PH stainless steel by using novel diamond burnishing tool confirmation assessment was performed. Optimum control factors selected for the confirmation test is given in Table 6.7. The predictable GRG $\gamma_{predicted}$ using optimal conditions of the machining factors can be computed by using Equation 6.8.

$$\gamma_{predicted} = \gamma_m + \sum_{i=1}^{k}(\gamma_0 - \gamma_m) \qquad (6.8)$$

Where γ_m is the average of total grey relation grade, γ_0 is the means of GRG at their optimal levels, and k is the number of machining factors that considerably affects the multiple performance characteristics.

Table 6.7 Confirmation test.

	Initial conditions	Optimal conditions	
		Prediction	Experimental
Level	$A_1B_1C_1$	$A_2B_1C_3$	$A_2B_1C_3$
Ra (µm)	0.12	----	0.07
H (HV)	387	----	416
Grey relation grade	0.459	0.8907	0.805
The improvement in grades of grey relation is 0.34			
The percentage improvement in GRG is **42.98**			

The confirmation experimentations have been carried out at the optimal levels of performance measures. The GRG values of the confirmation test, initial and predicted are shown in Table 6.7. It was observed that the GRG attained at optimum cutting parameters

combination is higher than that of the first experiment of Taguchi's L_9 orthogonal array. The improvement of GRG was observed to be 42.98%. From the GRA analysis, it was observed that the application of this technique was successful in improving the performance characteristics of the material after performing diamond burnishing under the cryogenic cooling condition.

6.7 SUMMARY

In this chapter, the diamond burnishing output responses, namely surface roughness, and surface hardness are optimized with respect to burnishing process conditions such as burnishing speed, burnishing feed and burnishing force at different levels. The 17-4 PH stainless steel was diamond burnished under the cryogenic environment by using a novel diamond burnishing tool. TGRA was successfully applied in the present research work to solve the multi-objective optimization problem effectively. The cryogenic cooling condition was proved to be essential in improving the performance characteristics of 17-4 PH stainless steel while performing diamond burnishing. The following conclusions were drawn from the experimental results.

- From the multi-response optimization outcomes, the optimal process parameters were found to be burnishing speed 73 m/min, burnishing feed 0.048 mm/rev and burnishing force 200 N to minimize the surface roughness and maximize the surface hardness.
- At the optimal condition, improvement in the surface finish and surface hardness was found to be 42% and 7% respectively.
- From the response table, it was observed that the burnishing force is the most influencing process parameter with a rank 1, followed by burnishing feed and the burnishing speed which has rank 2 and 3 respectively.
- ANOVA results prove that the burnishing force has the highest contribution of 48.29% and is the most influencing parameter on the diamond burnishing process. Next, most influencing process parameter is burnishing feed with a contribution of 37.58%. The least possible contribution of 13.52% is observed in burnishing speed.

- The enhancement of GRG from primary parameter specifically $A_1B_1C_1$, to the optimum parameter combination $A_2B_1C_3$, was found to be 0.34. The improvement of GRG was observed to be 42.98%.

CHAPTER-7

MODELING USING RESPONSE SURFACE METHODOLOGY AND GENETIC ALGORITHM

7.1 INTRODUCTION

In this chapter, an attempt has been made to propose a realistic cryogenic diamond burnishing condition for improvement of the process. RSM has been incorporated into the design of experiments. Initially, the impact of process conditions, namely burnishing force, burnishing feed, and burnishing speed on surface hardness and surface roughness was examined by experimental analysis. The significant influence of burnishing conditions on the output responses was established by ANOVA. The regression technique was used to develop an empirical model. Optimization of control factors for obtaining minimum surface roughness and maximum surface hardness was achieved by using MOGA. The results obtained by performing MOGA has been validated by confirmation experiments.

7.2 EXPERIMENTAL METHOD

The burnishing experiments have been carried out at different levels and process parameters as tabulated in Table 7.1. Based on the literature survey on diamond burnishing process and the set of trial experiments carried out on the 17-4 PH stainless steel workpiece, the set of control factors and their levels has been carefully chosen. The experiments were carried out in the cryogenic cooling condition by a novel diamond burnishing tool. The experiments were carried out by considering the RSM based face-centered CCD. The software used for the design of the experiment is Design Expert 10.0 and Table 7.2 tabulates the experimental results attained. The regression equation developed using RSM has been considered as the input to MOGA. The optimal results were obtained by

conducting the trial and error method. MOGA in Matlab optimization toolbox has been used to try different burnishing conditions and to attain the best feasible solution.

Table 7.1 Control factors and their levels.

Burnishing process parameters		**Levels**		
		1	2	3
Burnishing speed (s)	m/min	21	67	113
Burnishing feed (f)	mm/rev	0.048	0.072	0.096
Burnishing force (t)	N	50	125	200

Table 7.2 Experimental results obtained for RSM design.

Sl. No.	**Burnishing speed (m/min)**	**Burnishing feed (mm/rev)**	**Burnishing force (N)**	**Surface roughness (μm)**	**Surface hardness (HV)**
1	67	0.072	125	0.09	368
2	113	0.096	50	0.25	352
3	113	0.048	50	0.25	360
4	67	0.048	125	0.11	380
5	21	0.096	50	0.45	351
6	67	0.096	125	0.09	360
7	67	0.072	200	0.13	385
8	113	0.048	200	0.25	372
9	21	0.048	50	0.29	374
10	113	0.096	200	0.23	355
11	67	0.072	125	0.06	365
12	113	0.072	125	0.11	360
13	21	0.096	200	0.33	395
14	67	0.072	125	0.06	370
15	67	0.072	125	0.06	369
16	21	0.048	200	0.24	417
17	67	0.072	125	0.07	366
18	67	0.072	125	0.03	364
19	21	0.072	125	0.2	382
20	67	0.072	50	0.13	358

7.3 MODELING USING RSM

A quadratic model has been developed by RSM, and the optimization of the control factors has been performed by MOGA. The output responses considered for the study include surface hardness and surface roughness.

7.3.1 ANOVA for surface roughness

The regression model coefficient is represented in Equation (7.1).

$$Ra = +0.78679 - 5.86793E\text{-}003\ s - 8.11370\ f - 3.60181E\text{-}003\ t - 0.030571\ sf + 5.43478E\text{-}006\ st - 6.25000E\text{-}003\ ft + 4.83330E\text{-}005\ s^2 + 82.07071\ f^2 + 1.37374E\text{-}005\ t^2 \text{----------} \mu m \quad (7.1)$$

Table 7.3 ANOVA results attained for surface roughness.

Source	**Sum of squares**	**df**	**Mean square**	**F value**	**p value prob>F**	
Model	0.23	9	0.026	44.21	<0.0001	significant
A	0.018	1	0.018	30.48	0.0003	
B	4.410E-003	1	4.410E-003	7.62	0.0201	
C	3.610E-003	1	3.610E-003	6.24	0.0316	
AB	9.113E-003	1	9.113E-003	15.75	0.0027	
AC	2.813E-003	1	2.813E-003	4.86	0.0520	
BC	1.012E-003	1	1.012E-003	1.75	0.2154	
A^2	0.029	1	0.029	49.70	<0.0001	
B^2	6.145E-003	1	6.145E-003	10.62	0.0086	
C^2	0.016	1	0.016	28.37	0.0003	
Residual	5.787E-003	10	5.787E-004			
Lack of Fit	3.904E-003	5	7.807E-004	**2.07**	0.2214	not significant
Pure Error	1.883E-003	5	3.767E-004			
Cor Total	0.24	19				
Std. Dev.	0.024		R-Squared	0.9755		
Mean	0.17		Adj R-Squared	0.9534		
C.V.%	14.03		Pred R-Squared	0.8447		
PRESS	0.037		Adeq Precision	**21.902**		

The significance and adequacy of the regression model have been analyzed by ANOVA. The attained results are tabulated in Table 7.3. If the value of "P > F" is less than 0.05, then the regression model is said to be significant. The terms present in the model is said to have a significant impact on the responses if "P < 0.0001". It can be observed that the chances of obtaining a large value of F might be 0.01% due to noise. The terms in the model are said to be significant if "P > F" is less than 0.0500. The model terms which has a value greater than 0.1000 are considered to be not significant. The significant model terms are observed to be C^2, A, AB, C, A^2, B, and B^2. It can be improved by reduction of the insignificant model terms. "Lack of Fit F-value" of 2.07 indicates that the "lack of fit" is insignificant compared to the pure error. The chances of obtaining a large value of "Lack of Fit F-value" is only 22.14% due to noise. To fit the model, the lack of fit should be insignificant, and the same result was observed as charted in Table 7.3.

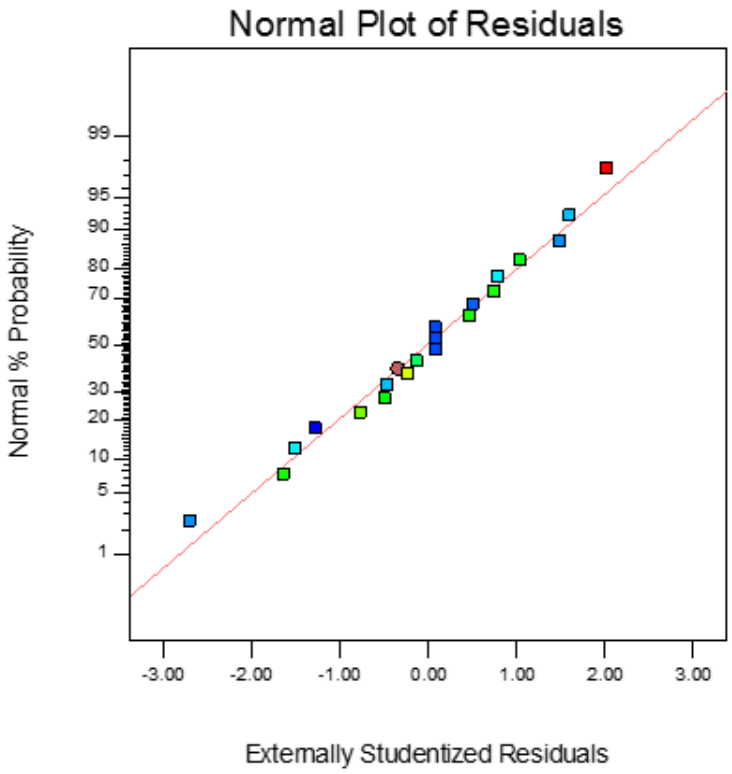

Figure 7.1 Normal probability plot for surface roughness.

To find the adequacy of the model, supplementary checks have to be performed. Major factors which need to be considered are the inspection of residuals and coefficients of determination (R^2). Always the value of R^2 should be between zero and one. The residuals are determined by calculating the difference between the predicted and observed responses. This investigation could be achieved by the plot of predicted vs. actual responses and the plot of residuals.

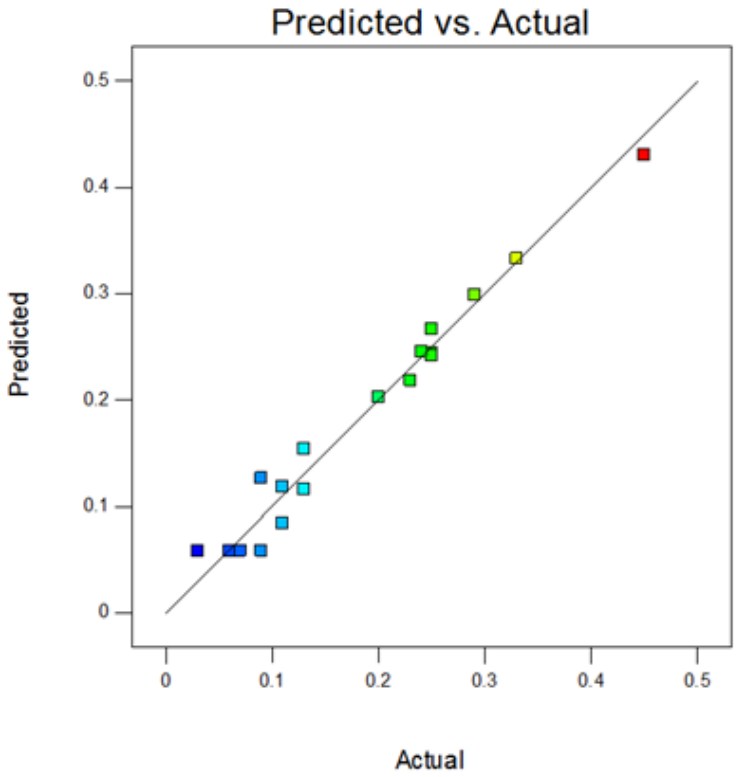

Figure 7.2 Predicted versus actual plot for surface roughness.

There are two ways to identify the adequacy of the model. The points on the normal probability graph should form a straight line, or the graph of predicted versus actual responses should not produce an obvious pattern. A straight line was formed by the points of the residuals as presented in Figure 7.1 which also designates that the errors are scattered normally. An obvious pattern was not observed as represented in Figure 7.2. Hence from these results, it can be said that the attained model for surface roughness satisfies all the conditions and it is an adequate model for predicting the surface roughness. Table 7.3

represents that the "Pred R-Squared" is in good agreement with "Adj R-Squared." The dissimilarity among them is under 0.2. "Adeq Precision" indicates the measurement of signal to noise ratio, and it is desirable only if it has a ratio beyond 4. The ratio of 21.902 confirms that the model is adequate and possible to navigate the design space.

7.3.2 Direct and interaction influence of parameters on surface roughness

To distinguish the impact of variables on any responses perturbation plot is used. The perturbation graph observed for the surface roughness is illustrated in Figure 7.3. A similar effect has been observed from the interaction of variables plot as displayed in Figure 7.4, Figure 7.5 and Figure 7.6 respectively.

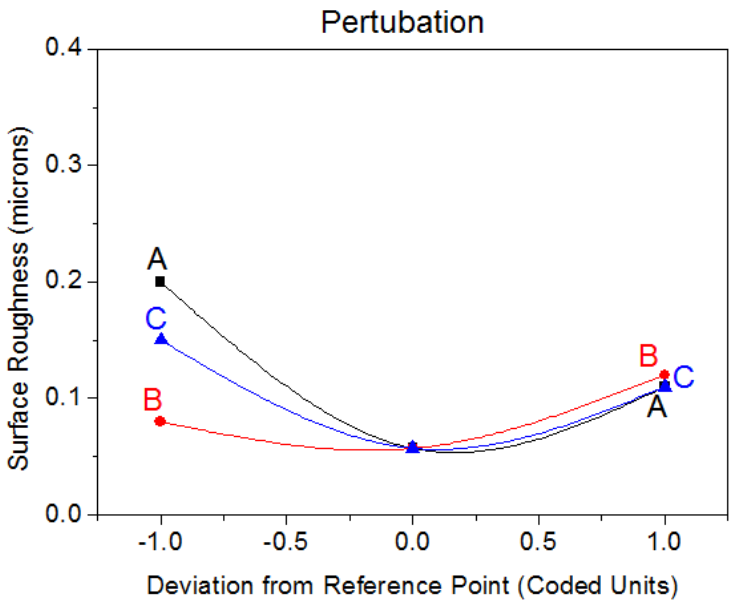

Figure 7.3 Perturbation plot for surface roughness.

The impact of burnishing speed on surface roughness is represented in Figure 7.4 and Figure 7.5. The surface roughness declines to the least possible value along with an increase in the burnishing speed. A further increase in the burnishing speed results in an increase in the surface roughness. Primarily, when the burnishing speed was increased, the reduction of surface roughness was observed owing to the fact that the diamond tip had further chances and time to push the irregularities into the valleys. The presence of chatter

is the main reason for the increase in the surface roughness at higher burnishing speed (El-Taweel and Ebeid, 2009; El-Khabeery and El-Axir, 2001).

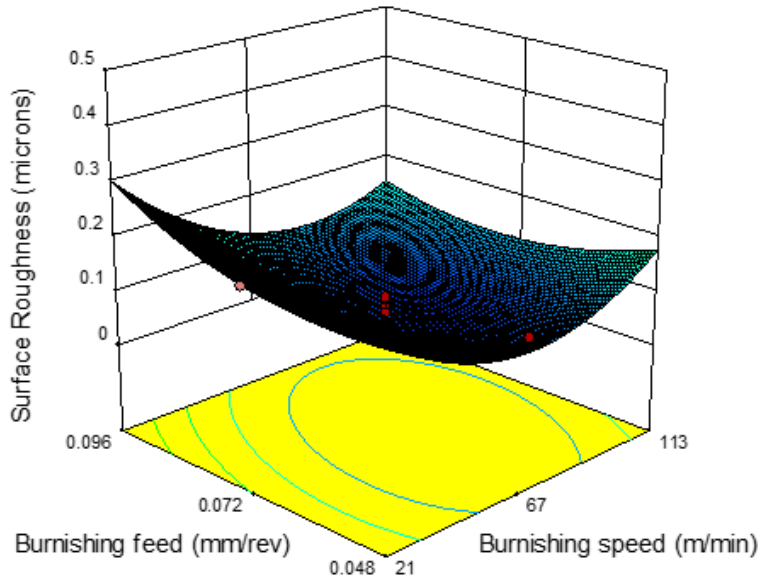

Figure 7.4 Interaction influence of burnishing feed and burnishing speed on surface roughness.

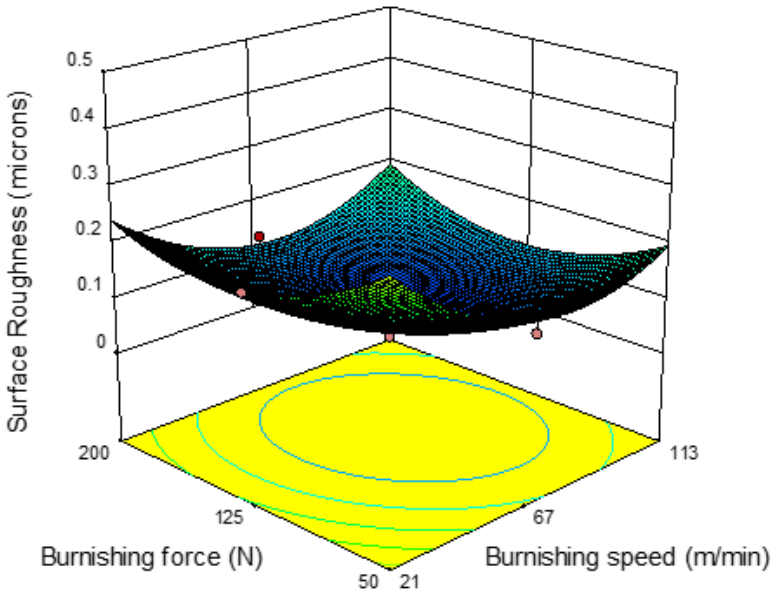

Figure 7.5 Interaction influence of burnishing force and burnishing speed on surface roughness.

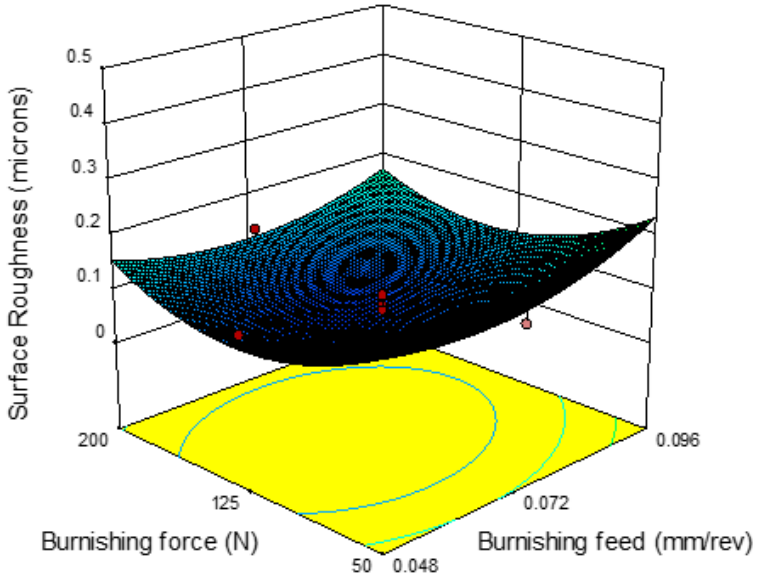

Figure 7.6 Interaction influence of burnishing force and burnishing feed on surface roughness.

Burnishing feed has an influence on surface roughness as illustrated in Fig 7.4 and Figure 7.6. It could be perceived that when the burnishing feed is at a lower range, the surface roughness drops to a minimum and a further increase in the burnishing feed causes an increase in the surface roughness. That's for the reason that the gap among the successive traces of the tool tip is small at lower burnishing feed and as the burnishing feed increases the surface roughness increases due to the more gap available among the successive traces of the tool (Santhanakrishnan et al. 2017; Liu and Wang, 1999).

The results of the diamond burnishing process will be affected by the variation of burnishing force as depicted in Figure 7.5 and Figure 7.6. The outcomes of the burnishing force show that the surface finish deteriorates as the burnishing force increases while the minimum surface roughness was observed for the middle level of burnishing force. It is due to the fact that higher forces lead to shear failure on the subsurface layer of the material and also another reason may be due to flaking (El-Taweel and El-Axir, 2009; El-Axir, 2000).

7.3.3 ANOVA for surface hardness

The regression equation for surface hardness is

$H = + 390.13289 – 0.20145\ s – 616.36748\ f + 0.29183\ t + 2.26449\ sf - 2.60870E\text{-}003\ st – 0.55556\ ft + 7.73329E\text{-}004\ s^2 + 1104.79798\ f^2 + 3.79798E\text{-}004\ t^2$-------HV (7.2)

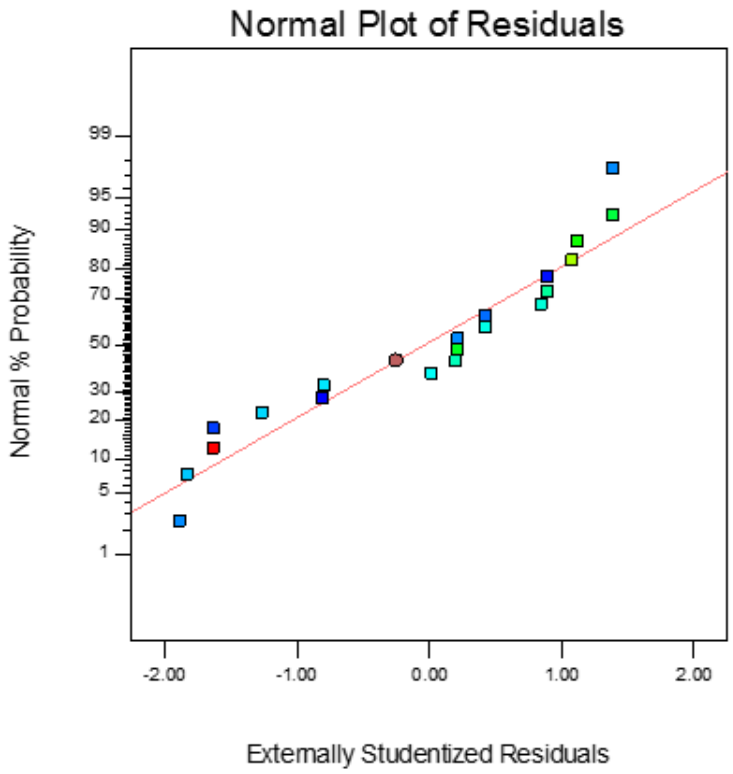

Figure 7.7 Normal probability plot for surface hardness.

The ANOVA results achieved for surface hardness is as tabulated in Table 7.4. The developed model for surface hardness was found to be significant. "Lack of fit value" was found to be not-significant which is good to fit a model. The F value of 80.44 shows the significance of the model. "Prob > F" which is less than 0.0500 represents the terms in the model are significant. According to the results attained A, B, C, AB, AC are significant terms. The values which are larger than 0.1000 are considered to be not significant. The model can be improved if the non-significant terms are reduced from the model. The "Lack

of fit F-value" of 1.32 shows that the "Lack of fit" is insignificant compared to the pure error. The chances of obtaining a large value of 38.54% could only be observed due to noise. It was also observed that a sensible agreement between the "Pred R-Squared" of 0.9052 and "Adj R-Squared" of 0.9741 had been observed and also the difference was observed to be 0.2. "Adeq Precision" ratio of 37.656 represents that the signal is adequate and possible to navigate the design space. Figure 7.7 and Figure 7.8 illustrated the normal graph of residuals and predicted versus actual graph for surface hardness. A similar methodology to surface roughness analysis has been followed to analyze the above-mentioned plots.

Table 7.4 ANOVA for surface hardness.

Source	**Sum of squares**	**df**	**Mean square**	**F value**	**p value prob>F**	
Model	4693.71	9	521.52	**80.44**	<0.0001	significant
A	1440.00	1	1440.00	222.10	<0.0001	
B	810.00	1	810.00	124.93	<0.0001	
C	1664.10	1	1664.10	256.66	<0.0001	
AB	50.00	1	50.00	7.71	0.0196	
AC	648.00	1	648.00	99.94	<0.0001	
BC	8.00	1	8.00	1.23	0.2926	
A^2	7.36	1	7.36	1.14	0.3116	
B^2	1.11	1	1.11	0.17	0.6873	
C^2	12.55	1	12.55	1.94	0.1943	
Residual	64.84	10	6.48			
Lack of Fit	36.84	5	7.37	**1.32**	**0.3854**	not significant
Pure Error	28.00	5	5.60			
Cor Total	4758.55	19				
Std. Dev.	2.55		R-Squared	0.9864		
Mean	370.15		Adj R-Squared	**0.9741**		
C.V.%	0.69		Pred R-Squared	**0.9052**		
PRESS	451.01		Adeq Precision	**37.656**		

It was perceived that the residuals followed a straight line in Figure 7.7 which designates that the model is adequate and significant. The residuals are less structured and also

obvious pattern was not observed as shown in Figure 7.8. Hence it was confirmed that the attained model is significant and adequate.

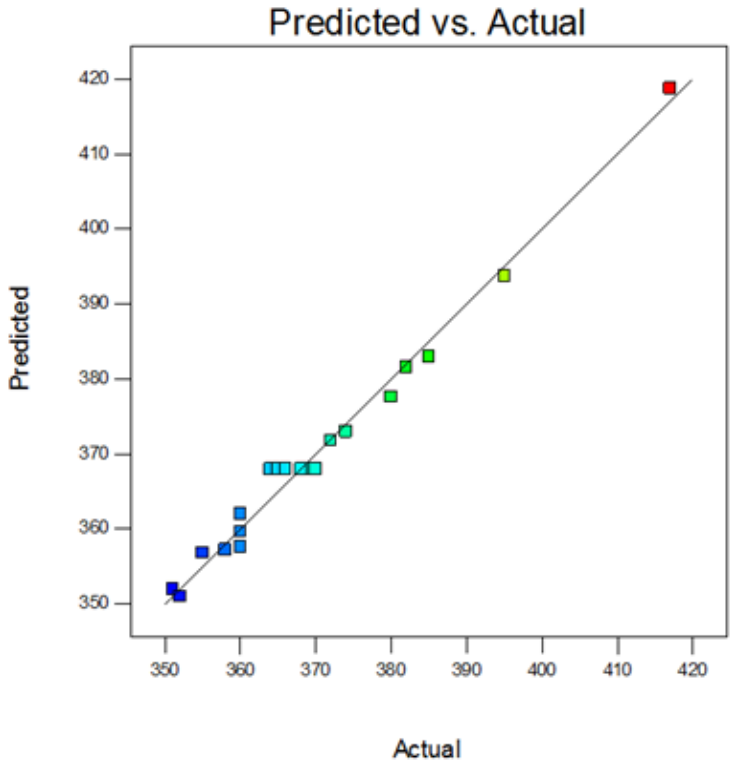

Figure 7.8 Predicted versus actual plot for surface hardness.

7.3.4 Direct and interaction influence of parameters on surface hardness

The perturbation graph as illustrated in Figure 7.9, demonstrates the trend of surface hardness observed for different variables used in the present study. A comparable effect has been found in the 3D surface hardness plot for all the variables which is as presented in Figure 7.10, Figure 7.11, and Figure 7.12. All the three variables are found to have their own interaction influence on the surface hardness.

The surface hardness variation with varying burnishing speed is as portrayed in Figure 7.10 and Figure 7.11. The surface hardness drops continuously with an increase in the burnishing speed. That's because of the chatter induced owing to the unsuitability of the diamond burnishing tool crossing over the work material (El-Axir, 2000).

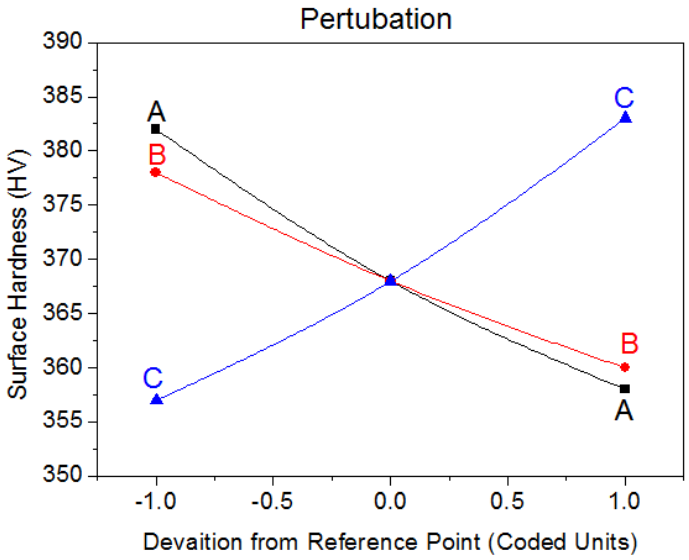

Figure 7.9 Perturbation plot for surface hardness.

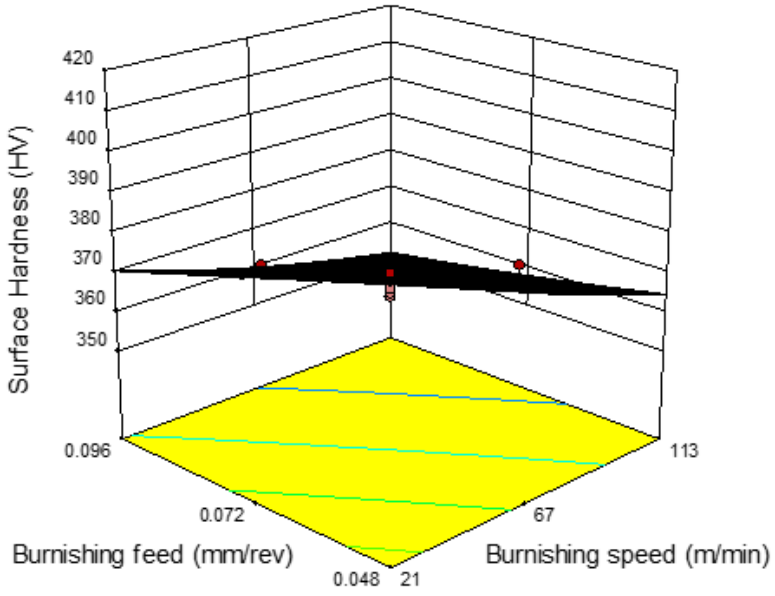

Figure 7.10 Interaction influence of burnishing feed and burnishing speed on surface hardness.

The impact of burnishing feed on surface hardness is as depicted in Figure 7.10 and Figure 7.12. The surface hardness diminishes when there is an increase in the burnishing feed. Maximum surface hardness was achieved at low burnishing feed. The reason for this drastic reduction in the surface hardness is ascribed to the overlap among the trenches at

lower burnishing feed was high which has been induced by the plastic deformation (Abrão et al. 2014).

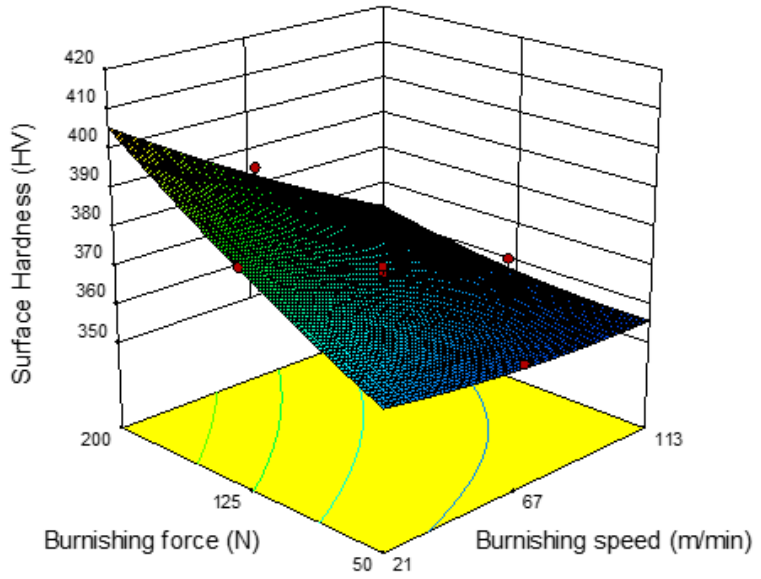

Figure 7.11 Interaction influence of burnishing force and burnishing speed on surface hardness.

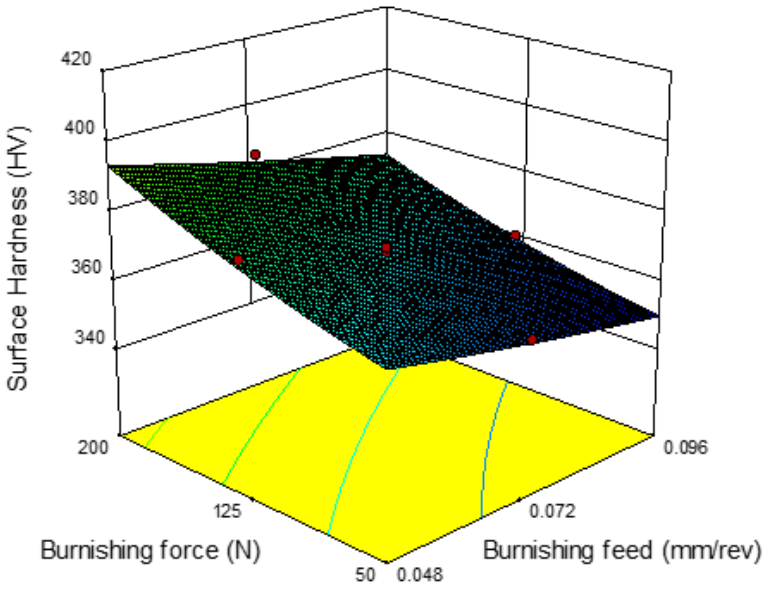

Figure 7.12 Interaction influence of burnishing force and burnishing feed on surface hardness.

For the enhancement of surface hardness of the material, burnishing force is treated to be one of the vital control parameters and the influence of it on surface hardness is as represented in Figure 7.11 and Figure 7.12. An increase in the surface hardness has been achieved with an increase in the burnishing force. That's because as the tool passes on the surface, the surface deformation increases. This is the reason for work hardening which has been generated because of the repeated plastic deformation (El-Taweel and Ebeid, 2009).

7.4 OPTIMIZATION USING MOGA

GA is a basic tool which works on the principle of natural selection and genetics. It is preferred to solve unconstrained and constrained problems to obtain an optimal solution with high probability (Çolak, 2014). Chromosomes are the initial set of a solution with which the process starts. Mutation, reproduction, and crossover are the genetic operators on which the convergence depends. To select good strings, the process starts with a step called reproduction. Splitting and combining one half of each chromosome with the other pair is performed in a crossover. The flipping of chromosomes is done by mutation. From the current population, GA uses individuals in random which is known as parents and children will be produced for the next generation (Kumar, 2018). An optimal solution of the population will be achieved from this generation. The best fitness criteria are achieved by repeating the same process. The prediction problems from the equations (7.1) and (7.2) attained from the RSM modeling has been considered as an objective function for obtaining the optimal solution. The solutions were recorded for both the output responses.

Some of the chromosomes considered in the present work are population size - 50, mutation function - adaptive feasible, crossover fraction - 0.8, and iterations - 500. The optimal results were attained by conducting the trial and error method. MOGA in Matlab optimization toolbox has been used to try different burnishing conditions and to accomplish at the best feasible solution. The feasible set of process parameters considered to perform MOGA are tabulated in Table 7.5. For all different combinations of operators and iteration, MOGA produces a different solution. The most suitable solution will be chosen based on

the priority of the output responses considered for the study. Equal priority has to be given for achieving minimum surface roughness and maximum surface hardness.

Table 7.5 MOGA parameters.

Variables	Values
Population size	50
Crossover fraction	0.8
Mutation function	adaptive feasible
Iteration	500

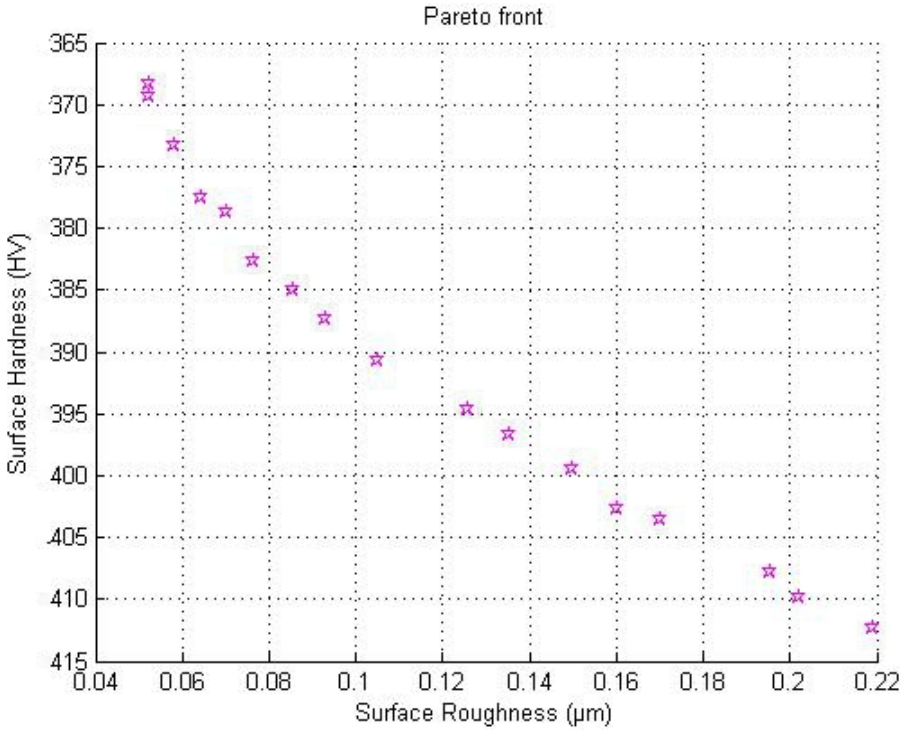

Figure 7.13 Plot of Pareto front attained using MOGA.

The solution for the best combination has been determined by a Pareto graph. Pareto graph for both the responses is depicted in Figure 7.13. From the previous discussion of RSM, the effect of control factors on each output response was studied and analyzed. Whereas in MOGA, multi-objective optimization has been carried out by considering the responses together and analyzing the influence of control factors on them. The optimal process

parameters recorded are burnishing feed = 0.068 mm/rev, burnishing speed = 74 m/min, and burnishing force = 132 N and the corresponding solution observed for surface roughness and surface hardness is 0.05 µm and 368 HV respectively by effective implementation of the MOGA technique as tabulated in Table 7.6.

7.4.1 CONFIRMATION TEST

With the aim of validating the accurateness of the results found using MOGA, confirmation test has been performed, and the outcomes achieved are as charted in Table 7.6. Five times the experiments were performed to obtain the accurate results, and the average reading was considered to be the final value. It was observed that a negligible deviation between experimental and MOGA results was noticed. It was attained because of the proper selection of MOGA process parameters. It was inferred that the results obtained are within the allowable limit. It has been concluded that it is possible to carry out multi-objective optimization of control factors involved in the diamond burnishing of 17-4 PH stainless steel under cryogenic cooling by MOGA which yields minimum surface roughness and maximum surface hardness at the optimal control factors.

Table 7.6 Confirmation results.

Responses	**Optimal conditions**	
	Burnishing speed = 74 m/min Burnishing feed = 0.068 mm/rev Burnishing force = 132 N	
	GA	**Confirmation experiment**
Surface roughness (µm)	0.05	0.04
Surface hardness (HV)	368	370

7.5 SUMMARY

RSM with CCD has been used for modeling and analyzing the performance of the responses. The significance and adequacy of the process parameters were studied. The best combination of the output responses was achieved by employing the optimal combination

of control factors which has been derived from the model. The conclusions were drawn as follows:

- The surface roughness declines to the lower value with an increase in the burnishing speed, burnishing feed, and burnishing force. Further increase in these parameters results in an increase in the surface roughness.
- A maximum surface hardness of 417 HV was achieved at low burnishing feed, low burnishing speed, and high burnishing force.
- The adequacy of the model is at 95% confidence level for the reason that a significant “lack of fit” was not found in the quadratic model. The attained model is adequate and accurate for predicting the responses for cryogenic diamond burnishing using a novel diamond burnishing tool.
- MOGA yields burnishing feed of 0.068 mm/rev, burnishing force of 132 N, and burnishing speed of 74 m/min as optimal process parameters which result in surface hardness of 368 HV and surface roughness of 0.05 µm.
- The accuracy of the results observed has been validated by confirmation experiments and the outcomes recorded for surface roughness = 0.04 µm and surface hardness = 370 HV, which are well within the acceptable limits.

CHAPTER-8

CONCLUSIONS AND SCOPE FOR FUTURE WORK

8.1 CONCLUSIONS

In the present investigation, the influence of diamond burnishing process parameters on the surface integrity characteristics of 17-4 PH stainless steel was performed in the cryogenic cooling, MQL, and dry conditions. A commercially available diamond burnishing tool and a novel diamond burnishing tool were used to improve the surface integrity characteristics of the material. A novel diamond burnishing tool was proved to be better in contrast with a commercially available tool under the cryogenic cooling environment. Further, optimization of the control factors was performed in the cryogenic cooling condition using TGRA. Finally, modeling and multi-objective optimization of the process parameters have been performed using RSM and MOGA respectively. The developed mathematical model was found to be adequate and accurate for predicting the responses. Based on the results, the following conclusions were drawn:

- The minimum surface roughness of 0.10 µm and maximum surface hardness of 404 HV was achieved under the cryogenic environment by a commercially available diamond burnishing tool.
- Surface finish improvement of 33% to 50%, 34 to 51%, and 25 to 40% respectively was observed using a novel diamond burnishing tool under the cryogenic environment in contrast with MQL and dry environment at all the levels of burnishing speed, burnishing feed and burnishing force. An improvement of 5% to 7%, 6% to 10%, and 6% to 9% respectively were observed in the surface hardness under the cryogenic environment when compared to MQL and dry environment.

- Highest subsurface microhardness was achieved under the cryogenic environment with a percentage improvement of 7% and 9% in contrast with MQL and dry environments using a novel diamond burnishing tool.
- The minimum surface roughness achieved by the cryogenic diamond burnishing at a diamond sphere diameter of 8 mm using a novel diamond burnishing tool was found to be 0.03 μm. Similarly, at a diamond sphere diameter of 6 mm, the maximum surface hardness was noticed to be 413 HV.
- From the multi-response optimization using GRA, the optimal process parameters were found to be burnishing speed 73 m/min, burnishing feed 0.048 mm/rev and burnishing force 200 N to minimize the surface roughness and maximize the surface hardness.
- The enhancement of GRG from primary parameter to the optimum parameter combination was found to be 0.34. The improvement of GRG was observed to be 42.98%.
- MOGA yields burnishing feed of 0.068 mm/rev, burnishing force of 132 N, and burnishing speed of 74 m/min as optimal process parameters which result in surface hardness of 368 HV and surface roughness of 0.05 μm.
- A minimum surface roughness of 0.02 μm was obtained by using a novel diamond burnishing tool in contrast with a conventional diamond burnishing tool under cryogenic environment.

8.2 SCOPE FOR FUTURE WORK

Even though the current investigation was able to yield improved surface integrity properties of the material, there is further scope for improvement. The present study implied future scope in the following areas:

- An exclusive study can be performed on the fatigue strength of diamond burnished components.
- The ultrafine grain refinement and Electron backscatter diffraction (EBSD) studies can be performed on the diamond burnished surface layer of the material.

- The investigation can be extended by considering the process parameters such as flow rate, supply angle, pressure and stand-off distance for the supply of coolant/lubricant from the nozzle to the tool-workpiece interface.

REFERENCES

Abelle, E., and Schramm, B. (2008). “Using PCD for machining CGI with a CO_2 coolant system.” *Prod. Eng*., 2, 165–169.

Abrão, A. M., Denkena, B., Breidenstein, B., and Mörke, T. (2014). “Surface and subsurface alterations induced by deep rolling of hardened AISI 1060 steel.” *Prod. Eng.*, 8, 551-558.

Adler, A., Yaniv, I., Solter, E., Freud, E., Samra, Z., Stein, J., Fisher, S., and Levy, I. (2006). “Catheter-associated bloodstream infections in pediatric hematology-oncology patients: Factors associated with catheter removal and recurrence.” *J. Pediatr. Hematol. Oncol.*, 28, 23-28.

Al-Qawabeha, U. F. (2007). “The effect of diamond pressing and roller burnishing of unheat treated carbon steel surfaces.” *Mach. Sci. Technol.*, 11(1), 145-155.

Amdouni, H., Bouzaiene, H., Montagne, A., Nasri, M., and Iost, A. (2017). “Modeling and optimization of a ball-burnished aluminum alloy flat surface with a crossed strategy based on response surface methodology.” *Int. J. Adv. Manuf. Technol.*, 88(1-4), 801-814.

Aoyama, T., Kakinuma, Y., Yamashita, M., and Aoki, M. (2008). "Development of a new lean lubrication system for near dry machining process". *CIRP Ann. - Manuf. Technol*., 57 (1), 125-128.

Autret, R., Liang, S. Y., and Woodruff, G. W. (2003). “Minimum quantity lubrication in finish hard turning.” *HNICEM.*, 03, 1-9.

Avilés, A., Avilés, R., Albizuri, J., Pallarés-Santasmartas, L., and Rodríguez, A. (2019). “Effect of shot-peening and low-plasticity burnishing on the high-cycle fatigue strength of DIN 34CrNiMo6 alloy steel.” *Int. J. Fatigue.*, 119, 338-354.

Aviles, R., Albizuri, J., Rodríguez, A., and De Lacalle, L. L. (2013). “Influence of low-plasticity ball burnishing on the high-cycle fatigue strength of medium carbon AISI 1045 steel.” *Int. J. Fatigue.*, 55, 230-244.

Babu, P. R., Ankamma, K., Prasad, T. S., Raju, A. V. S., and Prasad, N. E. (2011). “Effects of burnishing parameters on the surface characteristics, microstructure and microhardness in EN series steels.” *Trans. Indian Inst. Met.*, 64(6), 565-573.

Banh, Q. N., and Shiou, F. J. (2016). “Determination of optimal small ball-burnishing parameters for both surface roughness and superficial hardness improvement of STAVAX.” *Arab. J. Sci. Eng.*, 41, 639.

Baradie, M. A. (1996a). "Cutting fluids: Part I. Characterisation". *J. Mater. Process. Technol.*, 56 (1‑4), 786‑797.

Baradie, M. A. (1996b). "Cutting fluids: Part II. Recycling and clean machining". *J. Mater. Process. Technol.*, 56 (1–4), 798–806.

Bougharriou, A., Saï, W. B., and Saï, K. (2010). “Prediction of surface characteristics obtained by burnishing.” *Int. J. Adv. Manuf. Technol.*, 51(1-4), 205-215.

Boyce, Meherwan, P. (2006). “Gas Turbine Engineering Handbook.” Gulf Professional Boston, MA, 3rd edition.

Boyer, R. R. (1996). “An overview on the use of titanium in the aerospace industry.” *Mater. Sci. Eng. A.*, 213,103–114.

Bressana, D. P., Darosa, A., Sokolowskib, R. A., Mesquitac, C. A., and Barbosa. (2008). “Influence of hardness on the wear resistance of 17-4 PH stainless steel evaluated by the pin-on-disc testing.” *J. Mater. Process. Technol.*, 205, 353–359.

Cassin, C., and Boothroyd, G. (1965). “Lubricating action of cutting fluids.” *J. Mech. Eng. Sci.*, 7(1), 67–81.

Caudill, J., Huang, B., Arvin, C., Schoop, J., Meyer, K., and Jawahir, I. S. (2014). “Enhancing the surface integrity of Ti-6Al-4V alloy through cryogenic burnishing.” *Procedia CIRP*., 13, 243-248.

Caudill, J., Schoop, J., and Jawahir, I. S. (2018). “Correlation of surface integrity with processing parameters and advanced interface cooling/lubrication in burnishing of Ti-6Al-4V alloy.” *Adv. Mater. Process. Technol.,* 1-14.

Chetan, Ghosh, S., and Rao, P. V. (2016). "Environment friendly machining of Ni–Cr–Co based super alloy using different sustainable techniques". *Mater. Manuf. Process*., 31(7), 852-859.

Chomienne, V., Valiorgue, F., Rech, J., and Verdu, C. (2016). “Influence of ball burnishing on residual stress profile of a 15-5PH stainless steel.” *CIRP J. Manuf. Sci. Technol.*, 13, 90-96.

Çolak, O. (2014). “Optimization of machining performance in high-pressure assisted turning of Ti6Al4V alloy.” *J. Mech. Eng.*, 60, 675–681.

Cui, C., Hu, B., Zhao, L., and Liu, S. (2011). “Titanium alloy production technology, market prospects and industry development.” *Mater. Des.*, 32(3), 1684-1691.

Davim, J. P., Sreejith, P. S. and Silva, J. (2007). “Turning of brasses using minimum quantity of lubricant and flooded lubricant conditions.” *Mater. Manuf. Process*., 22, 45-50.

De Chiffre, L., Andreasen, J. L., Lagerberg, S., and Thesken, I. B. (2007). “Performance testing of cryogenic CO_2 as cutting fluid in parting/grooving and threading austenitic stainless steel.” *CIRP Ann. - Manuf. Technol*., 56(1), 101–104.

Deng, J. (1982). “Control problems of grey systems. *Syst. Control. Lett.*, 1(5), 288–294.

Denkena, B., Grove, T., and Maiss, O. (2017). “Surface texturing of rolling elements by hard ball-end milling and burnishing.” *Int. J. Adv. Manuf. Technol.*, 93(9-12), 3713-3721.

Dhar, N. R., Islam, M. W., Islam, S. and Mithu, M. A. (2006a). “The influence of minimum quantity of lubrication (MQL) on cutting temperature, chip and dimensional accuracy in turning AISI-1040 steel.” *J. Mater. Process. Technol.*, 171(1), 93- 99.

Dhar, N. R., Kamruzzaman, M. and Ahmed, M. (2006b). "Effect of minimum quantity lubrication (MQL) on tool wear and surface roughness in turning AISI-4340 steel". *J. Mater. Process. Technol.*, 172(2), 299–304.

Dhar, N. R., Paul, S. and Chattopadhyay, A. B. (2001). "The influence of cryogenic cooling on tool wear, dimensional accuracy and surface finish in turning AISI 1040 and E4340C steels". *Wear.*, 249(10–11), 932–942.

Dillon, O. W., De Angelis, R. J., Lu, W. Y., Gunasekera, J. S., and Deno, J. A. (1990). “The Effects of Temperatures on the Machining of Metals.” *J. Mater. Shaping Technol.*, 8, 23–29.

Dinesh, S., Senthilkumar, V., and Asokan, P. (2017). “Experimental studies on the cryogenic machining of biodegradable ZK60 Mg alloy using micro-textured tools.” *Mater. Manuf. Process.*, 32, 979–987.

Dix, M., Wertheim, R., Schmidt, G., and Hochmuth, C. (2014). “Modeling of drilling assisted by cryogenic cooling for higher efficiency.” *CIRP Ann. - Manuf. Technol.*, 63(1), 73–76.

El-Axir, M. H. (2000). “Investigation into roller burnishing.” *Int. J. Mach. Tools. Manuf.*, 40, 1603–1617.

El-Axir, M. H., and El-Khabeery, M. M. (2003). "Influence of orthogonal burnishing parameters on surface characteristics for various materials." *J. Mater. Process. Technol.*, 132(1-3), 82-89.

El-Axir, M. H., Othman, O. M., and Abodiena, A.M. (2008). “Study on the inner surface finishing of aluminum alloy 2014 by ball burnishing process.” *J. Mater. Process. Technol.*, 202, 435–442.

El-Khabeery, M. M., and El-Axir, M. H. (2001). “Experimental techniques for studying the effects of milling roller-burnishing parameters on surface integrity.” *Int. J. Mach. Tools. Manuf*., 41(12), 1705-1719.

El-Taweel T. A., and Ebeid S. J. (2009). “Effect of hybrid electrochemical smoothing-roller burnishing process parameters on roundness error and micro-hardness.” *Int. J. Adv. Manuf. Technol.*, 42, 643–655.

El-Taweel, T. A., and El-Axir, M. H. (2009). Analysis and optimization of the ball burnishing process through the Taguchi technique. *Int. J. Adv. Manuf. Technol.*, 41(3-4), 301-310.

El-Tayeb, N. S. M., Low, K. O., and Brevern, P. V. (2008). “Enhancement of surface quality and tribological properties using ball burnishing process.” *Mach. Sci. Technol.*, 12(2), 234-248.

El-Tayeb, N. S. M., Low, K. O., and Brevern, P. V. (2007). "Influence of roller burnishing contact width and burnishing orientation on surface quality and tribological behaviour of Aluminium 6061." *J. Mater. Process. Technol.*, 186(1-3), 272-278.

Ezugwu, E. O., Bonney, J., and Yamane, Y. (2003). “An overview of the machinability of aeroengine alloys.” *J. Mater. Process. Technol.*, 134(2), 233-253.

Fang, S., and Chuing, C. (2010). “Precision surface finish of the mold steel PDS5 using an innovative ball burnishing tool embedded with a load cell.” *Prec. Engg.*, 34, 76-84.

Gharbi, F., Sghaier, S., Al-Fadhalah, K. J., and Benameur, T. (2011). “Effect of ball burnishing process on the surface quality and microstructure properties of AISI 1010 steel plates.” *J. Mater. Eng. Perform.*, 20(6), 903-910.

Gharbi, F., Sghaier, S., Hamdi, H., and Benameur, T. (2012). “Ductility improvement of aluminum 1050A rolled sheet by a newly designed ball burnishing tool device.” *Int. J. Adv. Manuf. Technol.*, 60(1-4), 87-99.

Goel, B., Singh, S., and Sarepaka, R.V. (2015). “Optimizing single point diamond turning for mono-crystalline germanium using grey relational analysis.” *Mater. Manuf. Process*., 30(8), 1018-1025.

Grzesik, W., and Żak, K. (2014). “Characterization of surface integrity produced by sequential dry hard turning and ball burnishing operations.” *J. Manuf. Sci. Eng.*, 136(3), 031017.

Hassan, A. M. (1997a). “The effects of ball-and roller-burnishing on the surface roughness and hardness of some non-ferrous metals.” *J. Mater. Process. Technol.*, 72(3), 385-391.

Hassan, A.M. (1997b). “An investigation into the surface characteristics of burnished cast Al-Cu alloys.” *Int. J. Mach. Tools Manuf.*, 37, 813–821.

Hassan, A. M., Al-Jalu, H. F., and Ebied, A. A. (1998). “Burnishing force and number of ball passes for the optimum surface finish of brass components.” *J. Mater. Process. Technol.*, 83,176–179.

Hassan, A. M., and Al-Bsharat, A. S. (1996). “Influence of burnishing process on surface roughness, hardness, and microstructure of some non-ferrous metals.” *Wear*., 199, 1–8.

Hemanth, S., Harish, A., Bharadwaj, R. N., Bhat, A. B., and Sriharsha, C. (2018). “Design of roller burnishing tool and its effect on the surface integrity of Al 6061.” *Mater. Today: Proc.*, 5(5), 12848-12854.

Herbert, E. G. (1927). “The work hardening of steel by abrasion, with an appendix on the cloudburst test and super hardening.” *J. Iron. Steel.*, 11, 265-282.

Hiegemann, L., and Tekkaya, A. E. (2018). “Ball burnishing under high velocities using a new rolling tool concept.” *J. Manuf. Sci. Eng.*, 140(4), 041008.

Hong, S. Y., and Ding, Y. (2001a). “Micro-temperature manipulation in cryogenic machining of low carbon steel.” *J. Mater. Process. Technol.*, 116(1), 22-30.

Hong, S. Y., Ding, Y., and Ekkens, R. G. (1999). “Improving low carbon steel chip breakability by cryogenic chip cooling.” *Int. J. Mach. Tools Manuf.*, 39(7), 1065-1085.

Hong, S. Y., and Ding, Y. (2001b). “Cooling approaches and cutting temperatures in cryogenic machining of Ti-6Al-4V.” *Int. J. Mach. Tools Manuf.*, 41, 1417–1437.

Hong, S. Y., and Zhao, Z. (1999). “Thermal aspects, material considerations and cooling strategies in cryogenic machining.” *Clean Technol. Environ. Policy.*, 1(2), 107–116.

Huang, B., Kaynak, Y., Sun, Y., and Jawahir. I.S. (2015). “Surface layer modification by cryogenic burnishing of Al 7050-T7451 alloy and validation with FEM-based burnishing model. *Procedia CIRP*., 31, 1–6.

Jaffery, S. I., and Mativenga, P. T. (2009). “Assessment of the machinability of Ti-6Al-4V alloy using the wear map approach.” *Int. J. Adv. Manuf. Technol.*, 40(7-8), 687-696.

Jawahir, I. S., Attia, H., Biermann, D., Duflou, J., Klocke, F., Meyer, D., and Newman, S.T. et al. (2016). "Cryogenic manufacturing processes." *CIRP Ann.* 65(2), 713-736.

Jayal, A. D., Badurdeen, F., Dillon Jr, O. W., and Jawahir, I. S. (2010). “Sustainable manufacturing: modeling and optimization challenges at the product, process and system levels. *CIRP J. Manuf. Sci. Technol.*, 2, 144–152.

Jerez-Mesa, R., Travieso-Rodríguez, J. A., Landon, Y., Dessein, G., Lluma-Fuentes, J., and Wagner, V. (2018). “Comprehensive analysis of surface integrity modification of ball-end milled Ti-6Al-4V surfaces through vibration-assisted ball burnishing.” *J. Mater. Process. Technol*., 267, 230-240.

John, M. S., and Vinayagam, B. K. (2011). “Optimization of ball burnishing process on tool steel (T215Cr12) in CNC machining centre using response surface methodology.” *Arab. J. Sci. Eng.*, 36(7), 1407-1422.

John, M. S., Wilson, A. W., Bhardwaj, A. P., Abraham, A., and Vinayagam, B. K. (2016). "An investigation of ball burnishing process on CNC lathe using finite element analysis." *Simul. Model. Pract. Theory.*, 62, 88–101.

Kakinuma, Y., Yasuda, N., and Aoyama, T. (2008). "Micromachining of soft polymer material applying cryogenic cooling." *J. Adv. Mech. Des. Syst.*, 2(4), 560-569.

Kamata, Y. and Obikawa, T. (2007). "High speed MQL finish-turning of Inconel 718 with different coated tools." *J. Mater. Prorcess. Technol*., 192, 281-286.

Kaynak, Y., Lu, T., and Jawahir, I. S. (2014). "Cryogenic machining-induced surface integrity: a review and comparison with dry, MQL, and flood-cooled machining." *Mach. Sci. Technol.*, 18(2), 149–198.

Khan, Z., Prasad, B., and Singh, T. (1997). "Machining condition optimization by genetic algorithms and simulated annealing." *Comput. Oper. Res.*, 24, 647–657.

Kilickap, E., and Huseyinoglu, M. (2010). "Selection of optimum drilling parameters on burr height using response surface methodology and genetic algorithm in drilling of AISI 304 stainless steel." *Mater. Manuf. Process.*, 25, 1068–1076.

Kilickap, E., Huseyinoglu, M., and Yardimeden, A. (2011). "Optimization of drilling parameters on surface roughness in drilling of AISI 1045 using response surface methodology and genetic algorithm." *Int. J. Adv. Manuf. Technol.*, 52, 79–88.

Klocke, F., and Eisenblaetter, G. (1997). "Dry Cutting." *CIRP Ann.*, 46(2), 519-526.

Klocke, F., Bäcker, V., Wegner, H., Feldhaus, B., Baron, H. U., Hessert, R. (2009). "Influence of process and geometry parameters on the surface layer state after roller burnishing of IN718." *Prod. Eng.*, 3, 391–9.

Kochmański, P., and Nowacki, J. (2006). "Activated gas nitriding of 17-4 PH stainless steel". *Surf. Coatings Technol.*, 200(22–23), 6558–6562.

Korzynski, M., Dudek, K., Kruczek, B., and Kocurek, P. (2018a). “Equilibrium surface texture of valve stems and burnishing method to obtain it.” *Tribol. Int.*, 124, 195-199.

Korzynski, M., Dudek, K., Palczak, A., Kruczek, B., and Kocurek, P. (2018b). “Experimental models and correlations between surface parameters after slide diamond burnishing.” *Meas. Sci. Rev.*, 18(3), 123-129.

Kumar, K. V., and Sait, A. N. (2017). “Modelling and optimisation of machining parameters for composite pipes using artificial neural network and genetic algorithm.” *Int. J. Interact. Des. Manuf.*, 11, 435–443.

Kumar, S. L. (2018). “Experimental investigations and empirical modeling for optimization of surface roughness and machining time parameters in micro end milling using Genetic Algorithm.” *Meas.*, 124, 386-394.

Kuznetsov, V. P., Tarasov, S. Y., and Dmitriev, A. I. (2015). "Nanostructuring burnishing and subsurface shear instability." *J. Mater. Prorcess. Technol.*, 217, 327-335.

Kwak, J. S. (2005). “Application of Taguchi and response surface methodologies for geometric error in surface grinding process.” *Int. J. of Mac. Tools and Manufac*., 45, 327–334.

Li, F. L., Xia, W., Zhou, Z. Y., Zhao, J., and Tang, Z. Q. (2012). “Analytical prediction and experimental verification of surface roughness during the burnishing process.” *Int. J. Mach. Tools. Manuf*., 62, 67–75.

Li, L., Li, Z. Y., Wei, X. T., and Cheng, X. (2015). "Machining characteristics of Inconel 718 by sinking-EDM and wire-EDM". *Mater. Manuf. Process.*, 30(8), 968-973.

Liu, G., Huang, C., Zou, B., Wang, X., and Liu, Z. (2016). “Surface integrity and fatigue performance of 17-4PH stainless steel after cutting operations.” *Surf. Coatings Technol.*, 307, 182-189.

Liu, Y., and Wang, C. (1999). “Modified genetic algorithm based optimization of milling parameters.” *Int. J. Adv. Manuf. Technol.,* 15, 796–799.

Liu, Z., Nouraei, H., Spelt, J. K. and Papini, M. (2015). "Electrochemical slurry jet micromachining of tungsten carbide with a sodium chloride solution". *Precis. Eng.*, 40, 189-198.

Loh, N. H., and Tam, S.C. (1988). “Effects of ball burnishing parameters on surface finish - a literature survey and discussion.” *Prec. Engg*., 10, 215-220.

López de Lacalle, L. N., Rodriguez, A., Lamikiz, A., Celaya, A., and Alberdi, R. (2011). “Five-axis machining and burnishing of complex parts for the improvement of surface roughness.” *Mater. Manuf. Process*., 26(8), 997-1003.

Low, K. O., and Wong, K. J. (2011). “Influence of ball burnishing on surface quality and tribological characteristics of polymers under dry sliding conditions. *Tribol. Int.*, 44(2), 144-153.

Luo, H., Liu, J., Wang, L., and Zhong, Q. (2006). “The effect of burnishing parameters on burnishing force and surface microhardness.” *Int. J. Adv. Manuf. Technol.,* 28(7-8), 707-713.

Maawad, E., Brokmeier, H. G., Wagner, L., Sano, Y., and Genzel, C. H. (2011). “Investigation on the surface and near-surface characteristics of Ti–2.5Cu after various mechanical surface treatments.” *Surf. Coat. Technol*., 205, 3644–3650.

Mahesh, G., Muthu, S., Devadasan, S. R. (2015). “Prediction of surface roughness of end milling operation using genetic algorithm.” *Int. J. Adv. Manuf. Technol.,* 77, 369–381.

Maximov, J. T., Anchev, A. P., Duncheva, G. V., Ganev, N., and Selimov, K. F. (2017). “Influence of the process parameters on the surface roughness, micro-hardness, and residual stresses in slide burnishing of high-strength aluminum alloys.” *J. Brazilian Soc. Mech. Sci. Eng.*, 39(8), 3067-3078.

Maximov, J. T., Duncheva, G. V., Anchev, A. P., Ganev, N., Amudjev, I. M., and Dunchev, V. P. (2018). "Effect of slide burnishing method on the surface integrity of AISI 316Ti chromium-nickel steel." *J. Brazilian Soc. Mech. Sci. Eng.*, 40(4), 194.

Maximov, J. T., Duncheva, G. V., Anchev, A. P., Ganev, N., and Dunchev, V. P. (2019). "Effect of cyclic hardening on fatigue performance of slide burnished components made of low-alloy medium carbon steel." *Fatigue Fract Eng M*.

Mia, M., Khan, M. A., Rahman, S. S. and Dhar, N. R. (2017). "Mono-objective and multi-objective optimization of performance parameters in high pressure coolant assisted turning of Ti-6Al-4V." *Int. J. Adv. Manuf. Technol.*, 90(1-4), 109-118.

Mirzadeh, H., and Najafizadeh, A. (2009). "Aging kinetics of 17-4 PH stainless steel." *Mater. Chem. Phys.*, 116, 119–24.

Mirzadeh, H., Najafizadeh, A., and Moazeny, M. (2009). "Flow curve analysis of 17-4 PH stainless steel under hot compression test." *Metall. Mater. Trans. A.*, 40, 2950.

Mohanty, A., Gangopadhyay, S. and Thakur, A. (2016). "On applicability of multilayer coated tool in dry machining of aerospace grade stainless steel". *Mater. Manuf. Process.*, 31(7), 869-879.

Montgomery, D. C. (2005). *Design and Analysis of Experiments*, sixth edition, John Wiley & sons, Inc.

Morán, J., Granada, E., Míguez, J. L., and Porteiro, J. (2006). "Use of grey relational analysis to assess and optimize small biomass boilers." *Fuel Process. Technol.*, 87(2), 123-127.

Nalla, R. K., Altenberger, I., Noster, U., Liu, G. Y., Scholtes, B., and Ritchie, R. O. (2003). On the influence of mechanical surface treatments-deep rolling and laser shock peening-on the fatigue behavior of Ti–6Al–4V at ambient and elevated temperatures." *Mater. Sci. and Eng. A.*, 355(1-2), 216-230.

Nemat, M., and Lyons, A. C. (2000). “An investigation of the surface topography of ball burnished mild steel and aluminium.” *Int. J. Adv. Manuf. Technol.*, 16(7), 469-473.

Nestler, A., and Schubert, A. (2015). “Effect of machining parameters on surface properties in slide diamond burnishing of aluminium matrix composites.” *Mater. Today: Proc.*, 2, S156-S161.

Nestler, A., and Schubert, A. (2018). “Roller burnishing of particle reinforced aluminium matrix composites.” *Metals.*, *8*(2), 95.

Okada, M., Shinya, M., Matsubara, H., Kozuka, H., Tachiya, H., Asakawa, N., and Otsu, M. (2017). “Development and characterization of diamond tip burnishing with a rotary tool.” *J. Mater. Process. Technol.*, 244, 106-115.

Okada, M., Suenobu, S., Watanabe, K., Yamashita, Y., and Asakawa, N. (2015). “Development and burnishing characteristics of roller burnishing method with rolling and sliding effects.” *Mechatron.*, 29, 110-118.

Ozel, T., and Karpat, Y. (2005). “Predictive modeling of surface roughness and tool wear in hard turning using regression and neural networks.” *Int. J. Mac. Tools and Manufac*., 45, 467–479.

Patel, K. A., Brahmbhatt, P. K. (2017). “Response surface methodology based desirability approach for optimization of roller burnishing process parameter.” *J. Inst. Eng. Ser. C.*, 99(6), 729-736.

Phadke, M. S. (1989). Quality Engineering Using Robust Design, AT & T, Prentice Hall International, Englewood Cliffs, New Jersey.

Prevey, P. S., and Cammett, J. (2001). “Low cost corrosion damage mitigation and improved fatigue performance of low plasticity burnished 7075-T6.” *J. Mater. Eng. Perform.*, 10(5), 548-555.

Pu, Z., Outeiro, J. C., Batista, A. C., Dillon Jr, O.W., Puleo, D. A., and Jawahir, I. S. (2012a). "Enhanced surface integrity of AZ31B Mg alloy by cryogenic machining towards functional performance of machined components." *Int. J. Mach. Tools. Manuf.,* 56, 17–27.

Pu, Z., Song, G. L., Yang, S., Outeiro, J. C., Dillon Jr, O. W., Puleo, D. A., and Jawahir, I. S. (2012b). "Grain refined and basal textured surface produced by burnishing for improved corrosion performance of AZ31B Mg alloy." *Corros. Sci.*, 57, 192–201.

Pu, Z., Yang, S., Song, G. L., Dillon Jr, O. W., Puleo, D. A., and Jawahir, I. S. (2011). "Ultrafine-grained surface layer on Mg–Al–Zn alloy produced by cryogenic burnishing for enhanced corrosion resistance." *Scr. Mater.*, 65(6), 520-523.

Pusavec, F., Kramar, D., Krajnik, P. and Kopac, J. (2010). "Transitioning to sustainable production–part II: evaluation of sustainable machining technologies." *J. Clean. Prod.*, 18 (12), 1211-1221.

Radziejewska, J., and Skrzypek, S. J. (2009). "Microstructure and residual stresses in surface layer of simultaneously laser alloyed and burnished steel." *J. Mater. Process. Technol.*, 209(4), 2047-2056.

Rajesham, S., and Tak, J. C. (1989). "A study on the surface characteristics of burnished components." *J. of Mech. Working Tech*., 20, 129-138.

Rao, C. M., Rao, S. S., and Herbert, M. A. (2018). "Development of novel cutting tool with a micro-hole pattern on PCD insert in machining of titanium alloy." *J. Manuf. Process.,* 36, 93-103.

Reddy, V. C., Gowd, G. H., and Kumar, M. D. (2018). "Empirical modeling & optimization of laser micro-machining process parameters using genetic algorithm." *Mater. Today: Proc.,* 5(2), 8095-8103.

Revankar, G. D., Shetty, R., Rao, S. S., and Gaitonde, V. N. (2014). "Analysis of surface roughness and hardness in ball burnishing of titanium alloy." *Meas.*, 58, 256-268.

Rolls Royce. (2015). "The jet engine." John Wiley & Sons Inc., New York, USA.

Ross, P. J. (1996). “Taguchi techniques for quality engineering: loss function, orthogonal experiments, parameter and tolerance design.” McGraw-Hill, New York.

Ruseva, E. V., and Fuks, M. Y. (1978). “Surface layer properties after burnishing by different methods.” *Russian Eng. J.*, 58, 28–30.

Sachin, B., Narendranath, S., and Chakradhar, D. (2018a). “Experimental evaluation of diamond burnishing for sustainable manufacturing. *Mater. Res. Express.*, 5(10), 106514.

Sachin, B., Narendranath, S., and Chakradhar, D. (2018b). “Effect of cryogenic diamond burnishing on residual stress and microhardness of 17-4 PH stainless steel.” *Mater. Today: Proc.*, 5, 18393-18399.

Sachin, B., Narendranath, S., and Chakradhar, D. (2019a). “Effect of working parameters on the surface integrity in cryogenic diamond burnishing of 17-4 PH stainless steel with a novel diamond burnishing tool.” *J. Manuf. Processes.*, 38, 564-571.

Sachin, B., Narendranath, S., and Chakradhar, D. (2019b). “Sustainable diamond burnishing of 17-4 PH stainless steel for enhanced surface integrity and product performance by using a novel modified tool.” *Mater. Res. Express.*, 6(4), 046501.

Sachin, B., Narendranath, S., and Chakradhar, D. (2019c). “Selection of optimal process parameters in sustainable diamond burnishing of 17-4 PH stainless steel.” *J. Brazilian. Soc. Mech. Sci. Eng.*, 41(5), 219.

Sahin, Y., and Motorcu, A. R. (2004). “Surface roughness prediction model in machining of carbon steel by PVD coated cutting tools.” *Am. J. Applied Sci*., 1, 12-17.

Saï, W. B., and Lebrun, J. L. (2003). “Influence of finishing by burnishing on surface characteristics.” *J. Mater. Eng. Perform.*, 12(1), 37-40.

Salahshoor, M., and Guo, Y. B. (2011). “Surface integrity of biodegradable Magnesium–Calcium orthopedic implant by burnishing.” *J. Mech. Behav. Biomed. Mater.*, 4(8), 1888-1904.

Salahshoor, M., Li, C., Liu, Z. Y., Fang, X. Y., and Guo, Y. B. (2018). “Surface integrity and corrosion performance of biomedical magnesium-calcium alloy processed by hybrid dry cutting-finish burnishing.” *J. Mech. Behav. Biomed. Mater.*, 78, 246-253.

Saldana-Robles, A., Plascencia-Mora, H., Aguilera-Gomez, E., Saldana-Robles, A., Marquez-Herrera, A., and Diosdado-De la Peña, J. A. (2018). “Influence of ball-burnishing on roughness, hardness and corrosion resistance of AISI 1045 steel.” *Surf. Coatings Technol.*, 339, 191-198.

Santhanakrishnan, M., Sivasakthivel, P.S., and Sudhakaran, R. (2017). “Modeling of geometrical and machining parameters on temperature rise while machining Al 6351 using response surface methodology and genetic algorithm.” *J. Brazilian Soc. Mech. Sci. Eng.*, 39, 487–496.

Sarıkaya, M., and Güllü, A. (2015). “Multi-response optimization of minimum quantity lubrication parameters using Taguchi-based grey relational analysis in turning of difficult-to-cut alloy Haynes 25.” *J. Cleaner Prod.*, 91, 347-357.

Sayahi, M., Sghaier, S., and Belhadjsalah, H. (2013). “Finite element analysis of ball burnishing process: comparisons between numerical results and experiments.” *Int. J. Adv. Manuf. Technol.*, 67, 1665–1673.

Selvakumar, S., and Ravikumar, R. (2018). “A novel approach for optimization to verify RSM model by using multi-objective genetic algorithm.” *Mater. Today: Proc.*, 5, 11386-11394.

Senthilkumar, N., Tamizharasan, T., and Anandakrishnan, V. (2014). Experimental investigation and performance analysis of cemented carbide inserts of different geometries using Taguchi based grey relational analysis.” *Meas.*, 58, 520-536.

Sequera, A., Fu, C. H., Guo, Y. B., and Wei, X. T. (2014). “Surface integrity of inconel 718 by ball burnishing.” *J. Mater. Eng. Perform.,* 23(9), 3347-3353.

Shapiro, A. A. (1970). “Influence of surface work hardening on the fatigue properties of wrought iron.” *Russian Eng. J.,* 50(6), 52.

Sharma, V. S., Dogra, M., and Suri, N. M. (2009). "Cooling techniques for improved productivity in turning". *Int. J. Mach. Tools Manuf.,* 49(6), 435–453.

Shaw, M. C., Pigott, J. D. and Richardson, L. P. (1951). "Effect of cutting fluid upon chip–tool interface temperature". *Trans. ASME.,* 71(2), 45–56.

Shiou, F. J., Huang, S. J., Shih, A. J., Zhu, J., and Yoshino, M. (2017). “Fine surface finish of a hardened stainless steel using a new burnishing tool.” *Procedia Manuf.*, 10, 208-217.

Shokrani, A., Dhokia, V., and Newman, S. T. (2012). "Environmentally conscious machining of difficult-to-machine materials with regard to cutting fluids". *Int. J. Mach. Tools Manuf.,* 57, 83–101.

Silveira, E., Atxaga, G., and Irisarri, A. M. (2008). “Failure analysis of a set of compressor blades.” *Eng. Fail. Anal*., 15, 666-674.

Sivaiah, P., and Chakradhar, D. (2017). “Influence of cryogenic coolant on turning performance characteristics: A comparison with wet machining.” *Mater. Manuf. Process.*, 32, 1475–1485.

Sokovic, M., and Mijanovic, K. (2001). “Ecological aspects of the cutting fluids and its influence on quantifiable parameters of the cutting processes.” *J of Mater. Process Technol*., 109, 181–189.

Sova, A., Courbon, C., Valiorgue, F., Rech, J., and Bertrand, P. (2017). “Effect of turning and ball burnishing on the microstructure and residual stress distribution in stainless steel cold spray deposits.” *J. Therm. Spray Technol.*, 26(8), 1922-1934.

Sreejith, P. S. and Ngoi, B. K. A. (2000). “Dry machining – machining of the future.” *J of Mater. Process Technol*., 101, 289–293.

Suresh Kumar Reddy, N., and Venkateswara Rao, P. (2005). “A genetic algorithm approach for optimization of surface roughness prediction model in dry milling.” *Mach. Sci. Technol.,* 9(1), 63–84.

Swirad, S. (2011). “The surface texture analysis after sliding burnishing with cylindrical elements.” *Wear*, 271(3-4), 576-581.

Taguchi, G. (1986). “Introduction to quality engineering: designing quality into product and processes.” Asian Productivity Organisation, Tokyo.

Tang, J., Luo, H. Y., and Zhang, Y. B. (2017). “Enhancing the surface integrity and corrosion resistance of Ti-6Al-4V titanium alloy through cryogenic burnishing.” *Int. J. Adv. Manuf. Technol.,* 88(9-12), 2785-2793.

Tang, J., Luo, H., Qi, Y., Xu, P., Ma, S., Zhang, Z., and Ma, Y. (2018). “The effect of cryogenic burnishing on the formation mechanism of corrosion product film of Ti-6Al-4V titanium alloy in 0.9% NaCl solution.” *Surf. Coatings Technol.,* 345, 123-131.

Teimouri, R., Amini, S., and Bami, A. B. (2018). “Evaluation of optimized surface properties and residual stress in ultrasonic assisted ball burnishing of AA6061-T6.” *Meas.*, 116, 129-139.

Thorat, S. R., and Thakur, A. G. (2018). “Optimization of burnishing parameters by taguchi based gra method of AA 6061 aluminum alloy.” *Mater. Today: Proc.*, 5(2), 7394-7403.

Tian, Y., and Shin, Y. C. (2007). "Laser-assisted burnishing of metals." *Int. J. Mach. Tools Manuf.,* 47(1), 14-22.

Timoshchenko, V. A., and Dubenko, V. V. (1976). “Selection of optimum technological parameters for diamond burnishing of chromium coated blanks.” *Russian Eng. J.*, 56, 57–58.

Toboła, D., and Kania, B. (2018). “Phase composition and stress state in the surface layers of burnished and gas nitrided Sverker 21 and Vanadis 6 tool steels.” *Surf. Coatings Technol.*, 353, 105-115.

Tolga Bozdana, A. (2005). “On the mechanical surface enhancement techniques in aerospace industry-a review of technology.” *Aircraft Eng. and Aero. Technol.*, 77(4), 279-292.

Travieso-Rodríguez, J. A., Gras, G. G., Peiró, J. J., Carrillo, F., Dessein, G., Alexis, J., and Rojas, H. G. (2015). “Experimental study on the mechanical effects of the vibration-assisted ball-burnishing process.” *Mater. Manuf. Process.*, 30(12), 1490-1497.

Tsai, C. H., Chang, C. L., and Chen, L. (2003). “Applying grey relational analysis to the vendor evaluation model.” *Int. J. Comput. Inter. and Manag.*, 11(3), 45-53.

Wakabayashi, T., Sato, H. and Inasaki, I. (1998). “Turning using extremely small amounts of cutting fluids.” *JSME Int. J.*, 41, 143-148.

Wang, T., Wang, D. P., Gang, G., Gong, B. M. and Song, N. X. (2009). “40Cr nano crystallization by ultrasonic surface rolling extrusion processing.” *J. of Mech. Eng.*, 45(4), 177–183.

Wang, Z., Jiang, C., Gan, X., Chen, Y., and Ji, V. (2011). “Influence of shot peening on the fatigue life of laser hardened 17-4PH steel.” *Int. J. Fatigue.*, 33(4), 549-556.

Wen, K. L. (2004). “The grey system analysis and its application in gas breakdown and var compensator finding.” *J. Comput. Cognit.*, 2(1), 21-44.

Yang, S., Puleo, D. A., Dillon, O. W., and Jawahir, I. S. (2011). “Surface layer modifications in Co-Cr-Mo biomedical alloy from cryogenic burnishing.” *Procedia Eng.*, 19, 383-388.

Yang, S., Umbrello, D., Dillon Jr, O. W., Puleo, D. A., and Jawahir, I. S. (2015). "Cryogenic cooling effect on surface and subsurface microstructural modifications in burnishing of Co–Cr–Mo biomaterial." *J. Mater. Prorcess. Technol*., 217, 211-221.

Yildiz, Y., and Nalbant, M. (2008). "A review of cryogenic cooling in machining processes." *Int. J. of Mac. Tools and Manufac*., 48, 947–964.

Yu, X., and Wang, L. (1999). "Effect of various parameters on the surface roughness of an aluminium alloy burnished with a spherical surfaced polycrystalline diamond tool." *Int. J. of Mac. Tools and Manufac*., 39(3), 459-469.

Yuan, X. L., Sun, Y. W., Gao, L. S., and Jiang, S. L. (2016). "Effect of roller burnishing process parameters on the surface roughness and microhardness for TA2 alloy." *Int. J. Adv. Manuf. Technol.*, 85(5-8), 1373-1383.

Yuan, X., and Li, C. (2017). "An engineering high cycle fatigue strength prediction model for low plasticity burnished samples." *Int. J. Fatigue.*, 103, 318-326.

Yuan, X., Sun, Y., Li, C., and Liu, W. (2017). "Experimental investigation into the effect of low plasticity burnishing parameters on the surface integrity of TA2." *Int. J. Adv. Manuf. Technol.*, 88(1-4), 1089-1099.

Zaborski, A., Tubielewicz, K., and Major, B. (2000). "Contribution of burnishing to the microstructure and texture in surface layers of carbon steel." *Arch. of Metall*., 45(4), 333–341.

Zhang, P., and Lindemann, J. (2005). "Effect of roller burnishing on the high cycle fatigue performance of the high-strength wrought magnesium alloy AZ80." *Scr. Mater.*, 52(10), 1011-1015.

Zhang, P., and Liu, Z. (2015). "Effect of sequential turning and burnishing on the surface integrity of Cr–Ni-based stainless steel formed by laser cladding process." *Surf. Coatings Technol.*, 276, 327-335.

Zhang, S., Li, J. F., Sun, J., and Jiang, F. (2010). “Tool wear and cutting forces variation in high-speed end-milling Ti-6Al-4V alloy.” *Int. J. Adv. Manuf. Technol.*, 46(1-4), 69-78.

Zhang, T., Bugtai, N., and Marinescu, I. D. (2015). “Burnishing of aerospace alloy: a theoretical–experimental approach.” *J. Manuf. Syst.*, 37, 472-478.

NATIONAL INSTITUTE OF TECHNOLOGY KARNATAKA, SURATHKAL

LIST OF PUBLICATIONS BASED ON PH.D. RESEARCH WORK

Sl. No.	Title of the paper	Authors	Name of the Journal/Copyrights/Conference/ Symposium, Vol., No., Pages	Month, Year of Publication	Category*
1.	Enhancement of surface integrity by cryogenic diamond burnishing toward the improved functional performance of the components	Sachin B, Narendranath S, D Chakradhar	Journal of the Brazilian Society of Mechanical Sciences and Engineering, 41, 396 doi:10.1007/s40430-019-1918-1	October 2019	1
2.	Selection of optimal process parameters in sustainable diamond burnishing of 17-4 PH stainless steel	Sachin B, Narendranath S, D Chakradhar	Journal of the Brazilian Society of Mechanical Sciences and Engineering, 41, 219 doi:10.1007/s40430-019-1726-7	May 2019	1
3.	Effect of working parameters on the surface integrity in cryogenic diamond burnishing of 17-4 PH stainless steel with a novel diamond burnishing tool	Sachin B, Narendranath S, D Chakradhar	Journal of Manufacturing Processes, 38, 564-571 doi:10.1016/j.jmapro.2019.01.051	February 2019	1
4.	Sustainable diamond burnishing of 17-4 PH stainless steel for enhanced surface integrity and product performance by using a novel modified tool	Sachin B, Narendranath S, D Chakradhar	Material Research Express, 6(4), 046501 doi:10.1088/2053-1591/aaf900	January 2019	1
5.	Experimental evaluation of diamond burnishing for sustainable manufacturing	Sachin B, Narendranath S, D Chakradhar	Material Research Express, 5(10), 106514 doi:10.1088/2053-1591/aadb0a	August 2018	1

6.	Effect of cryogenic diamond burnishing on residual stress and microhardness of 17-4 PH stainless steel	Sachin B, Narendranath S, D Chakradhar	Materials Today: proceedings, 5(9), 18393–18399 doi:10.1016/j.matpr.2018.06.179	March 2018	3
7.	Analysis of surface hardness and surface roughness in diamond burnishing of 17-4 PH stainless steel	Sachin B, Narendranath S, D Chakradhar	IOP conference series: material science and engineering	(In Press)	3
8.	Optimization of Cryogenic Diamond Burnishing Process Parameters on 17-4 PH Stainless Steel using Taguchi Method	Sachin B, Narendranath S, D Chakradhar	International Conference on Contemporary Design and Analysis of Manufacturing and Industrial Engineering Systems, NIT-Trichy	January 2018 (Received best paper award)	3
9.	Empirical modeling and experimental evaluation for optimization of hardness and surface roughness parameters in cryogenic diamond burnishing using Genetic Algorithm	Sachin B, Narendranath S, D Chakradhar	Measurement	(Revision submitted)	1
10.	Improvements in the surface integrity of 17-4 PH stainless steel by cryogenic diamond burnishing	Sachin B, Narendranath S, D Chakradhar	Arabian Journal for Science and Engineering	(Revision submitted)	1
11.	Application of desirability approach to optimize the control factors in cryogenic diamond burnishing	Sachin B, Narendranath S, D Chakradhar	Arabian Journal for Science and Engineering	(Under Review)	1
12.	Diamond burnishing tool	Sachin B, Narendranath S, D Chakradhar	Copyrights	(Under Review)	5

*Category:
1: Journal paper, full paper reviewed
2: Journal paper, Abstract reviews
3: Conference/Symposium paper, full paper reviewed
4: Conference/Symposium paper, abstract reviewed
5: Others (including papers in Workshops, copyrights/patents, NITK Research Bulletins, Short notes etc.)

Mr. Sachin. B	Prof. Narendranath. S	Dr. D. Chakradhar
Research Scholar	Research Guide	Research Guide
Name & Signature, with Date	Name & Signature, with Date	Name & Signature, with Date

VITAE

Name	Mr. Sachin B
Father's Name	Sri. Chandrakanth B
Communication Address	Sri Rama Kuteera Chikkamudnoor Post Krishnanagara, Puttur (D.K) Karnataka, India-574203
E-Mail	sachinraobc@gmail.com
Telephone a) Mobile	+91 9900529811
Nationality	Indian

ACADEMIC CREDENTIALS

DEGREE	YEAR	INSTITUTE	DISCIPLINE
Ph.D.	2019	National Institute of Technology Karnataka, Surathkal, India	Mechanical Engineering
M. Tech.	2013	Dayananda Sagar College of Engineering, Bengaluru, Karnataka, India	Computer Integrated Manufacturing
B.E.	2011	Vivekananda College of Engineering & Technology, Puttur (D.K), Karnataka, India	Mechanical Engineering

PROFESSIONAL EXPERIENCE

- Working as **Assistant Professor** in the Department of Mechanical Engineering, **NITTE Meenakshi Institute of Technology, Bengaluru, Karnataka, India (an Autonomous Institution)**.

RESEARCH FOCUS

- Advanced Machining
- Diamond Burnishing
- Sustainable Manufacturing
- Product Design

I declare that above information is true and correct to best of my knowledge.

(Sachin B)